Tumor distribution and efficacy of antiangiogenic receptor tyrosine kinase inhibitors

Ph.D. Dissertation

Szilvia Török

Semmelweis University
Clinical Medicine Ph.D. School

Consultants: Dr. Balázs Döme, MD, PhD , head of department
Dr. György Marko-Varga, PhD, professor

Official reviewers: Dr. Anna Sebestyén, PhD, senior research fellow
Dr. Zsolt Horváth, MD, PhD, associate professor

Head of the final Examination Committee:
Dr. András Matolcsy, DSc, professor
Members of the Final Examination Committee:
Dr. Béla Szende, DSc, professor emeritus
Dr. Krisztina Vellainé Takács, PhD, associate professor

Budapest
2016

1. TABLE OF CONTENTS

1. TABLE OF CONTENTS 2

2. ABBREVIATIONS 4

3. INTRODUCTION 8

3.1 Angiogenesis 8

3.2 Tumor-induced angiogenesis 10

3.2.1 Main receptor families and signalization pathways in tumor-induced angiogenesis 12

3.2.1.1 VEGFR family 15

3.2.1.2 PDGFR family 17

3.2.1.3 FGFR family 19

3.2.1.4 TIE receptor family 21

3.2.1.5 TGFβR family 23

3.2.1.6 Notch receptor family 24

3.2.2 Mechanisms of tumor-induced angiogenesis 26

3.2.2.1 Sprouting angiogenesis 26

3.2.2.2 Vessel incorporation or co-option 27

3.2.2.3 Intussusceptive microvascular growth 27

3.2.2.4 Glomeruloid angiogenesis 28

3.2.2.5 Postnatal vasculogenesis 28

3.2.2.6 Vessel-like structures, formed by tumor cells 29

3.2.3 Characteristics of tumor blood vessels 30

3.2.4 Inhibition of the tumor vasculature 32

3.2.4.1 Conventional chemotherapeutic agents 32

3.2.4.2 Vacular disrupting agents 32

3.2.4.3 Vasoactive agents 33

3.2.4.4 Angiogenesis inhibitors 34

3.2.5 Resistance to antiangiogenic tyrosine kinase inhibitor therapy 40

3.3 TKI imaging 41

4. AIMS 44

5. METHODS 45

5.1 In vivo tumor models and treatments 45

5.1.1 Tumor models 45

5.1.2 Drugs 45

5.1.3 In vivo treatment 47

5.2 Analysis of vascular parameters and target receptors 47

5.3 Detection of the compounds and analysis of drug distribution and intensity 49

5.3.1 Ionization technique and instrumentation 49

5.3.2 Compound characterization 56

5.3.3 Compound detection in the blood 57

5.3.4 Tissue imaging of antiangiogenic RTKIs 57

5.3.5 Quantification of the compounds 58

5.4 Statistical analysis 58

6. RESULTS 60

6.1 Tumor growth inhibititon 60

6.2 Immunohistochemical analysis 61

6.3 Mass spectrometric analysis 77

6.3.1 Compound characterization 77

6.3.2 Precursor compound and metabolite detection in the blood 79

6.3.3 Tissue imaging of antiangiogenic RTKIs 87

7. DISCUSSION 95

8. CONCLUSIONS 99

9. SUMMARY 100

10. ÖSSZEFOGLALÁS 101

11. REFERENCES 102

12. PUBLICATIONS 147

13. ACKNOWLEDGEMENT 149

2. ABBREVIATIONS

AC: alternate current

ACN: acetonitrile

ADME: adsorption, distribution, metabolism and elimination

AGC: automatic gain control

AI: angiogenesis inhibitor

AKT: protein kinase with transforming capabilities developed in the Ak strain of mice

ALK: activin receptor-like kinase

Ang: angiopoietin

ANOVA: analysis of variance

ARNT: aryl hydrocarbon receptor nuclear translocator

ARRIVE: animal research: reporting of rn vivo experiments

BAMBI: BMP and activin membrane-bound inhibitor homologue

BCR-ABL: break point cluster- abelson

BM: basement membrane

BMP: bone morphogenic proteins

CA4P: combretastatin A-4 phosphate

CSC: cancer stem cells

CBP: CREBB binding proein

c-FMS: colony-stimulating factor-1 receptor

CHCA: α-cyano-4-hydroxycinnamic acid

CID: collision-induced dissociation

c-KIT: cellular homolog of the feline sarcoma viral oncogene v-kit

c-MYC: cellular myelocytomatosis transcription factor

COX: cyclooxygenase

CRC: colorectal cancer

CSF-1R: colony stimulating factor 1 receptor

CSL: CBF1/Su(H)/Lag-1) transcription factor

C-Trap: curved linear trap

CXCR4: SDF receptor

DC: direct current

DFG motif: Asp-Phe-Gly motif

APE motif: Ala–Pro–Glu motif

DHB: 2,5-dihydroxybenzoic acid

DLL: delta-like ligand

DTC: differentiated thyroid carcinoma

EC: endothelial cell

ECM: extracellular matrix

EGF/EGFR: epidermal growth factor/ epidermal growth factor receptor

EMEA: European Medicines Agency

EPAS: endothelial PAS domain-containing protein

EPC: endothelial progenitor cell

ErbB: erythroblastic leukemia viral oncogene homologue

ERK: extracellular signal-regulated kinase

FAK: focal adhesion kinase

FDA: Food and Drug Administration

FGF/FGFR: fibroblast growth factor/ fibroblast growth factor receptor

FLK: fetal liver kinase

FLT: fms-like tyrosine kinase

FT-MS: Fourier transform-mass spectrometry

GDF: growth and differentiation factor

GIST: gastrointestinal stromal tumor

HCC: hepatocellular carcinoma

HCD: high energy collisional dissociation

HE: haematoxylin&eosin

HER: human epidermal growth factor receptor

HGF: hepatocyte growth factor

HIF: hypoxia-inducible factor

HPLC: high-peformance liquid chromatography

HRE: hypoxia-response element

HSP27: heat shock protein 27

IC50: the half maximal inhibitory concentration

IGF/IGFR: insuline-like growth factor/ insuline-like growth factor receptor

IL: interleukin

ITK: interleukin-2-inducible T-cell kinase

JNK: c-Jun N-terminal kinase

KDR: kinase domain-containing receptor

LCK: lymphocyte-specific protein tyrosine kinase

LC-MS: liquid chromatography-mass spectrometry

LYN: Lck/Yes novel tyrosine kinase

LTQ: linear trap quadrupole

mAB: monoclonal antibody

MALDI: matrix-assisted laser desorption ionization

MAPK: mitogen-activated protein kinase

MEK: MAPK/ERK Kinase

MIS: mullerian inhibitory substance

MMP: matrix metalloproteinases

MS: mass spectrometry

MSI: mass spectrometry

mTOR: mammalian target of rapamycin

MVD: microvessel density

m/z: mass to charge ratio

NCE: normalized collision energy

NF-κB: nuclear factor kappa-light-chain-enhancer of activated B cells

NICD: Notch intracellular domain

NRP: neuropilin

NSCLC: non-small cell lung cancer

PA/PAI: plasminogen activator /plasminogen activator inhibitor

PDGF/PDGFR: platelet-derived growth factor/ platelet-derived growth factor receptor

PHD: prolyl-hydroxylase domain-containing protein

PI3K: phosphatidilinositole 3-kinase

PIP2: phosphatidylinositol 4,5-bisphosphate

PKB: protein kinase B

PKC: protein kinase C

PLCγ: phospholipase C gamma

PlGF: placental growth factor

pNET: pancreatic neuroendocrine tumors

PTEN: phosphatase and tensin homolog

RAS: rat sarcoma viral oncogene homolog gene

RAF: rapidly accelerated fibrosarcoma

RCC: renal cell cancer

RET: rearranged during transfection

RTK/RTKI: receptor tyrosine kinase/ receptor tyrosine kinase inhibitors

SAPK: stress-activated kinase

s.c.: subcutan

SDF: stromal derived factor

SH2-domain: Src homology 2 domain

SEM: secondary electron multiplyer

SEM: standard error of the mean

SMA: smooth muscle actin

SNP: single nucleotid polymorphism

Src: sarcoma

STAT: signal transducer and activator of transcription

TFA: trifluoroacetic acid

TGF: transforming growth factor

TIC: total ion current

TIE: tunica intima endothelial receptor

TNF: tumor necrosis factor

TOF: time of flight

uPA/uPAR: urokinase plasminogen activator/ urokinase plasminogen activator receptor

VDA: vascular disrupting agents

VEGF/VEGFR: vascular endothelial growth factor/ vascular endothelial growth factor receptor

VHL: von Hippel-Lindau

VSMC: vascular smooth muscle cell

3. INTRODUCTION

3.1 Angiogenesis

The word “angiogenesis” was first mentioned in 1787 in the work of John Hunter, an English surgeon who studied the process in the growing antlers of deers (1). In contrast to vasculogenesis, which means the development of the vascular system during embryogenesis, angiogenesis is the process when new blood vessels are formed from preexisting ones.

Under physiological conditions, angiogenesis is activated in response to low oxygen level. The process is regulated by the HIF (hypoxia-inducible factor) complex. HIFs are basic helix-loop-helix DNA binding transcription factor proteins of the Per-Arnt-Sim family, and function as heterodimers consisting of an oxygen-regulated alpha subunit and a stably expressed beta subunit (2). The alpha subunits are encoded by three genes in mammals: HIF1α, HIF2α (EPAS1: Endothelial PAS domain-containing protein 1) and HIF3α (2-4). Also three forms of the beta subunit have been identified until now, the HIF1β (aryl hydrocarbon receptor nuclear translocator: ARNT), ARNT2 and ARNT3 (5,6). The structure, regulation and function of all HIFs seem to be similar, but compared to their homologs (HIF1α and ARNT) the members of the HIF2 and -3 family have been reported to have a more restricted pattern of expression and thus may play more specialized roles in oxygen delivery than the HIF1 subunits (6,7).

Under normal oxygen tension, the alpha subunits are hydroxylated at the prolyl residues, a process that is catalyzed by the prolyl-hydroxylase domain-containing protein (PHD). This hydroxylation promotes interaction with the von Hippel-Lindau (VHL) ubiquitin ligase and, consequently, they undergo proteasomal degradation (8,9). Thus the half-life of alpha subunits is measurable in minutes and the protein is hardly detectable at all (10). The degradation process is regulated not only by the VHL protein, but p53 as well (11).

In case of hypoxia, the HIF alpha and beta subunits form a complex, recruits its co-activator, p300/CBP (CREBB Binding Protein) and binds to the Hypoxia Responsive Element (HRE) of the target genes, thus modifying their transcription (12). Several of these target genes are responsible for inducing angiogenesis in order to increase the oxygen delivery of the tissue, such as vascular endothelial growth factor (VEGF),

VEGF receptor 1, tunica intima endothelial receptor 2 (TIE2), angiopoietin 2 (Ang2), erythropoietin, Insulin-like growth factor 2 (IGF2), Transforming Growth Factor β3 (TGFβ3), c-MET, adrenomedullin, NO Synthase 2, plasminogen activator inhibitor-1 (PAI1) (3,13-21). Regulation of oxygenation via the HIF molecule is depicted in **Figure 1.**

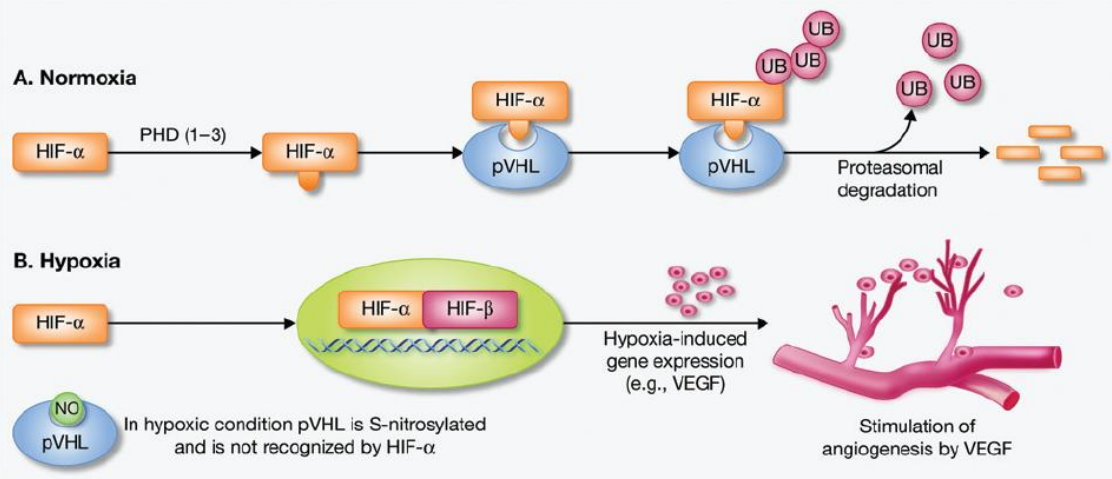

Figure 1. Regulation of oxygenation via the HIF molecule (22). Degradation of HIFα via ubiquitination in normoxia (**A.**) and angiogenesis stimulation in hypoxia (**B.**).

VEGF is considered to be the key hypoxia dependent cytokine for endothelial sprouting (23). Besides, many other factors are also able to positively influence the process of angiogenesis such as platelet-derived growth factors (PDGFs) (24-26), fibroblast growth factors (FGFs) (27,28), placental growth factor (PlGF) (29), angiopoietins (30), Jagged (31), epidermal growth factor (EGF) (32), hepatocyte growth factor (HGF) (33) and interleukin-8 (IL-8) (34). These ligands bind to their receptors on the surface of endothelial cells and act in an autocrin or paracrin manner. Binding the growth factor leads to the activation of signaling cascades, influencing the survival, proliferation and migration of endothelial cells and thus the maintenance of existing- and development of new vessels. Moreover, these pathways regulate further processes involved in angiogenesis, such as secretion of additional growth factors (35), upregulation of angiogenic receptors (36), alterations in cell-cell and cell-matrix interactions by matrix metalloproteinases (MMPs) (37), and activation of the members of endothelial cell (EC) adhesion molecule family (38). After the new capillary is formed by ECs, PDGF-BB and bFGF secreted by the endothelium recruits PDGFRβ or FGFR expressing pericytes and vascular smooth muscle cells (VSMCs) (36,39). These supporting cells provide

structural stability for the new blood vessel, promote EC survival and regulate blood flow via influencing vasoconstriction and -dilatation. Moreover, via the secretion of VEGF pericytes also promote EC sprouting and survival (40). By binding to their receptor, TGFß1 (41), Ang1 (42) and sphingosine-1-phosphate (43) stabilize the interaction between mural cells and ECs.

The healthy body controls angiogenesis by balancing a series of angiogenesis stimulating and inhibiting factors. Thus, in a healthy adult ECs have long half-life, and angiogenesis is only activated under special conditions, such as the reproducible processes of women or wound healing.

If tissues cannot produce adequate amounts of angiogenic growth factors, blood vessel growth becomes inadequate leading to improper circulation and eventually to necrosis. Insufficient angiogenesis occurs in diseases such as coronary artery disease, stroke and chronic wounds. In these pathological features therapeutic angiogenesis is aimed to stimulate the sprouting of new vessels with growth factors being developed to treat these conditions.

On the other hand, by overexpressing the angiogenesis stimulating factors, blood vessel growth becomes highly intensive in some pathological conditions, such as endometriosis, atherosclerosis, psoriasis, rheumatoid arthritis, inflammation, ischaemia, ocular neovascularization and cancer (44).

3.2 Tumor-induced angiogenesis

After the experiments of Hunter, more than a century had passed until an interest in the angiogenesis of tumors was piqued. Until the 1930-40s these investigations were restricted mostly to the observation of the morphology of tumor blood vessels (45). Later the process of neovascularization was also observed, but it had not become the focus of research until 1971, when Judah Folkman postulated that above a certain size (about 1-2 mm diameter) intratumoral diffusion is no longer sufficient and tumors are incapable of growing and metastatizing, unless they develop their own blood supply to ensure the necessary oxygen and nutrient level of the cells. He also assumed that tumor cells secrete growth factors to facilitate the process of angiogenesis, ie. capillary growth is induced by the communication between tumor blood vessels and the tumor tissue (46).

This communication is mediated by the HIFα proteins, which are stabilized in hypoxic tumor cells, and thus facilitate the expression of angiogenic proteins. Moreover, the expression level of HIF1α is controlled not only by oxygen tension, but also by reactive oxygen species, that are secreted in response to carcinogens (47,48).

Moreover, oncogenes, such as activated EGFR (49), ErbB-2/Her2 (50) mutant RASv12 (51), mTOR (52) and Src (53) also augments HIF mediated gene expression. On the other hand, some tumor suppressor genes also play an important role in the regulation of HIF1α, therefore loss of function of these gene products may influence angiogenesis in tumor tissues. The product of the tumor suppressor gene PTEN attenuates hypoxia mediated HIF1-α stabilization through the inhibition of AKT (54), while pVHL (9) and p53 (11) regulate the ubiquitination and degradation of the HIF complex, thus mediating the expression of angiogenic molecules.

Furthermore, solid tumors and their microenvironment secrete and often overexpress a range of growth factors, cytokines and hormones that coordinate the complex series of events of new capillary growth. Among them ie. VEGFA (55), IL1β, insuline (56), heregulin (50), EGF (57), IGF1,-2 (13) TGFβ (58), Tissue Necrosis Factor α (TNFα) (59) enhance HIF expression, activating a vicious circle in the angiogenic process.

HIF independent regulation of the VEGF pathway also occurs in tumors, as some oncogenes and tumor suppressor genes (cSrc (60), BCR-ABL (61), RAS (62), p53 (63)); cellular receptors (activated EGFR (64), IGF-1R (65) and overexpressed HER2 (66)); and cytokines (COX-2 (67), PDGF-AA (68)) can also influence VEGF production. These changes in the HIF-VEGF protein system drive the activity of angiogenesis in tumors, which can be further modulated by the expression of other angiogenic growth factors.

The schematic process of tumor-induced angiogenesis is depicted in **Figure 2.**

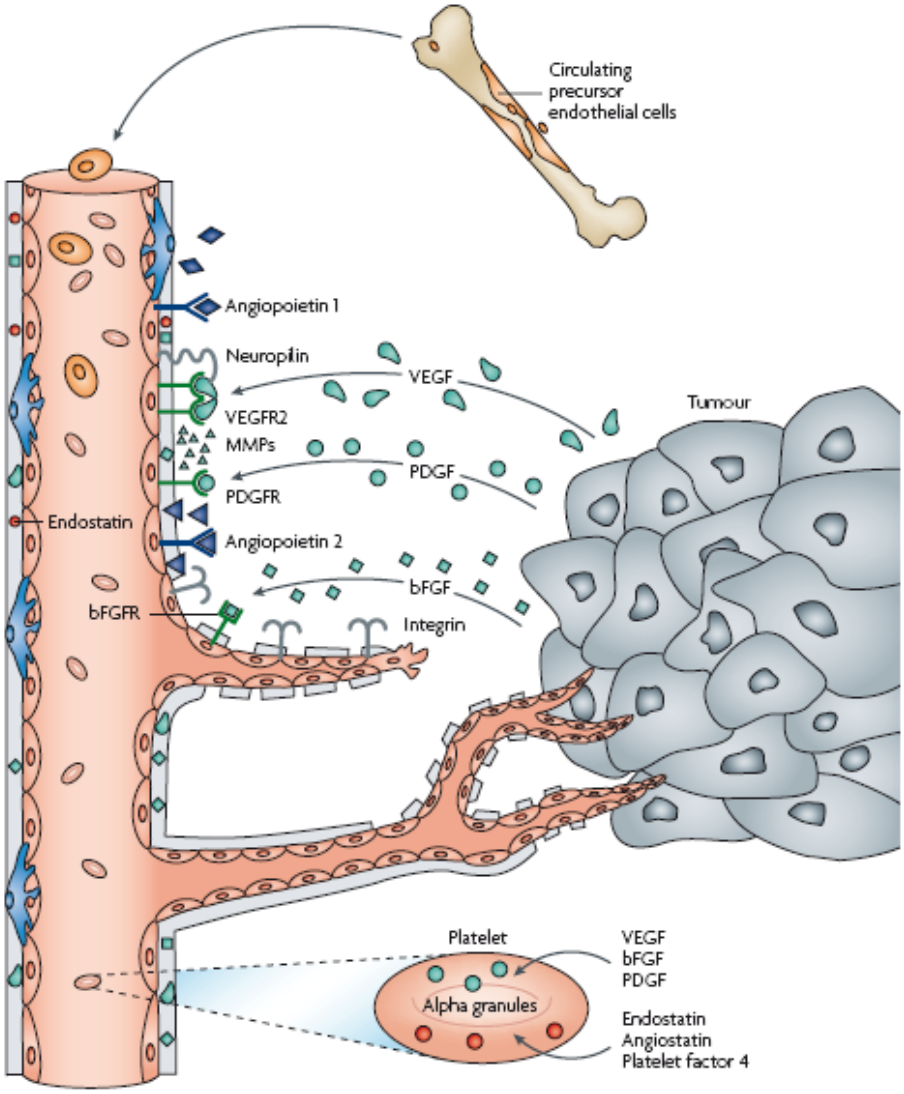

Figure 2. The process of tumor-induced angiogenesis (69). Main angiogenic growth factors (VEGF, PDGF, bFGF) are secreted by tumor cells or platelets and bound to their transmembrane receptors on ECs. The process is further regulated by integrins, MMPs and intrinsic angiogenesis inhibitors, such as endostatin, angiostatin or platelet factor-4.

3.2.1 Main receptor families and signalization pathways in tumor-induced angiogenesis

Kinases are phosphotransferase enzymes that transmit the terminal phosphate group of a high-energy donor molecule, such as adenosine triphosphate (ATP), to their substrate.

Protein kinases can be divided into a larger group of serin/threonine kinases and a smaller tyrosine kinase group, based on the amino acid they target. Besides, atypical kinases also exist.

Another classification is based on the localization of the kinase. Receptor kinases are membrane bound and essential for the transduction of extracellular signals into the cell. Non-receptor kinases are responsible for intracellular communication. Angiogenesis is mainly regulated by receptor tyrosine kinases (RTKs).

RTKs have a variable extracellular part for ligand binding, a transmembrane region to anchore the molecule to the cell membrane, and they all share a conserved intracellular secondary structure. This consists of (i) a bi-lobed catalytic core, responsible for binding ATP in a deep cleft, located between the lobes (hinge region); (ii) a substrate binding site, where interacting proteins can bind and (iii) an activation loop, containing Asp-Phe-Gly (DFG) and Ala–Pro–Glu (APE) motifs at the N- and C-terminal part of the loop, respectively.

The ATP-binding site is divided into the following subregions (**Figure 3.**): adenine region, sugar region and phosphate binding region, based on the part of the ATP it binds. The sugar- and phosphate binding regions form a hydrophilic channel. Besides, a hydrophobic pocket (selectivity pocket) is also formed near the ATP binding region by the activation loop in the inactive conformation. This is not used by ATP, but ensures selectivity of receptor tyrosine kinase inhibitors. Moreover, ATP does not use the hydrophobic channel either, which provides a slot to open for solvents and it can be exploited to gain binding affinity.

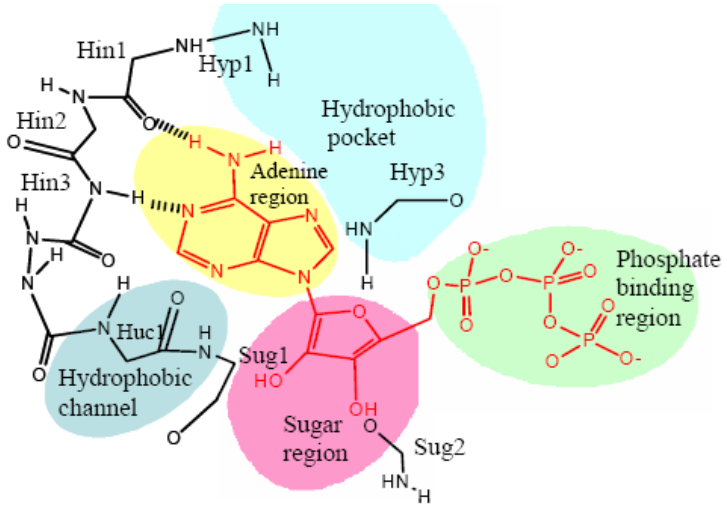

Figure 3. Binding of ATP to receptor tyrosine kinases (70). The ATP-binding site is divided into the following subregions: adenine region, sugar region and phosphate binding region, based on the part of the ATP it binds. The sugar- and phosphate binding regions form a hydrophilic channel. Note that the hydrophobic pocket and the hydrophobic channel are not used by ATP, but ensures binding affinity and selectivity of RTKIs.

The activation loop can form a number of conformations. In the "out" conformation it creates a hydrophobic pocket near the ATP-binding cleft, thus blocking the accessibility of the receptor for ATP. Ligand binding of the extracellular domain triggers receptor dimerization, resulting in transphosphorylation of specific tyrosine residues in the activation loop, juxtamembrane- and C terminal regions. As a result, the receptor turns to the "in" conformation, which opens the hinge region for ATP. ATP binds in the cleft via the adenine ring, which forms 2 hydrogen bonds with the kinase 'hinge'. The ribose and triphosphate group of ATP bind in a hydrophilic channel that extends to the substrate binding site, which is essential to the catalysis of autophosphorylation.

After autophosphorylation, the receptor recruits interacting proteins that bind to certain phosphorylation sites, which subsequently phosphorylate other proteins. These activation signaling pathways eventually lead to biological responses, such as cell activation, proliferation, differentiation, migration, survival and vascular permeability, (70,71). Activation of RTKs is depicted in **Figure 4.**

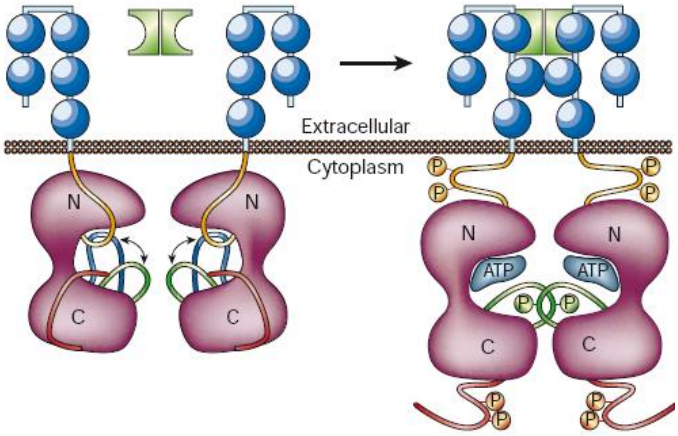

Figure 4. Activation of RTKs (71). Ligand binding of the extracellular domain triggers receptor dimerization, resulting in transphosphorylation of specific tyrosine residues in the activation loop, juxtamembrane- and C terminal regions. As a result, the receptor turns to the "in" conformation, which opens the hinge region for ATP.

The most important angiogenic RTKs are VEGFRs, PDGFRs, FGFRs, and the TIE receptors. Beside tyrosine kinases, serine-threonine kinases also regulate the process of neovascularization. These act similar to RTKs. Main examples are the members of TGF receptor family. Other receptors exert their effect not by phosphorylating partner molecules, but by regulating potential transcriptional activators. Of these, the Notch receptor family is the predominant member of angiogenic signalling.

3.2.1.1 VEGFR family

The VEGF family consists of the following growth factors in mammals: VEGFA (VEGF), VEGFB, VEGFC, VEGFD and PlGF. They are homodimeric polypeptides, although naturally occurring heterodimers of VEGFA and PlGF have also been described (72,73). Splicing and processing regulates the ability of the growth factors to bind to the appropriate receptors or co-receptors. Ligands can bind to three different receptors, VEGFR1-3 (FLT1: fms-like tyrosyl kinase-1, FLK1/KDR: Fetal liver kinase-1/Kinase Domain-containing Receptor and FLT4 respectively) (74). The receptors have a ligand-binding extracellular domain consisting of seven immunoglobulin-like loops, a transmembrane domain, a juxtamembrane domain, and a split tyrosine kinase domain followed by a C-terminal tail (75). As co-receptors neuropilin 1-2 (NRP1, -2) and heparan sulphate play a role in the regulation of angiogenesis by increasing the binding affinity of specific ligands to the receptors (76-78).

VEGFA is the ligand of both VEGFR1 and VEGFR2, but while VEGFR1 has much higher affinity for binding the growth factor, than VEGFR2, its kinase activity is weakly induced (79). Moreover, beside being highly expressed on immune cells, hematopoietic cells, vascular endothelial and -smooth muscle cells and several tumor cells (79-84), this receptor exists partly in a soluble form, thus it rather acts as a „trap receptor" for the angiogenic growth factors (85). As VEGFB and PlGF bind just to VEGFR1, their proangiogenic role is limited (86).

VEGFR2 binds VEGFA and proteolitically processed VEGFC, -D (87-89). VEGFR2 is highly expressed not only on lymphatic and vascular endothelial cells but on hematopoietic and tumor cells as well (90-94). Soluble antiangiogenic form of the receptor also exists, but as its binding affinity is much smaller than that of VEGFR1, its trap function is also less important (95).

VEGFC binds with a higher affinity to VEGFR3 than to VEGFR2, while VEGFD has similar affinity for both receptors in human, but does not bind to VEGFR2 in mouse (96,97). VEGFR3 is expressed in the venous endothelial cells in the cardial vein during the later stages of embryogenesis, which gives rise to lymphatics, thus in adults VEGFR3 can be found mainly in lymphatic endothelium and to a lesser extent in vascular endothelial cells (98). It is disputed, whether it can be found on tumor cells (99). Soluble VEGFR3 suppresses lymphangiogenesis and lymphatic metastasis in

different cancer types (100,101). Consequently, the VEGFA-VEGFR2 axis is the predominant mediator of tumor-induced angiogenesis.

Alternative mRNA splicing of VEGFA gives rise to several distinct isoforms. The splice variants are noted as VEGFxxx (xxx means the number of amino acids present in the proteins without the signal peptide) (102). These isoforms differ not only in their expression pattern but their biochemical and thus biological properties as well. Also exon 8b containing less angiogenic or antiangiogenic variants of VEGFxxx are documented (103), and seem to be able to inhibit neovascularization. Moreover, they might be responsible for the failure of antiangiogenic therapies targeting VEGFs (104). **Figure 5.** shows the main ligands and receptors of the VEGF superfamily.

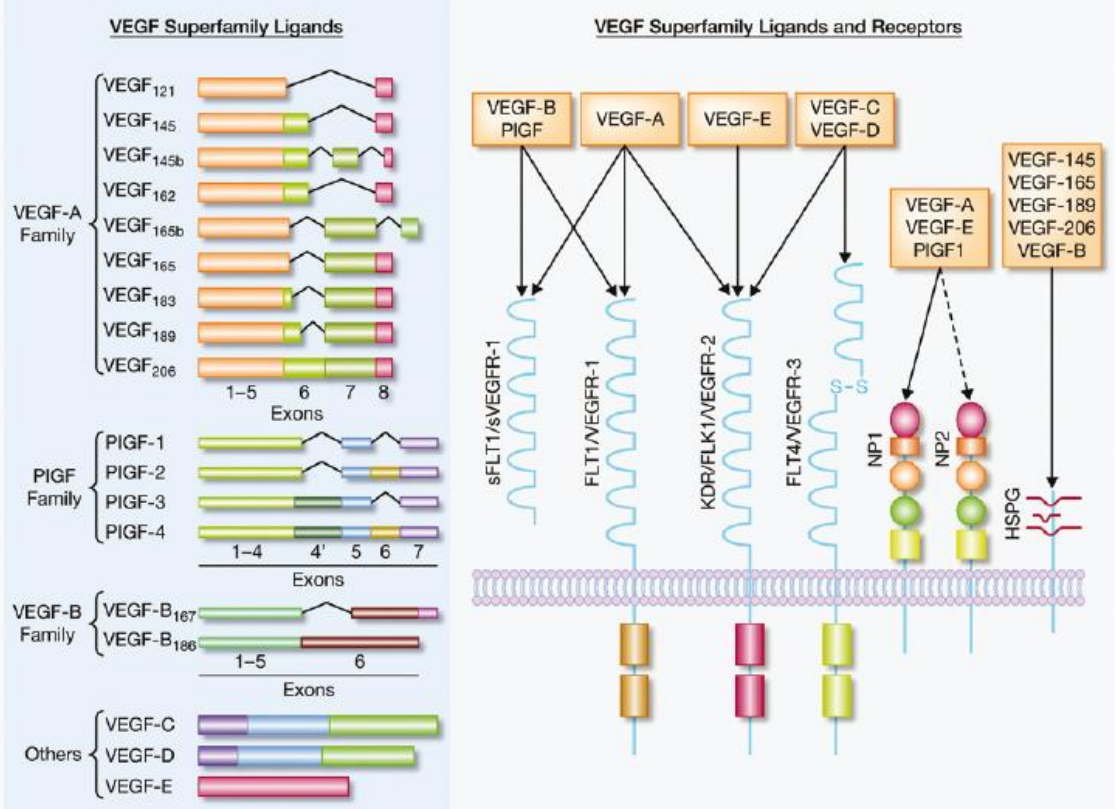

Figure 5. VEGF Superfamily Ligands and receptors (22).

VEGFs can either bind to the receptors freely or be presented by co-receptors. Ligand binding results in receptor homo-, or heterodimerization, followed by changes in the intracellular domain conformation. This leads to the liberalization of the ATP binding site of the receptor and binding of ATP results in the auto- or transphosphorilation of tyrosine residues on the receptor and downstream signal transducers (105).

The VEGF ligands are produced by most parenchymal cells, and paracrine VEGF signaling is essential for the angiogenic cascade, proliferation, survival, permeability responses and endothelial differentiation. Moreover, autocrine VEGF signaling also exists, but only conveys survival signals (106).

After ligand binding the receptor dimerizes and activates the PLCγ/Ras/Raf/MEK/ERK pathway, leading to the regulation of gene expression and cell proliferation (89). With PI3K activation they modulate AKT signaling and thus the survival of receptor expressing cells (107). Via the elevation of intracellular Ca^{2+} or NO level, induced by PI3K or PLC they can also enhance vascular permeability (108). Cell migration is regulated by the PKC/p38/MAPK2-3/HSP27 pathway and the FAK or the STAT cascade (109). Signalization pathways activated by VEGFR2 are shown in **Figure 6**.

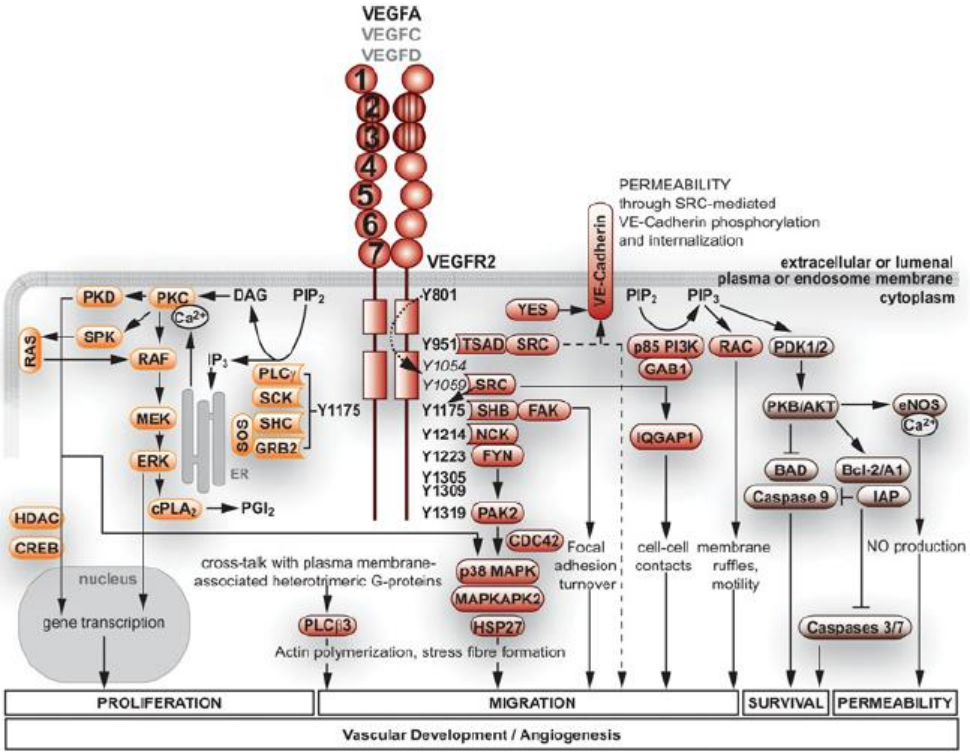

Figure 6. Signalization pathways of VEGFR2 (110).

Overexpression, mutation of the receptors and elevation of VEGF have also been related to enhanced angiogenesis and tumor development (111-113).

3.2.1.2 PDGFR family

The PDGF family consists of four ligand chains, PDGF-A, PDGF-B, PDGF-C and PDGF-D, which create five disulphide bonded dimeric isomorphs, PDGF-AA, PDGF-

BB, PDGF-AB, PDGF-CC and PDGF-DD (114). The ligands can bind to three membrane bound dimeric receptors, PDGFRαα, PDGFRββ, and PDGFRαβ (115). Moreover, low density lipoprotein receptor-related protein and NRP1 seem to mediate PDGFR signaling as co-receptors (116,117).

PDGF synthesis is enhanced in response to low oxygen tension (118), thrombin (119), or other growth factors and cytokines (120). A number of cells secrete PDGFs, ie. cells associated with reproductive processes (121,122), vascular functions (123,124), cells of the nervus system (125-127), immune cells (128) and some other cell types (129,130).

PDGF isoforms are synthesized as precursor molecules and after dimerization they are proteolytically processed to the active forms that bind to their receptors. PDGF-AA binds only to PDGFRαα, while PDGF-BB can bind to all three dimeric receptors. PDGF-AB and PDGF-CC can activate dimeric receptors containing at least one PDGFRα monomer, while PDGF-DD those, containing at least one PDGFRβ monomer. By binding to PDGF receptors, PDGFs target a broad spectrum of mesoderm-derived cells, like fibroblasts, smooth muscle cells, pericytes, mesangial- and glia cells (131-135). Soluble form of both PDGFRα and -β are detected and compete with cell-associated PDGF receptors for ligand binding, antagonizing the effects of their membrane bound counterparts (136,137).

The extracellular parts of the PDGF receptors contain 5 Ig-like domains, of which domain 2 and 3 are responsible for ligand binding, while domain 4 stabilizes the dimer by a direct receptor-receptor interaction. The intracellular parts contain split tyrosine kinase domains (138). Ligand-induced dimerization of the receptors is followed by autophosphorylation, which activates their kinase activity and creates docking sites for SH2-domain-containing signaling molecules (139).

The PDGFs play crucial roles during development, and they are essential in wound healing and inflammation (140,141). Increased PDGF activity has been linked with several disorders and pathological conditions, such as atherosclerosis, fibrosis and malignant diseases (142,143). Most solid tumors secrete PDGF and express their receptors on tumor-, endothelial- or perivascular cells (144,145). Both overexpression, and different mutations of either the ligands or the receptors is associated with tumorigenesis (146-148). Moreover, all PDGF ligands are documented to be involved in the process of angiogenesis by activating signaling pathways triggering endothelial cell

proliferation (24-26). On the other hand, as pericytes and VSMCs express PDGFRβ, processes driven by this receptor, such as mural cell recruitment to capillaries stabilize the vasculature, thus inhibiting tumor cell extravasation and metastatization (149).

Due to the high structural similarities with VEGFRs - all have a split kinase domain - they induce similar signaling cascades. PI3K and PLC mobilizes Ca^{2+} from intracellular stores, regulating vascular permeability (150,151). The RAS/RAF/MEK pathway is implicated in the stimulation of cell proliferation, migration, and differentiation (152). By enhancing the serine/threonine kinase AKT/PKB pathway, it mediates antiapoptotic effects (153). PDGFRs are also involved in the activation of the JNK/SAPK pathway, thus regulating cell migration (154). Binding of PDGF isoforms to PDGF receptors, with the subsequent signalization is depicted in **Figure 7.**

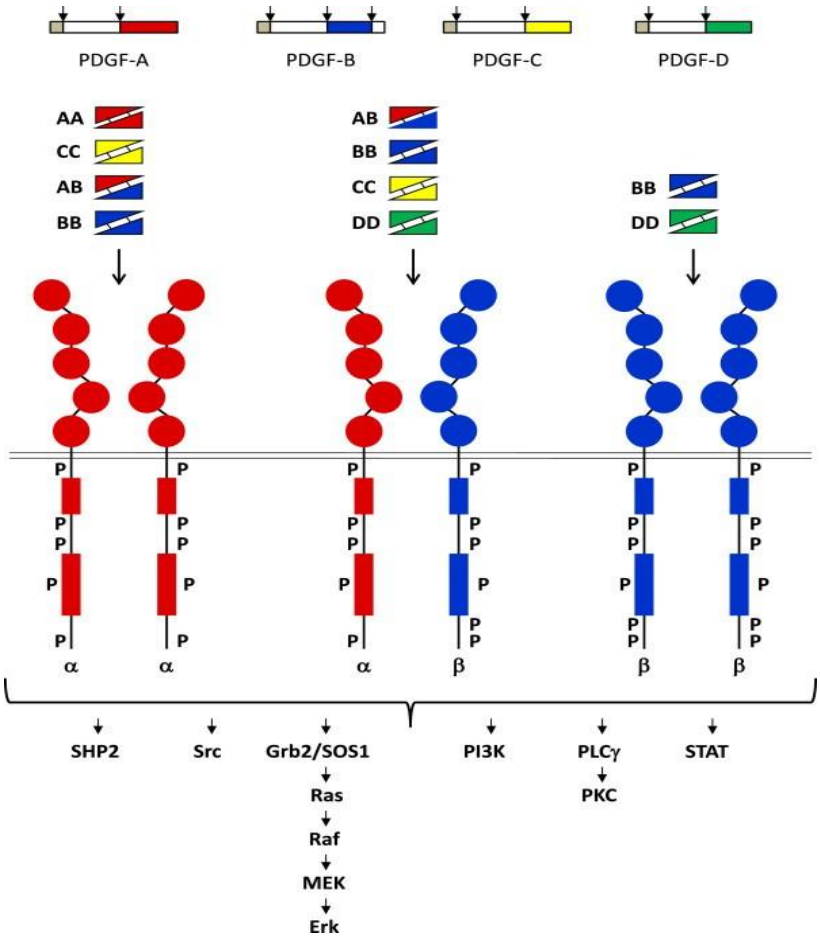

Figure 7. Binding of PDGF isoforms to PDGF receptors, and subsequent signalization (155).

3.2.1.3 FGFR family

The FGF family consists of 23 ligands, of which 18 can be secreted and bound to 4 high-afinity cell surface receptors, FGFR1-4 in mammals (156). Four FGFs do not bind

to FGF receptors, while one ligand is only expressed in mice (157). Despite most ligands act in an autocrine or paracrine manner, endocrine members of the family have also been identified (158). FGFs share a central core of 140 amino acids that is highly homologous between all family members (159,160). The ligands have strong affinity for the glycosaminoglycan side-chains of not only cell surface proteoglycans, but heparin sulphate proteoglycans and heparin-like glycosaminoglycans as well (161,162). They may protect ligands from degradation and stabilise the FGF ligand–receptor complex. A specific FGF ligand can bind to more FGFRs, although it may have a preference for a particular one (163). Ligands are produced in either epithelial or mesenchymal cells and usually activate receptors of the opposite tissue specificity.

The extracellular ligand-binding part of the receptors contains three immunoglobulin-like domains, which are important in receptor dimerisation. Different isoforms of FGFR1–3 are generated by alternative expression of the IgIII domain. Upon the presence of exon 8 or 9 they either express the "b or c" splice variant of domain III. Different isoforms are expressed in different tissues and have distinct binding specificities. FGFR4 has only one possible form (164). Truncated receptor splice variants coded by IgXa (X refers to the Ig domain being shortened by alternative splicing) are also secreted and may function as an inhibitor for FGFs (165). Structure and splicing of FGFRs are shown in **Figure 8.**

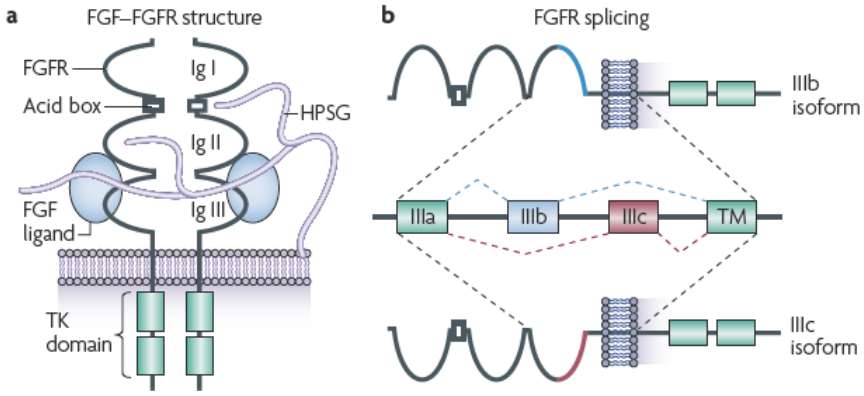

Figure 8. Structure (**A.**) and splicing (**B.**) of FGFR (166). The extracellular ligand-binding part of the receptors contain three immunoglobulin-like domains, which are important in receptor dimerisation. Different isoforms of FGFR1–3 are generated by alternative expression of the IgIII domain. Upon the presence of exon 8 or 9 they either express the "b or c" splice variant of domain III.

The FGFR signaling pathway plays a key role in embryonic development, wound healing and angiogenesis. Deregulated FGFR signalling contributes to pathological

conditions, including different malignancies. Both the receptors and the ligands are expressed by different tumor cell types (167-170). Beside translocation of FGFRs in hematological malignancies, amplification, overexpression, activating mutation or SNP of the receptors can also lead to tumorigenesis (156). Moreover, abnormalities of different FGFs are also linked to tumor progression (171,172).

Binding of bFGF (FGF2) to FGFR1IIIc is considered to be the major regulator of FGF induced angiogenesis, being the most intensively expressed both on ECs and smooth muscle cells (173). Thus it has also a diverse role, by triggering EC proliferation and stabilizing vessel walls.

Ligand binding leads to the activation of signaling cascades similar to the ones of VEGFRs and PDGFRs because of the resemblance of their kinase domain. Receptor dimerization results in the recruitment of adaptor proteins to activate RAS/RAF/MEK pathways, that regulate gene expression and cell proliferation (174). Recruitment of PI3K activates an AKT and mTOR dependent antiapoptotic pathway (175). Hydrolysis of phosphatidylinositol 4,5-bisphosphate (PIP2) by PLCγ triggers the release of intracellular Ca^{2+} (176), enhancing vascular permeability. The p38/MAPK cascade is responsible for the translocation of FGF1 to the nucleus (177), while activation of the JAK/STAT pathway, or the p70 S6 kinase also plays important roles in the regulation of FGFR signaling by mediating immunity, proliferation and apoptosis (178,179).

3.2.1.4 TIE receptor family

The family consists of two tyrosine kinase receptors, the TIE receptor 1 and 2 which can bind four ligands, Angiopoietin 1-4 (Ang1-4). The ligands are secreted glycoproteins, composed of an N-terminal superclustering domain, responsible for the creation of the higher order multimers of the ligands; a coiled-coil domain, responsible for ligand homo-oligomerization, which is essential for receptor activation and a C-terminal fibrinogen-like domain, responsible for receptor binding. The laters are separated by the linker region (180,181). The extracellular part of TIE1 and TIE2 consists of three Ig-like domains that are flanked by three EGF-like cysteine repeats followed by three fibronectin type III domains. The intracellular part has a split kinase domain. Ligands bind to the Ig- and EGF-like domains of the TIE receptors (182). The structure and binding of Angs and TIE receptors are shown in **Figure 9.**

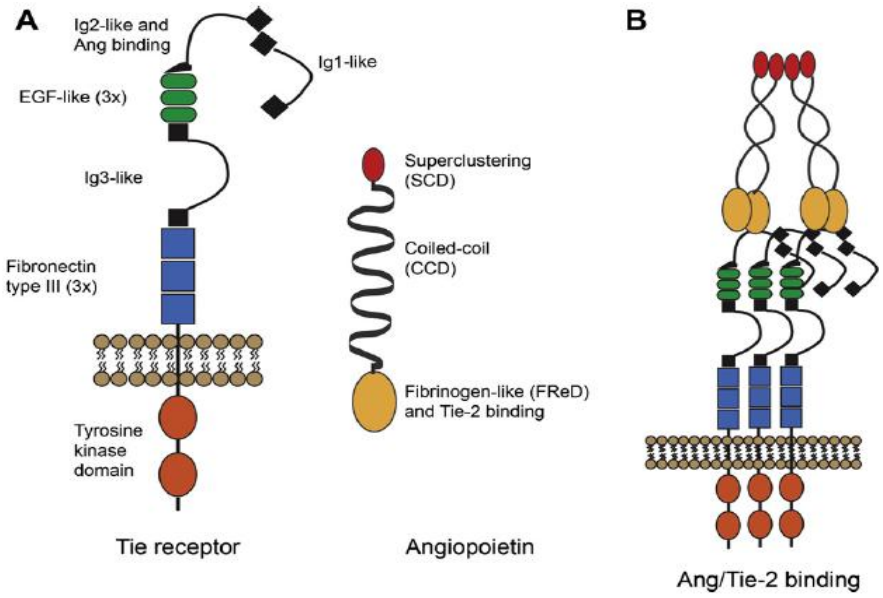

Figure 9. Structure (**A.**) and binding (**B.**) of TIE receptors and angiopoietins (183).

Ang1 is primarily secreted by mesenchymal cells, such as perivascular cells and fibroblasts, and acts in a paracrine manner on the endothelium (184,185). Ang2 is expressed by ECs (186) and retinal neurons (187). Following cytokine activation of the endothelium, it is rapidly released and acts in an autocrine manner on ECs (188). Ang1 and Ang2 bind to TIE2 with similar affinity (182). Ang1 acts as an agonist of the TIE2 receptor, activating EC survival, integrity and vessel maturation (189), whereas Ang2 is thought to be an antagonist, displacing the more active ligand Ang1. However, Ang2 has also been reported to induce receptor phosphorylation in a context-dependent manner (190). The molecular basis for these contradictory functions has not been unraveled. However, a number of factors have been implicated in controlling agonistic versus antagonistic functions (191,192). When functioning as a TIE2 antagonist, Ang2 enhances pericyte dissociation from the vessels and increases vascular permeability (193). In the absence of VEGF these unstable vessels die, but in the presence of VEGF they migrate or proliferate, depending on whether they are located at the sprouting tip or the stalk part of a newly forming blood vessel (194). Ang3 and -4 are counterparts of the same gene locus found in mouse and human, respectively, but with divergent functions. Moreover, while Ang3 is secreted by a number of mouse tissues, Ang4 is expressed to a high level only in the human lung (195).

The full length or proteolytically cleaved orphan receptor, TIE1 heterodimerize with TIE2 (196), and thus act as a co-receptor. Both TIE1 and -2 are expressed by

(lymph)endothelial cells (197,198), but TIE2 is present on hematopoietic cells and endothelial precursor cells as well (199,200). In addition to TIE receptors, angiopoietins have been found to bind integrins as well (201). Following context dependent binding of the ligands, the receptors are autophosphorylated, and intracellular signaling pathways are activated, mediating endothelial survival (202), migration, and permeability (203). Ang1 and TIE2 are shown to be essential in the recruitment of pericytes and their interaction with endothelial cells (204).

The Ang-TIE system plays a key role during vessel maturation, stabilization and remodeling, thus abnormalities of either member of the family results in diseases manifested in vascular malformations. Both Ang1 and Ang2 can be expressed by tumor cells and tumor endothelial cells (205). Despite pericyte coverage of the tumor vasculature is massively increased and thereby stabilized in response to Ang1 overexpression (206), the role of Ang1 in tumor-associated angiogenesis and metastasis remains controversial (207). Angiogenesis enhancing functions of Ang2 during VEGF or FGF induced angiogenesis has been demonstrated (208). On the other hand, an agonistic effect of Ang2 on TIE2 has also been documented (190). Furthermore, both TIE1 and -2 are present on both tumor cells and tumor ECs (209), and their expression is upregulated during angiogenesis (210,211). These findings suggest that tumor growth promoting or inhibiting functions of angiopoietins are possibly dependent on the tumor cell type and the balance between both angiopoietins and TIE1/TIE2 (190).

3.2.1.5 TGFβR family

The TGFβR family includes TGFβ ligands: TGF-β1-3, bone morphogenic proteins (BMPs), growth and differentiation factors (GDFs), activins, inhibins, leftys, nodal and the mullerian inhibitory substance (MIS). Ligands can be secreted by tumor or a number of stromal cells (212). The receptors of the superfamily include the Type I receptors: Alk (activin receptor-like kinase) receptors, and Type II receptors: TGFβ RII, BMP RII, Act RII (activin type II receptor) and RIIB, and MIS RII. Co-receptors of the family include TGFβRIII/betaglycan, endoglin, BAMBI (BMP and activin membrane-bound inhibitor homologue) Crypto and Cryptic (213).

TGFβ and its receptor, TGFβR are key molecules in cancer development and progression. On one hand, TGFβ can inhibit tumorigenesis by suppressing cell cycle

progression and stimulating apoptosis in early stages of cancer (214). On the other hand, it can also promote cancer development and spreading by the suppression of anti-tumor immunity (215), modulation of cell invasion via modification of the microenvironment (216), induction of epithelial-mesenchymal transition (217) and degradation of the extracellular matrix (ECM) (218).

ECM and basement membrane (BM) degradation is a critical step in tumor invasion and metastasis. TGFβ plays an important role in ECM degradation via upregulating MMP2 expression in different tumor types (219), and facilitates tumor cell infiltration by degrading basement membrane components via the regulation of protease expression (220). TGFβ also plays a crucial role in angiogenesis by promoting endothelial cell proliferation and migration through signalling via ALK1 and by causing vessel maturation through ALK5 (41). Highly expressed ligands of the other family members, such as endoglin, can antagonize the inhibitory effects of TGFβ and contribute to proliferation, migration, and capillary formation of endothelial cells (218).

3.2.1.6 Notch receptor family

Four receptors (Notch1-4), and five ligands, Jagged 1-2 and delta-like ligand (DLL) 1, 3-4 of the Notch family have been described in mammals. The receptors and the ligands are both type I transmembrane proteins, and activation requires contact of the sender and the receiver cell. The activation of Notch signaling involves three proteolytic events, resulting in the release of Notch intracellular domain (NICD) into the cytoplasm and from there it translocates to the nucleus (221). With the binding of NICD, the CSL family is converted into a transcriptional activator by displacing corepressors and by recruiting coactivators to induce transcription of Notch target genes (222).

Notch signaling plays an important role in cell proliferation, survival, apoptosis and differentiation, as their targets include proteins and factors involved in the control of cell cycle and survival (p21, cyclin D3), transcription factors (c-MYC, NF-κB), growth factor receptors (HER/ErbB, IGF1-R) and regulators of apoptosis (survivin) (223-229). Recently, non-canonical Notch signaling that does not involve CSL or require cleavage has also been identified. This induces development via interaction with other molecules, such as members of the the IL6/JAK/STAT-, the Wnt pathway, the uPA/uPAR axis or BCR-ABL (230-233). Activation of target genes via Notch is shown in **Figure 10.**

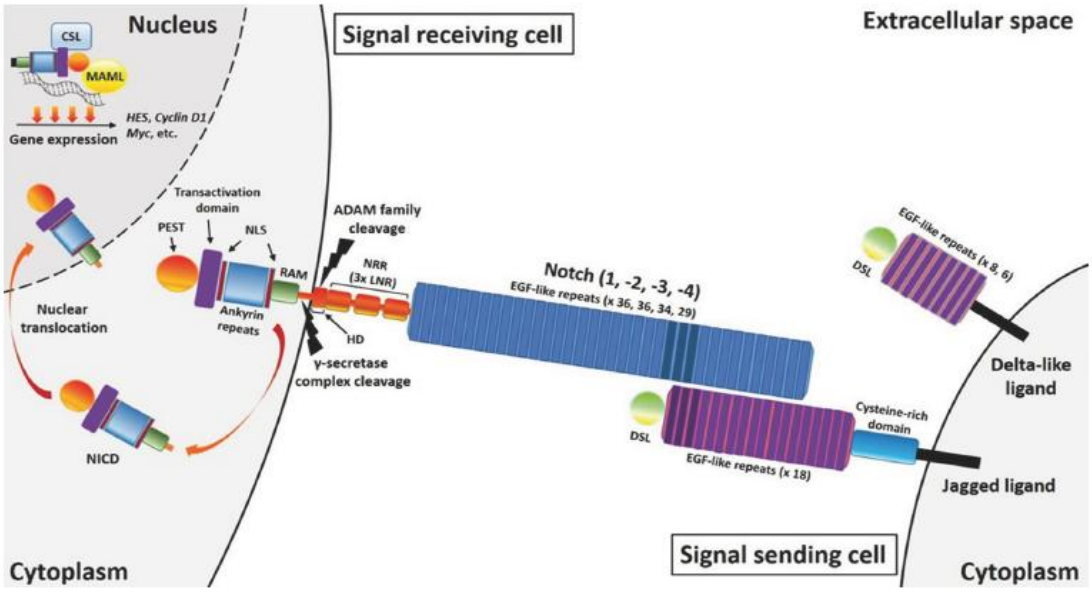

Figure 10. Activation of the Notch signaling pathway (234). Three proteolytic events result in the release of NICD into the cytoplasm and from there it translocates to the nucleus. With the binding of NICD, the CSL family is converted into a transcriptional activator to facilitate transcription of Notch target genes.

Although classically known for its role in embryonic development, the Notch pathway have been shown to mediate tumorigenesis (235) by regulating the formation of cancer stem cells (236), and epithelial- or endothelial-mesenchymal transition (237,238). Aberrant activation of Notch signaling is implicated in various neoplastic processes. Somatic gain-of-function mutations in Notch receptors have been identified first in T-cell acute lymphoblastic leukemia and later in other malignancies as well (239).

Functional studies have demonstrated the key role of Notch signaling in vascular development and postnatal angiogenesis (240), which is emphasized by the involvement of both ligands and receptors in vascular diseases. The cerebral autosomal dominant arteriopathy with subcortical infarcts and leukoencephalopathy (CADASIL) and the Alagille syndrome can be traced back to mutations in Notch3 and Jagged1, respectively (241,242). In the endothelium, as well as in VSMCs, both Notch receptors and ligands are highly expressed (243-250). DLL4 is generally considered as a marker of arterial and tip cell phenotype (244), moreover, it is more robustly expressed in tumor ECs, compared to the neighburing normal vessels (251). Thus it is the main ligand expressed in tumor neoangiogenesis (252).

The “tip” cell is located on the leading edge of an angiogenic sprout. It is highly migratory because of the presence of filopodia and expresses high levels of VEGFR2

and -3 (253,254). Stalk cells are located adjacent to the tip cell, extend fewer filopodia but form lumen, and proliferate to support sprout elongation. The sprouting process is maintained until proangiogenic signals decrease, and quiescence is reestablished (255). It has been proposed that in response to VEGF, DLL4 is induced on tip cells. High DLL4 expression on tip cells lead and guide new sprouts, and is thought to activate Notch and suppress the tip phenotype on adjacent (stalk) ECs. As a result, Notch activity is high in stalk cells but low in tip cells, and a VEGF feedback loop is activated, whereby Notch activation causes reduction of VEGFR2 and VEGFR3 and induction of VEGFR1 on stalk cells. The absence of Notch signaling in the tip cells results in high VEGFR2 and VEGFR3 expression, causing enhanced sensitivity to external VEGF, while decreased VEGF receptor expression on the stalk cells limit sprouting and ensures the proper number of tip cells at the angiogenic front (254,256-258). Inactivation of DLL4-Notch leads to the formation of a highly branched and dense vascular network with excessive filopodia. Moreover, these vessels are often not fully lumenized, thus are unable to deliver the necessary amount of oxygen and nutrients to the tissue (252). In contrast, upregulation of DLL4 inhibits VEGF-induced endothelial cell proliferation (259) and downregulates VEGFR2 expression (260).

3.2.2 Mechanisms of tumor-induced angiogenesis

3.2.2.1 Sprouting angiogenesis

The first identified form of angiogenesis is endothelial sprouting. It was originally described by Ausprunk and Folkmann in 1977. According to their hypothesis, in response to the NO mediated VEGF signal, the postcapillary venules become dilatated, cell-cell interactions get lost, the basement membrane (BM) degrades, and thus the vessel becomes fenestrated. Endothelial cells lose their polarity and migrate to the connective tissue. Then a tube is formed from the ECs, which is followed by lumen formation, synthetization of a new BM and recruitment of pericytes (261). This hypothesis has been developed further by Paku and Paweletz in 1991. According to their model, in response to Ang2, tumor cells secrete MMPs and plasminogen activators, which digest the pericytes on the vessel wall. Consequently, the electron density of the mother vessel is changed. A gel-sol transition occurs in the BM, this is maintained by MMP2, which binds $\alpha_v\beta_3$ integrin. Growth factors are liberated from the

BM, such as bFGF and VEGF, thus inducing migration of ECs with a maintained polarity, lumen and except from tip cells, a maintained BM. As the sprouts grow the BM on the tip is continuously synthesized, pericytes are recruited in response to bFGF and PDGF and the interaction between ECs and mural cells is stabilized by TGF-β1 and Ang1 (262). This hypothesis provides explanations missing from the former model of Ausprunk and Folkmann. These include the losening and then regaining ECs polarity, the fact that there is de- and redifferentiation in the same process and that the lumen is formed before the synthesis of the BM, although formation of BM is known to be the facilitator for lumen formation.

3.2.2.2 Vessel incorporation or co-option

In 1987 WD Thompson raised the possibility that tumors acquire their vasculature by vessel incorporation, instead of vessel ingrowth (263). This theory was proven by Josephine Holash in 1999 (264,265). Angiogenesis by vessel incorporation usually occurs,when tumors grow or metastatize into well vascularized tissues, such as lung, liver or skin. Tumor cells grow along the preexisting, well developed vessels of the host tissue, thus annexing its vasculature. The process is faster than sprouting angiogenesis, as it does not require EC proliferation. Moreover, on the periphery of the tumor these vessels provide surface for sprouting angiogenesis. Meanwhile, in response to the locally predominant antiangiogenic factors, ECs can undergo apoptosis in the centre. This in one hand causes necrosis of the tumor mass, but on the other hand it also triggers the extravasation and metastatization of tumor cells. Maintenance of incorporated vessels is secured by the interaction of Ang1-TIE2.

3.2.2.3 Intussusceptive microvascular growth

Intussusceptive microvascular growth was first described by Sybill Patan in 1996 in a human colon adenocarcinoma model (266). This type of vessel growth is characterized by the incorporation of peritumoral capillaries, which are then separeted by connective tissue pillars. The original model of Caduff has been redrawn by Paku and his collegues in 2011. After the formation of an intraluminal endothelial bridge the BM is locally degraded, thus the EC can attach to a collagene bundle from the underlying collagene layer. The actin cytoskeleton of the EC exerts pulling force to the collagene bundle,

which in turn is transported through the vessel lumen. Finally, connective tissue cells are immigrated to the pillars and new collagenous connective tissue is deposited (267), thus the process results in lots of vessels with big lumens, providing surface for EC sprouting. In the absence of EC proliferation, the process is faster than sprouting and does not involve permeability of the vessel wall. This suggests and some experimental data also supports, that intussusception does not rely on VEGF signalization, but instead is regulated by physiologic stimuli and cytokines, that lead to vessel maturation, such as bFGF (268), PDGF-BB (269), Ang1-TIE2 complex (270), ephrin-ephrin receptor (271). However, the role of VEGF in the process is still contested (269,272,273).

Moreover, it is also shown, that in response to some antiangiogenic treatment, such as vatalanib or the mTOR inhibitor sirolimus, experimental tumors switch from endothelial sprouting to intussusceptive angiogenesis (274,275).

3.2.2.4 Glomeruloid angiogenesis

In 1992 Hauro Ohtani described coiled vascular structures in human gastrointestinal carcinoma. As they resemble renal glomeruli, they were called glomeruloid structures (276). These are characterized by many, tightly associated capillary loops with different thickness of BMs. The molecular mechanism behind the process is still not clear. On one hand, Sundberg et al. suggests that VEGF is a key mediator of inducing glomeruloid body formation and maintaining these vessels (277). On the other hand, it was also shown that the glomeruloid structure is created by proliferating and migrating tumor cells, which pull the capillaries and their branching points into the tumor cell nests. Thus, this type of vascular growth cannot be termed as true angiogenesis, but rather a reorganization of tumor blood vessels, which does not require EC proliferation (278). Moreover, these vessels seem to be able to provide enough oxygen and nutrients to the cells, as no necrosis was observed in tumors developing them. As a result, glomeruloid bodies are not only diagnostic markers of glioblastoma, but also poor prognostic factors in many cancer types (279).

3.2.2.5 Postnatal vasculogenesis

Postnatal vasculogenesis refers to the process, in which bone marrow derived VEGFR2+, TIE2+, AC133+, CD34+ endothelial progenitor cells (EPCs) incorporate

into the EC layer of the tumor capillary network in response to tumor derived VEGF (280) and other proangiogenic factors. After incorporation into the EC layer, EPCs are differentiated to mature ECs. Thereafter, by producing pro-angiogenic factors, such as VEGF and PlGF, they mediate the attraction of additional EPCs to the tumor vasculature. VEGF mobilizes these cells from the bone marrow via the stromal derived factor (SDF) and its receptor, CXCR4. The process of postnatal vasculogenesis was described by Takayuki Asahara and his group both in physiologic and pathologic conditions at the end of the 1990s (281).

3.2.2.6 Vessel-like structures, formed by tumor cells

It has been shown, that not only ECs, but aggressive tumor cells can also form vessel-like structures, which facilitate tumor perfusion.

In 1941 Béla Kellner described tumor sinusoids in soft tissue sarcomas (282). These are lumens, which are covered exclusively by tumor cells, and are responsible for the transport of blood cells within the tissue.

It is also possible that tumor cells form a lumen together with ECs, without expressing endothelial or embrional markers. These structures are called mosaic vessels and were also first described in the 1940s (283). The genesis of these types of vessels is still not well understood. They are considered to be formed either by the apoptosis of incorporated ECs, which is followed by the occupacy of the lumen or invasion of the vessel by tumor cells. The process is thus thought to be mediated via Ang2 signalling.

Vasculogenic mimicry refers to the process, when tumor cells express differential markers to completely resemble BM covered ECs. The process was first described by the group of Mary J Hendrix in uveal melanoma, where highly agressive melanoma cells formed vessel-like channels and upregulated endothelial genes and genes involved in microvascular channel formation. Meanwhile, these cells downregulate classical melanoma markers. None of the main angiogenic cytokines, such as VEGF, PDGF, bFGF, TGF-β, Ang, Notch, TNF-α seem to induce the formation of these channels (284).

Different types of vascularization mechanisms in cancer are shown in **Figure 11.**

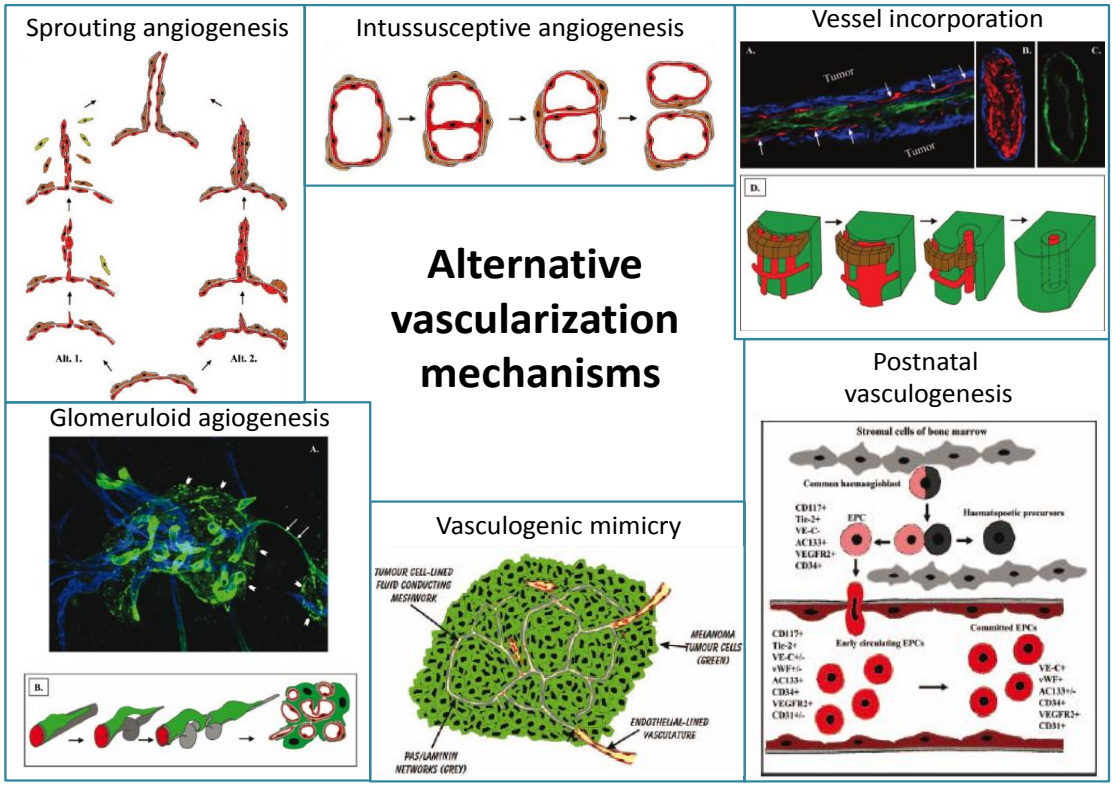

Figure 11. Alternative vascularization mechanisms in cancer (285).

3.2.3 Characteristics of tumor blood vessels

Because of the dominance of proangiogenic factors in malignant tissues, tumor blood vessels differ from the normal ones both in function and structure. In a healthy adult, ECs have a long half-life with a well differentiated BM (286), which is stabilized by pericytes and VSMCs, to influence permeability and contractility of the vessel wall. (287). Moreover, they secrete a minor amount of survival factors for the ECs, such as VEGF and Ang1. In case of Ang2 and MMP effect pericytes and VSMCs get detached from the BM and after their apoptosis, ECs also get prepared for cell death (288). In a healthy adult the endothelial tube is connected with cell-cell junctions. Maintenance of the vessel is supported by autocrin factors and signals launched by the oxygen sensors, such as the PHD2, which secures the appropriate blood flow (289).

In contrast, tumor blood vessels usually have deficient pericyte and VSMC coverage, which are not tightly attached to the ECs. They are often immature, less contractile and their shape is abnormal (290,291). The BM is often degraded and loosely attached to the EC, or it is thick and thus hinder contraction and perfusion (292). The morphology of ECs are changed and cell-cell connections are often lost (293). As a result, vessels get

dilated negatively impacting the ratio of vessel surface, which supplies the tumor tissue with oxygen and nutrients. Tumor cells can press in the instable vessel wall, thus vessel diameter becomes uneven (294). Because of this and the altered EC morphology, vessels get curved and form serpentine-like structures, and may also create high amount of anastomosis within the vessel wall (291). This is further supported by the impaired cell junctions, resulting in the loss of the signals of oxygen sensors, eventually leading to abnormal flow in the tumor vasculature (295). Because of the degraded BM, ECs lose their polarity, thus get detached from the endothelial layer and may form a plug in the lumen resulting in thrombosis and further injury of the vessel wall. This leads to enhanced metastatization capacity and the creation of mosaic blood vessels (296). Moreover, degraded mural cells and BM leads to fenestrated vessel walls, and thus not only metastatizing tumor cells may intravasate to the lumen (297), but vessels get hyperpermeabilized as well, causing an increase in the interstitial fluid pressure, which cannot be restored because of the decreased lymphatic function (298,299). Thus, the oxygen supply of the tumor decreases, resulting in an increased glycolitic activity to provide energy and the necessary building material for the growing tumor (300). The altered acidic microenvironment and abnormal morphology of tumor vessels increase the invasion and metastatization ability of malignus cells, creating a vicious circle in tumor progression. This microenvironment selects for hypoxia resistant, aggressive tumor cells (301). Because of the high intratumoral pressure, intersticial fluid, often containing tumor cells may infiltrate to lymphatic vessels, thus enhancing lymphatic tumor spread (302). Furthermore, some immune cells also promote invasion in these circumstances (303). Unlike in tumors, in case of physiological angiogenesis, these processes are balanced by the generation of antiangiogenic factors. Moreover, as a result of the inadequate blood flow, the resulting hypoxia and/or the tightened BM, efficacy of conventional anticancer therapies are inadequate due to limited penetration.

These abnormalities of tumor blood vessels and the resulting aggressiveness of cancers, accompanied by decreased efficacy of conventional treatment led Rakes Jain to the elaboration of the vessel normalization theory (304). Accordingly, the inhibition of the signal of proangiogenic factors and the subsequent normalization of tumor blood vessels has become a critical step in cancer therapy. Proposed structures of normal, tumorous, normalized and inadequate blood vessels are shown in **Figure 12**.

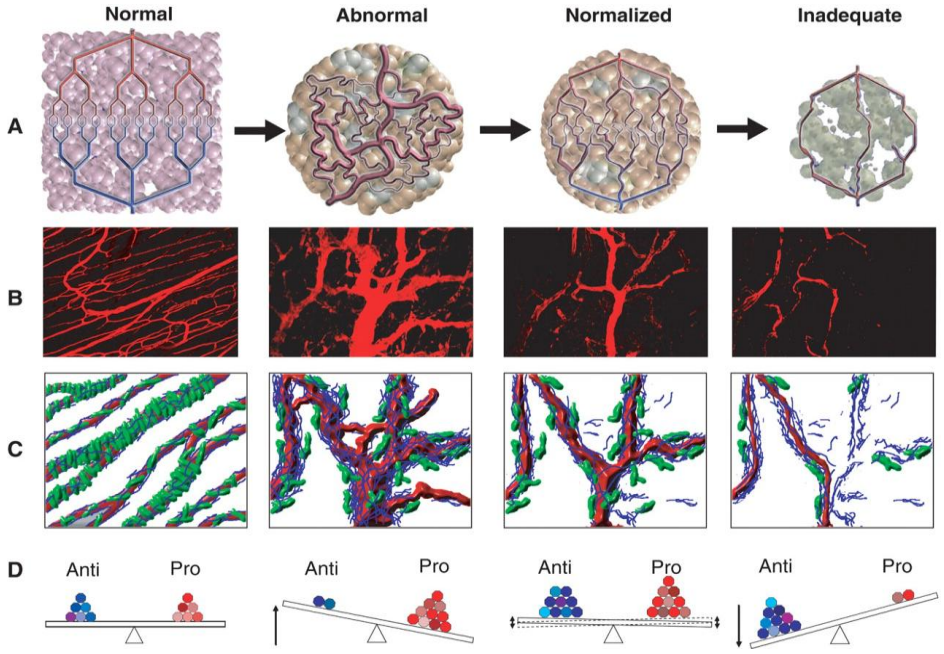

Figure 12. Proposed structures of normal, tumorous, normalized and inadequate blood vessels. (A.) Schematic structures of the vascular system. (B.) Two-photon images of normal blood vessels in skeletal muscle and subsequent images showing human colon carcinoma vasculature in mice at day 0, day 3, and day 5 after administration of VEGFR2-specific antibody. (C.) Diagrams depicting the changes in pericyte (green) and basement membrane (blue) coverage. (D.) Changes in the balance of pro-, and antiangiogenic factors in the tissue (305).

3.2.4 Inhibition of the tumor vasculature

In the complex processes outlined above, several differently acting agents are capable of blocking the blood supply of a tumor. It can be suppressed in distinct cells and also in diverse levels and modes.

3.2.4.1 Conventional chemotherapeutic agents

Conventional therapeutic agents have been found to have antiangiogenic functions as "side effect". These include microtubule targeting agents, such as Vinca-alkaloids or Taxanes, that block endothelial cell proliferation (306). Beside other drugs, thalidomide and lenalidomide also have complex antiangiogenic functions (307,308).

3.2.4.2 Vacular disrupting agents

Vascular disrupting agents (VDAs) selectively target tumor vessels, causing fast and dynamic effects (309). They destroy rapidly dividing endothelial cells in the tumor

tissue by targeting the colchicine binding site of tubulins (tubulin-binding agents) (310) or induce vascular collapse through TNF-α (flavonoid-type VDAs) (311). As a result, vascular supply shuts down, causing necrotization in response to the insufficient oxygen and nutrient delivery (312,313). By this strategy both preexisting and newly formed vessels can be targeted, with the inhibition of the metastatic potential as well. VDAs mostly act on advanced tumors, which are resistant for conventional therapy. However, their effect is very short, and can cause serious cardial toxicities (314). Moreover, vessel density is higher at the edge of tumors, so targeting it with VDAs is not effective enough. Consequently, often there is no visible tumor shrinkage following VDA therapy. Furthermore, as tumors can also be fed by diffusion from nearby tissues, the monotherapy can leave a surviving rim at the edge of the tumor, which allows rapid tumor regrowth (315). Combretastatin A-4 Phosphate (CA4P), 5,6 dimethylxanthenone-4-acetic acid (DMXAA) and NPI-2358 are the most investigated VDAs.

3.2.4.3 Vasoactive agents

Vasoactive agents also combinatorially block existing vessels and suppress the formation of new ones. Moreover, they do not target preferentially the larger vessels in the tumor center, but also the small ones in the periphery, causing hyperabnormalization and hyperpermeability of the vessels. This allows chemotherapeutic agents better access to the tumor. However, these drugs are highly toxic when administered systemically, thus local, small dose and metronomic application is preferable.

The most often used vasoactive agents are inflammatory modulators. Among them the most important are the followings:

IL-2, a cytokine, that induces T cells, augments natural killer cell activity and demonstrates vasopermeability activity (316).

TNF-α, an inflammatory cytokine, that is principally produced by activated macrophages and monocytes and has direct effects on tumor cells. After exposure to low-dose TNF-α, hyperpermeability, hemorrhagic necrosis, extravasation of erythrocytes, edema and vessel congestion were observed (317), leading to an increased intratumoral chemotherapeutic drug concentration or effect of radiation (318). In the clinic combination therapy of melphalan and TNF-α is a popular approach to treat patients with unresectable advanced sarcoma and advanced melanoma (319).

Histamine is an inflammatory modulator that causes edema in small vessels by locally increasing the lymph flow into the extracellular space and by promoting hyperpermeability of the endothelium (320).

3.2.4.4 Angiogenesis inhibitors

Angiogenesis inhibitors (AIs) block the formation of new vessels from preexisting ones, but do not affect already established vasculature. Despite the fact that they are used in advanced tumors in the clinic, they are tought to mainly act on small vessels of the tumor edge, mostly at the early stage of tumorigenesis or metastatization.

As discussed above, endothelial sprouting is activated in physiological angiogenesis in response to hypoxia, thus, suppression of HIF1 to bind to the HRE of proangiogenic molecules is one of the main options to block the process. In the absence of selective HIF inhibitors (321) and the presence of a number of factors that also regulate angiogenic growth factor expression in tumors, the common way is to target molecules downstream of HIF by the blockade of receptor - ligand communication.

Growth factors can be targeted with either monoclonal antibodies (mABs) or soluble „trap/decoy" receptors. mABs are produced from a common germ cell and have affinity for a specific antigen, thus inhibiting their binding to the corresponding receptors (322). Although having just one target, their effectiveness may be broad, as angiogenic growth factors usually bind to a number of isoforms of their target receptors. mABs are usually given intravenously, and because of their high molecular weight, their half-life is long (weeks). The resulting more prolonged inhibition allows less frequent dosing. The high molecular weight of mABs reduces diffusional capacity, thus renal filtration is limited, but their penetration into the brain is also impeded. Antiangiogenic antibodies as single agents exhibit only limited clinical activity, thus they are usually applied in combination that significantly improves their therapeutic effect.

Decoy receptors are soluble proteins that compete with their membrane bound counterparts with high affinity for their ligands. In the absence of transmembrane and intracellular domains, they fail to mediate signal, thus function as a trap for angiogenic growth factors (323). These traps can either be physiologically present, as a result of proteolytic cleavage of their transmembrane counterparts (eg. soluble VEGFR1), or designed and added as external therapy (324,325).

Receptors on ECs can be targeted at their extracellular part by mABs, thus blocking ligand binding, or by RTKIs at the tyrosine kinase domain, which serve as a docking site for molecules mediating the angiogenic signal (326,327). Anti-receptor mABs can usually target only one of the receptors, thus do not mediate widespread effect.

RTKIs can be divided to five subgroups:

- Type I kinase inhibitors recognize the active conformation of the receptor. They typically consist of a heterocyclic ring system that occupies the purine binding site of the enzyme, and form one to three hydrogen bonds by that part of the inhibitor, which mimick the purine ring of the adenine moiety, thus actively competing with ATP. Extra interactions may also be formed at hydrophobic regions adjacent to the hinge region. The hydrophilic region of the enzyme can be exploited for maximizing the solubility of the compounds. Since the targeted ATP pocket is conserved through the kinome, Type I inhibitors usually have low kinase selectivity, thereby enhancing the potential for off-target side effects. Examples of type I tyrosine kinase inhibitors targeting the VEGF pathway are sunitinib and pazopanib.
- Type II inhibitors recognize the inactive, unphosphorilated conformation of the kinase and indirectly compete with ATP by occupying the hydrophobic pocket, which is created by the DFG-out conformation of the activation loop. It is also known as the allosteric site, thus type II inhibitors can modulate kinase activity in an allosteric way. The DFG-out conformation is unique to all receptors, thus the hydrophobic interactions with the DFG pocket confer a high degree of selectivity. Some type II inhibitors are able to form a hydrogen bond directly to the ATP-binding site, but this is not necessary for their functionality. Sorafenib is a type II kinase inhibitor (328).
- Type III or allosteric inhibitors bind outside the catalytic domain of the kinase, in regions that are involved in the regulatory activity of the enzyme. They block the binding of ATP by modulating the conformation of the receptor. As they exploit the binding sites and regulatory mechanisms that are unique to the target, a high degree of kinase selectivity is exhibited. Additionally, allosteric modulators can provide delicate regulation of kinases, which is not easily performed with ATP-competitors.
- Type IV kinase inhibitors also act allosterically by forming a reversible interaction outside the ATP binding pocket, in the kinase substrate binding site, thus are not

competing with ATP. Since this area is unique for the substrate, it also ensures high degree of selectivity.

- The fifth class of kinase inhibitors are known as ‘covalent’ inhibitors. These bind covalently to cysteines proximal to the ATP binding site. Sulfur, an electron-rich atom is present in the cysteine residue, and reacts with the electrophilic groups of the inhibitor. As a result, by sharing electrons, they bind irreversibly, thus allowing the inhibitor to prevent the binding of ATP. The cysteine residue, and thus the binding site of the inhibitor can be variably located in the kinase domain. Examples of covalent tyrosine kinase inhibitors are quinazoline-based inhibitors (329) such as vandetanib.

Most small-molecule kinase inhibitors developed to date compete with ATP, thus target (nearby) the ATP-binding site. This region is common to all RTKs, thus selectivity is ensured by the region of the inhibitor, which is not similar to the structure of ATP.

In contrast to the mABs, RTKIs are much smaller, which on one hand may result in penetration to the brain, but also in decreased stability. The subsequent shorter half-life (hours) makes daily dosing necessary. Fortunately oral application is possible, which allows more comfort for the patient. However, absorption is often influenced by food and concomitant medications. Interactions in absorption and broad metabolism of RTKIs may be responsible for their limited activity or increased toxicity.

The toxic effects of antiangiogenic RTKIs can in part be attributed to their lack of selectivity. However, selective inhibitors may also induce toxicities, because their target kinases are not exclusively expressed by endothelial cells. As discussed above, although normal vasculature remains quiescent during adulthood, growth factor signaling in normal endothelial cells is still important for their survival and the maintenance of vascular integrity. Moreover, as specific kinases are involved in the normal physiology of organs like kidneys and the thyroid gland, specific toxicities, such as nephrotic syndrome might be related to the interference of RTKIs with the normal function of these organs (330). Furthermore, bleeding and wound healing abnormalities may be caused by the disturbance of the close interaction of PDGFR, FGFR and fibroblasts (331). In line with that, most common toxicities of antiangiogenic tyrosine kinase inhibitor therapy include hypertension, bleeding, fatigue, diarrhea, nausea, vomiting, hand-foot syndrome, and myelosuppression (332).

In order to enhance their effect, antiangiogenic agents can be combined, resulting in either vertical or horizontal blockade. Horizontal combinations have targets at the same level of the pathway, like different growth factors or different RTKs. Vertical combination, for example blocking the ligand and its receptor simultaneously leads to more effective suppression of a given pathway (333).

Because of the structural similarities of the main angiogenic RTKs (VEGFRs, PDGFRs and FGFRs), they activate overlapping signaling cascades. As a result, most antiangiogenic RTKIs block more than one isoforms of these receptors, (albeit with different affinity), thus horizontal blockade can be achieved by using them alone (multi-target RTKIs). This makes tumors less prone to swich from one driver angiogenic molecule to another, and may result in enhanced tumor growth inhibition (334). Moreover, the target receptors of antiangiogenic RTKIs are often expressed not only by endothelial-, but tumor cells as well, exhibiting direct antitumor properties beside the blockade of the vasculature. On the other hand, inhibition of PDGFR and FGFR signaling and the subsequent loss of mural cell function can also result in vascular destabilization and enhanced tumor leakiness, which may support metastatization (335). Furthermore, simultanous receptor blockade may lead to increased toxicity (336).

Antiangiogenic agents approved for the treatment of cancer are shown in **Table 1**.

Table 1. Antiangiogenic agents approved for the treatment of cancer. Target status defined as half maximal inhibitory concentration (IC50)<1000 nM. Approval of FDA, if not, labelled.

Name	**Target receptor/Type**	**Developer**	**Indication**
mAB			
Bevacizumab (Avastin)	Recombinant humanized anti-VEGF mAB (337)	Genentech	Metastatic colorectal cancer (CRC); metastatic non-small cell lung cancer (NSCLC); progressive glioblastoma; metastatic renal cell carcinoma (RCC); metastatic cervical cancer; platinum resistant ovarian, fallopian tube, or

			primary peritoneal cancer
Ramucirumab (Cyramza, IMC-1121B)	Full human Anti-VEGFR2 mAB (338)	ImClone Systems Inc.	Metastatic CRC; metastatic NSCLC; advanced gastric or gastroesophageal junction adenocarcinoma
RTKI			
Axitinib (Inlyta, AG013736)	VEGFR1-3, PDGFRα, -β, c-KIT, FLT3, CSF-1R (339)	Pfizer	Advanced RCC
Cabozantinib (Cabometyx, XL184, BMS907351)	VEGFR1-3, PDGFRβ, TIE2, c-MET, KIT, FLT3, AXL, RON (340)	Exelixis	Advanced RCC
Nintedanib (Vargatef, BIBF1120)	VEGFR1-3, PDGFRα, -β, FGFR1-4, IGF1R, insuline receptor, FLT3, LCK, Src, LYN (341)	Boehringer Ingelheim	Advanced lung adenocarcinoma (EMEA)
Pazopanib (Votrient, GW786034B)	VEGFR1-3, PDGFRα, -β, FGFR1, -3-4, c-KIT, c-FMS, LCK, ITK, FAK (342)	GlaxoSmith Kline	Advanced soft tissue sarcoma; advanced RCC
Regorafenib (Stivarga, BAY 73-4506)	VEGFR1-3, PDGFRβ, FGFR1, TIE2, BRAF, BRAF (V600E), RAF-1, RET, KIT (343)	Bayer	Advanced gastrointestinal stromal tumor (GIST); metastatic CRC
Sorafenib (Nexavar, BAY 43-	VEGFR2-3, PDGFRβ, FGFR1, EGFR, HER2,	Bayer	Advanced RCC; unresectable hepatocellular carcinoma; progressive differentiated

9006)	BRAF, BRAF (V599E), RAF-1, IGF1R, FLT3, C-KIT, ERK1, MEK1 (344)		thyroid carcinoma
Sunitinib (Sutent, SU11248)	VEGFR2, PDGFRβ, FGFR1, EGFR, FLT3, Kit (345)	Pfizer	progressive well differentiated pancreatic neuroendocrine tumors (pNET); metastatic RCC; GIST after disease progression, or intolerance to imatinib mesylate
Vandetanib (Caprelsa, ZD6474)	VEGFR2-3, EGFR (346)	AstraZeneca	Advanced thyroid cancer
Trap receptor			
(Ziv-) Aflibercept (Zaltrap, AVE0005)	Recombinant fusion protein of the extracellular domains of human VEGFR1 - 2 (347)	Sanofi and Regeneron	Metastatic CRC

The role of VEGF and its receptor as an important factor in the vascularization, metastatization and proliferation of human colorectal cancer was already postulated in the mid-1990s (348). The first drug inhibiting the VEGF-VEGFR axis in colorectal cancer (CRC), bevacizumab was approved in 2004 (349). The other antiangiogenic mAB, ramucirumab was just approved in 2015 (350). Ziv-Aflibercept was approved by the FDA in 2012 (351). Beside the spread of antiangiogenic RTKIs in the clinic, regorafenib, a dual VEGFR2-TIE2 blocking drug is the only antivascular RTKI, being used for the treatment of CRC since 2012 (352). All other classical VEGFR inhibitors have failed to demonstrate unequivocal benefit in this patient population.

3.2.5 Resistance to antiangiogenic tyrosine kinase inhibitor therapy

Initially, no resistance to antiangiogenic tyrosine kinase inhibitors was expected, because they target genetically stable ECs and therefore unlikely to develop mutations. In spite of that, drug resistance in patients treated with antiangiogenic therapies is an important clinical problem. Both primary (no initial response is shown to therapy) and secondary (after a short regression period, the tumor recovers) resistances have been documented. The following mechanisms are considered to explain the phenomenon:

Although VEGF signaling is the predominant stimulator of angiogenesis, as seen above, several other pathways are involved in the promotion of neovascularization. Thus, inhibition of VEGFR-mediated pathways may not be sufficient to completely inhibit vessel growth. Activation of alternative angiogenic pathways may circumvent inhibition by antiangiogenic tyrosine kinase inhibitors (353).

In line with that, as discussed above, VEGF signalization does not drive all forms of angiogenesis, and thus by activating alternative vascularization mechanisms, vascular development can be achieved in spite of effective VEGFR inhibition.

Resistance to kinase inhibitors can also result from a mutation in the target site of the receptor even on endothelial cells, although resistance is less likely to arise if multiple receptors are being targeted at the same time. Moreover, multi-target inhibitors mostly hit the ATP binding site, thus they are less precisely linked to their target receptor and for that reason, are less sensitive for dislodging due to a mutation of the target kinase. In spite of that, several studies reported mutations in target kinases recently that correlate with resistance to antiangiogenic RTKIs (354,355).

Decreased vessel number is accompanied by hypoxia as a result of antiangiogenic therapy, but hypoxia may select for more resistant tumor cells, thus increasing tumor aggressiveness and invasion (356).

The metastatization potential might also be enhanced by the loss of tumor vessel integrity, because of thrombic events (357) or the decreased number of pericytes as a result of PDGFR and FGFR inhibiting functions of multi-target RTKIs (358).

Beside the above mechanisms, probably the most important cause of resistance is suboptimal pharmacokinetics and/or the localization of the drug out of the target site. Multidrug resistance proteins (MDRs) may also be involved in the removal of antiangiogenic RTKIs from the tumor tissue (359).

3.3 TKI imaging

Mass spectrometry (MS) is an analytical chemistry technique, which generates ions from molecules by excitation energy, and helps to identify the structure and relative intensity of molecules from their mass to charge ratio (*m/z*). By virtue of its speed and sensitivity, MS has become a key technique in medical research and drug development.

In the last decades MS technology has been dramatically improved and had an impact on the research field of angiogenesis as well. The first proteomic study of HUVECs was published in 2003, when 53 proteins were identified using Time of flight (TOF) MS (360). Since then, the number of detected proteins has increased, and also those being differentially expressed upon pro/antiangiogenic stimulation have been identified (361). Moreover, stable isotope labeling with amino acids (SILAC) of ECs enables accurate quantitative proteomic analysis of cell cultures (362).

MS technology can be used in several fields of angiogenesis research. For example, the proteome of subcellular compartments can be studied (363). Of that area, the cellular secretome is of particular interest, because it allows investigation of the communication between ECs and surrounding cells (364). Cellular regulatory mechanisms such as protein trafficking, posttranslational modifications or phosphorilation of molecules can also be examined by MS (365). It allows the characterization of the cellular and molecular cascades that regulate developmental angiogenesis (366). MS analysis can be further extended to mice treated with (anti)angiogenic therapeutics to detect molecular changes in the vasculature that are critical for tumour progression. The combination of mass spectrometry and separation techniques, such as liquid-chromatography and electrophoresis has already identified numerous disease biomarkers from various body fluids (367). Moreover, using laser capture microdissection, the highest regional selectivity could be applied for down to single cell analyses (368), which helps to build a picture about spatial distribution of the analytes. The need for this spatial information and the time consuming, arduous nature of laser capture microdissection promoted the spread of mass spectrometry imaging techniques. This ensures visualization of molecules on complex surfaces to identify and localize elements, lipids, peptides, proteins, pharmaceuticals and metabolites in biological tissues (369-373).

Although the last half century has witnessed dramatic advances in the field of medical imaging, there is still an urgent need for the development of more advanced techniques

in the drug discovery process. This is particularly important in the narrowing of the selection of potential hits and leads as candidates for further development. One of the reasons this has been difficult to accomplish in the past is that until recently, the only avenue for visualizing the in vivo distribution of drugs in targeted tissues was the use of labels, commonly radioactive and such, a safety risk. Methods, like positron emission tomography and autoradiography can provide information on the distribution of a radio-labelled compound even at cellular level (374). However, both of these methods rely on quantitative data based upon the relative strength of the label rather than the relative concentration of the drug. If a drug is metabolized, the label can follow the altered structure, that is neither active, nor the precursor of an active form, and the readout of distribution may have little to do with the mode of action or the actual efficacy of the drug (374). For these reasons, unlabeled i.e. "cold compound" would provide evidence that relate only to the drug structure and not to the chemistry of labeling material in a modified drug molecule. Other methods rely on the use of isotopes with relatively short half-lives or fluorescent tags which makes long-term pharmacological analysis impossible or alters the chemical structure of the drug and thus, the binding affinity and/or avidity to its target molecule (375). From this point of view, it is particularly important that the applied methods can be used to investigate the characteristics of the unaltered native compound (i.e. the same agent that is being administered to patients).

Meanwhile the pharmacological properties of novel drug candidates are routinely characterized during the preclinical phase of drug development, in-depth and routine determination of the adsorption, distribution, metabolism and elimination (ADME) of compounds became the focus of research only in the last decades. Although ADME can fundamentally influence the therapeutic benefit of different drugs, until recently, extensive ADME studies were conducted rather late in the process of drug development, mainly in phase I clinical studies. This may be one of the key factors behind the low, 11%, overall first-in-man to registration rate of novel drug candidates in the 1990s. This proportion was especially poor (5%) among drugs in the field of oncology (376).

Mass spectrometry is a powerful technique, enabling the parallel determination of label-free drugs and their metabolites from different tissue compartments, that gives researchers the opportunity to analyse the adsorption, distribution and elimination of the native drug and its active/toxic metabolites as well.

One of the best techiques for such complex experiments is matrix-assisted laser desorption ionization (MALDI) MS (377). Briefly, a suitable matrix material is added to the sample surface, which extracts the analytes, helps the formation of analyte-doped crystals on the surface, and absorps the laser energy for soft-ionization of sample molecules (378). Thus, sample preparation is crucial for successful detection of the desired molecule (379). Then, a pulsed laser irradiates the sample, triggering ablation and desorption of the sample-matrix mixture. Finally, the analyte molecules are ionized by being protonated or deprotonated in the hot plume of ablated gases, and then are accelerated into the mass spectrometer linked to analyse them. The use of MALDI mass spectrometry in pharmacological studies dates back to the mid 1990s when in vitro metabolites were characterized by this technique (380).

The development of MALDI mass spectrometry imaging (MSI) sources for high mass resolution and mass accuracy analysers allows for the separation of ions with the same nominal mass and confident assignment of elemental formulas. Furthermore, various MS/MS techniques are available to link with FT-MS systems. This, by fragmenting the precursor molecule and yielding a structure specific fragment ion map, further ensures the identification of the desired molecule. This technology has recently been employed to determine the exact tissue compartment localization of small drug molecules (381).

Although localization of antitumor molecules in their target site is considered to be important to show their efficacy, studies published to date focus mainly on the measurements of compounds from the blood, urine and occasionally from tissue homogenates (382). Consequently, the lack of greater clinical success of anticancer agents is, at least in part, due to our limited knowledge of their pharmacokinetic profile, bioavailability and distribution at the tumor tissue. Antiangiogenic drug imaging is also still in its infancy, as the only study reported so far on the distribution of an antiangiogenic antibody, detected by MALDI-MSI was published in 2014 (383). Our group was the first to show imaging data on the distribution of antiangiogenic RTKIs.

However, considering that the inhibition of the tumour vessel network may influence the dispersal of the antiangiogenic drug itself, such spatial distribution data could greatly help researchers to better understand their mode of action and to identify the best potential therapeutic schedules of these agents.

4. AIMS

The clinical experiences with antiangiogenic RTKIs are controversial, despite their predicted inhibitory and normalizing effects on vessel growth. No biomarker of tumor response has yet been linked to the effect of these agents. Taken into consideration that ADME can fundamentally influence the therapeutic benefit of different drugs, the following specific aims have been defined:

1. to develop a method for the detection of antiangiogenic RTKIs and their metabolites in different tissues.

2. to analyse the intratumoral distribution and levels of different antiangiogenic receptor tyrosine kinase inhibitors (RTKIs) of mice bearing subcutaneously growing murine tumors by using MALDI-MSI.

3. to evaluate the potential associations between intratumoral antiangiogenic drug levels and distributions and **3.1.**/ tumor growth inhibition; **3.2.**/ blood vessel density and area; **3.3./** blood vessel integrity (basement membrane, pericyte and α-smooth muscle actin (SMA) coverage **3.4.**/ the size and localization of hypoxic areas of the tumor tissue; **3.5.**/ the expression and distribution of receptors targeted by the RTKIs.

5. METHODS

5.1 In vivo tumor models and treatments

5.1.1 Tumor models

Two different mouse colon adenocarcinoma models, C26 and C38 were used for our experiments. The C26 cell line was cultured in RPMI 1640 medium with 10% fetal bovine serum and 1% penicillin/streptomycin (all from Sigma Aldrich, Steinheim, Germany) in a humidified atmosphere at 37°C, 5% CO_2. Groups of six 8-week-old female Balb/C mice from the colony of the National Oncology Institute, Budapest were inoculated subcutaneously (sc.) with $2x10^6$ C26 cells. The C38 tumors were maintained by serial s.c. transplantations in 8-week-old female C57Bl/6 mice. Tumors were cut into cubes measuring 5×5×5 mm. Animals were anesthetized and one piece of tumor tissue was transplanted into the back of each mouse.

All animal-model protocols were developed and conducted in accordance with the ARRIVE guidelines (384) and the animal welfare regulations of the Department of Experimental Pharmacology, National Institute of Oncology, Budapest, Hungary (permission number: 22.1/722/3/2010). Mice were kept on a daily 12-h light/12-h dark cycle and held in conventional animal house in microisolator cages with water and laboratory chow ad libitum.

5.1.2 Drugs

For drug treatment of C26 bearing mice, 5 antiangiogenic RTKIs either approved by both the FDA and the EMEA (pazopanib, sorafenib, sunitinib) or investigated in Phase III trials (motesanib, vatalanib) were selected. In the C38 model a vatalanib-treated and a control group was generated.

Drugs were purchased from LC Laboratories, (Woburn, MA, USA, CAS. No. for motesanib: 453562-69-1; pazopanib: 444731-52-6; sorafenib: 284461-73-0; sunitinib: 557795-19-4 and vatalanib: 212141-54-3) at >99% purity and suspended in 2% carboxymethylcellulose with 2 mg/mL methyl-4-hydroxibenzoate (both from Sigma Aldrich). Control animals received the suspending medium only.

These RTKIs are known to have significant IC50 values of the main angiogenic receptor, VEGFR2, and may also inhibit PDGF- and FGF receptors (342,344,385-387).

The IC50 values (nM) of the applied compounds against the main antiangiogenic receptors as measured in a cell-free assay are shown in **Table 2**.

Table 2. IC50 values (nM) of the main antiangiogenic RTKIs against human angiogenic receptors measured in a cell free assay. IC50 values of the corresponding mouse receptors are shown in brackets. ND: not defined. *not defined which FGFR is tested.

Target receptor	Motesanib	Pazopanib	Sorafenib	Sunitinib	Vatalanib
VEGFR1	2	10	ND	ND	77
VEGFR2	3 (6)	30	90 (15)	9	37 (270)
VEGFR3	6	47	(20)	ND	660
PDGFRα	ND	71	ND	ND	ND
PDGFRβ	84	84	(57)	8	580
FGFR1	>2800*	140	580	830	ND
FGFR2	ND	ND	ND	ND	ND
FGFR3	ND	130	ND	ND	ND
FGFR4	ND	800	ND	ND	ND
TIE1	ND	ND	ND	ND	ND
TIE2	ND	4520	ND	ND	ND
Ref.	(385)	(342)	(344)	(386)	(387)

Pazopanib, sunitinib, and vatalanib are Type I inhibitors, while motesanib and sorafenib belong to the group of Type II inhibitors (327,388). Out of this five compounds pazopanib, sorafenib and sunitinib are already used for cancer therapy. All three are approved for advanced RCC. Besides RCC, pazopanib is effective in advanced soft tissue sarcoma (389). Sorafenib is used for the treatment of unresectable hepatocellular carcinoma and locally recurrent or metastatic, progressive differentiated thyroid carcinoma, refractory to radioactive iodine treatment (41). Sunitinib therapy is approved in progressive well-differentiated pNET and GIST after disease progression or intolerance to imatinib mesylate (390). Several completed or still ongoing clinical trials have assessed the effects of these approved antiangiogenic RTKIs in colorectal cancer with controversial results (352,391-395). Motesanib and vatalanib have been investigated in clinical trials in different tumor types. In colorectal cancer, the only study completed to date with motesanib in first- or second line treated CRC patients demonstrated modest efficacy (396), while vatalanib is showing promising results in CRC patients only with activated vessel density (high phospho-VEGFR expressing vessels) or low lactate dehydrogenase levels (397,398).

5.1.3 In vivo treatment

The administration and dose level for each compound was chosen to be tolerable and effective according to the literature (385,399-402). Moreover, to mimic the clinical situation, RTKIs were administered orally.

Accordingly, in case of the C26 model, treatment began 14 days after tumor cell injection and was performed per os with a feeding tube once daily, at a dose of 100 mg/kg, 5 times a week for two weeks. In the C38 model, treatment began 9 days after tumor implantation and was performed as in the C26 model.

During the growth of tumors animals were weighed three times per week and monitored daily for tumor related symptoms. To evaluate the in vivo effects of the different antiangiogenic RTKIs, two diameters of the tumors were measured three times a week, and tumor volume was calculated with the formula $width^2$ x length x $\pi/6$.

To assess intratumoral hypoxia, a bolus of i.p. pimonidazole (60 mg/kg; Hypoxyprobe Inc., MA, USA) was administered 1 hour before the mice were sacrificed. Pimonidazole is activated by reduction in hypoxic cells and forms adducts with thiol groups in proteins, peptides and amino acids.

Two hours after the last oral treatment, peripheral blood was drawn from the canthus and mice were sacrificed. Tumors and normal organs were removed, tumor weight was measured and samples were snap frozen by submerging the tissues into dry ice cooled isopentane. Frozen tissues were stored at -80 ^{o}C until utilization.

5.2 Analysis of vascular parameters and target receptors

For the analysis of vascular parameters and target receptor expressions, 10 serial frozen sections were cut from each tumor. Sections #5 and #7 were used to analyse the distribution and levels of the given RTKI by MALDI-MSI and for subsequent haematoxylin&eosin (HE) staining. Sections #1-4 were labeled with either of the following primary antibodies: anti-FGFR1, anti-PDGFRα, anti-PDGFRβ and anti-VEGFR2. For hypoxia detection (section #6), we used the Hypoxyprobe-1 Plus Kit. Sections #8-10 were labeled with either of the following primary antibodies: anti-laminin (for endothelial basement membrane labeling), anti-desmin (for pericyte labeling) and anti-α-smooth muscle actin (anti-αSMA). All of the above primary antibodies were developed with an appropriate fluorescent secondary antibody. For

intratumoral microvessel density (MVD) and microvessel area measurements, sections #1-4, #6 and #8-10 were co-stained with anti-mouse CD31 antibody, followed by a counterstain with Hoechst 33342 before mounting under glass coverslips in ProlongGold Antifade Reagent (Invitrogen, Carlsbad, CA, USA; Catalog number: P36930). Primary and secondary antibodies and dyes used for immunohistochemical labeling are listed in **Table 3.**

Slides were scanned by TissueFAXS using a 20x objective and analysed by TissueQuest 4.0.0140 (both from TissueGnostics GmbH, Vienna, Austria) and ImageJ software packages.

For microvessel density and microvessel area measurements, images of ten different viable intratumoral regions were assessed separately for each section. Microvessel areas were calculated by measuring the number of CD31-positive pixels, while MVD was estimated by counting the number of vessels in all ten fields of view, and calculating the average of them. For quantification of VEGFR2 expression, both signal area and density were calculated similarly to CD31. In case of VEGFR2, positively labelled vessels and tumor cells were also counted for data analysis. The percentages of microvessels that were positive for laminin, desmin or αSMA were also calculated. For quantification of hypoxia, PDGFRα, PDGFRβ and FGFR1 expressions, the percentages of the areas of positively labeled cells were determined across the entire section.

Table 3. Specifications of different antibodies and the nucleic acid stain used in our experiments.

Antibody	**Species**	**Manufacturer**	**Catalog No.**	**Dilution**
Primary				
Anti-CD31	rat monoclonal	BD Pharmingen, BD Biosciences, Franklin Lakes, NJ, USA	550274	1:50
Hypoxyprobe-1 Plus Kit (FITC-Mab1)	mouse monoclonal	Hypoxyprobe Inc., Middlesex Turnpike Burlington, MA, USA	HP1-100Kit	1:100
Anti-Laminin	rabbit polyclonal	DAKO, Glostrup Denmark	Z0097	1:200

Anti-Desmin	rabbit polyclonal	Abcam, Cambridge, UK	Ab32362	1:200
Anti-αSMA	mouse monoclonal	DAKO, Glostrup Denmark	M0851	1:200
Anti-FGFR1	rabbit polyclonal	Cell Signaling Technology, Danvers, MA, USA	9740	1:50
Anti-PDGFRα	rabbit polyclonal	Cell Signaling Technology, Danvers, MA, USA	3174	1:50
Anti-PDGFRβ	rabbit polyclonal	Cell Signaling Technology, Danvers, MA, USA	4564	1:50
Anti-VEGFR2	rabbit polyclonal	Cell Signaling Technology, Danvers, MA, USA	2479	1:50
Secondary				
Alexa 488	Anti-mouse goat $F(ab')_2$	Cell Signaling Technology, Danvers, MA, USA	4408	1:1000
Alexa 488	Anti-rabbit goat $F(ab')_2$	Cell Signaling Technology, Danvers, MA, USA	4412	1:1000
Alexa 555	Anti-rat goat $F(ab')_2$	Cell Signaling Technology, Danvers, MA, USA	4417	1:1000
Nucleic acid stain				
Hoechst 33342		Molecular probes, Eugene, OR, USA	H3570	1:10000

5.3 Detection of the compounds and analysis of drug distribution and intensity

5.3.1 Ionization technique and instrumentation

MALDI-MS was used for the detection of RTKIs. MALDI-MS is a soft ionization technique, thus it is mostly used to detect and analyse molecules which tend to be fragile and fragment when ionized by conventional ionization methods.

As a matrix, molecules with mobile electron system are suitable, which are showing light absorption in the wavelength of the laser, thus transmit the laser energy to the analyte molecule. This process facilitates the ionization of the sample. Besides, the matrix is able to block the aggregation of analyte molecules.

For the analysis of small molecules, the most commonly used matrices are 3,5-dimethoxy-4-hydroxycinnamic acid (sinapinic acid), α-cyano-4-hydroxycinnamic acid (CHCA) and 2,5-dihydroxybenzoic acid (DHB). A solution of one of these matrices is usually made of a mixture of highly purified water and an organic solvent such as acetonitrile (ACN), acetone, chlorophorm, methanol or ethanol. The most suitable matrix is variable among different molecular structure analytes, thus more matrices should be tested to reach maximal quality of the mass spectrum and highest signal intensity of the analyte. A counter ion source such as trifluoroacetic acid (TFA) is usually added to generate the [M+H] ions (quasimolecular ions). The analyte molecules are mixed with the matrix solution either on a target plate or on tissue surface. The mixture of a hydrophil (water) and a hydrophob (organic solvent) component of the matrix solution allows both hydrophobic and hydrophilic molecules to dissolve into the solution. The solvents vaporize in a few seconds, while matrix molecules co-cristallize with the analyte molecules embedded into matrix cristals.

MALDI (**Figure 13.)** makes it possible to detect molecules of interest with high accuracy and sensitivity from small amounts of complex samples, as one of the main advantage of this ionization technique is that it has great tolerance towards salts and puffers, being present in physiological samples (403). However, matrix application can result in the generation of high background signals below 500 Da mass range (404).

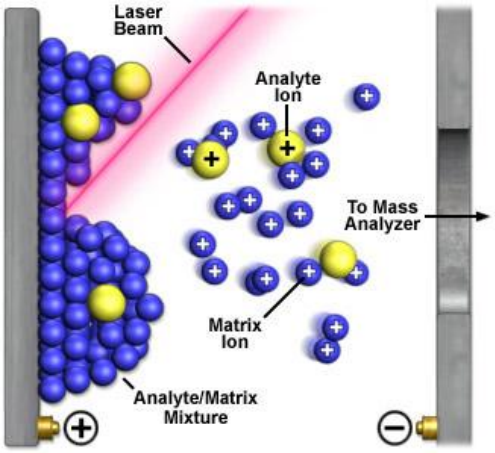

Figure 13. Ionization of the analyte molecule (yellow) with matrix (blue) using MALDI (405). Solution of the matrix is applied to the surface of the sample. In turn, analyte molecules dissolve into the solution. The solvents vaporize, while matrix molecules co-cristallize with the analyte molecules embedded into matrix cristals, thus blocking their aggregation. The matrix (a molecule with mobile electron system) absorbs light in the wavelength of the laser and transmits the laser energy to the analyte molecule. This process facilitates the ionization of the sample.

Both for compound characterization and drug detection in blood on a MALDI target plate, as well as for tissue imaging a MALDI LTQ Orbitrap XL mass spectrometer (**Figure 14.**, Thermo Fisher Scientific, Bremen, Germany) was used.

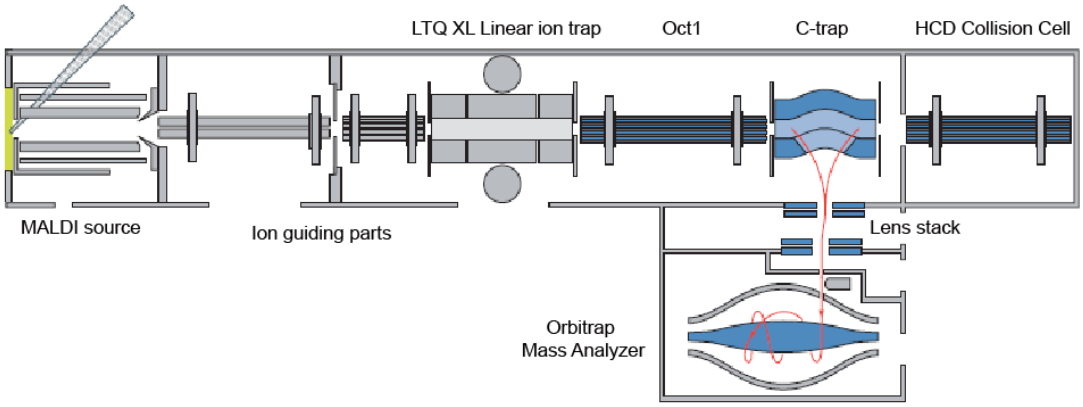

Figure 14. Structure of the MALDI LTQ Orbitrap XL mass spectrometer (406).

After the insertion of the plate, the sample is targeted by a nitrogen laser at the UV range. By absorbing light in the wavelenght of the laser, the matrix gets excited, ionized and desorbed from the surface of the sample. Finally matrix molecules transfer/remove protons to/from the analyte molecules, which also get into gas phase by desorption from the sample surface. The analyte molecules in turn get singly or multiply charged depending on the matrix, the laser intensity and the applied voltage. One of the main advantages of the MALDI technique is that the laser is operated in a pulsed mode, thus generation of ions is a discrete process, and if the analysis is linked in time with ion generation, hardly any sample is wasted. This is one reason of the high sensitivity of the MALDI technique, as even fmol (10^{-15}) of analyte molecules can be detected (407). On the other hand, pulsed laser is the reason, why MALDI ionization cannot be linked with some specific mass analysers. After the ion beam is formed, ions are accelerated and sent to the mass analyser part of the instrument.

The mass analyser can either be responsible for fragmentation of the gas phase analyte molecules, or separation of both precursor molecules and their fragment ions based on their *m/z* ratio, depending on the scan type used. Moreover, they transfer ions to the detector. The mean free path in the analyser (the average distance traveled by an ion between collisions) has to be larger than the length of the instrument. That means that collision with the wall of the insrument is more likely than it is with other ions. This is

of major importance, because collisions may modify the direction or energy of ions, which mainly impact data outcome. Therefore, analysers are operated in high vacuum.

The instrument used in our experiments has a hybrid linear quadrupole ion trap (LTQ)-orbitrap mass analyser, and both of the mass analysers function as mass detectors as well. Compared to other hybrid instruments, LTQ-Orbitrap is characterized by high ion transmission (30%–50%) (406).

The LTQ (**Figure 15.**) part consists of 4 parallel metal rods, which conduct electricity. Direct current (DC) and alternate current (AC) voltages are both switched to the rods in such manner, that the opposite rods have the same potential, while the neighbouring rods have potentials with opposite signs. Ions leave the ion source and enter the quadrupole in response to accelerating voltages. Here the positive potential rods toss the positive ions, while attract the negative ions. The negative rods do the opposite. As a result of the AC voltage the relative charge of the rods is changing from time to time, thus, the ions oscillate while passing through the rods. In a quadrupole mass analyser, the correct magnitude of the radio frequency and DC voltages applied to the rods allow ions of specific *m/z* to maintain stable trajectories from the ion source to the detector, whereas ions with different *m/z* values are unable to maintain stable trajectories.

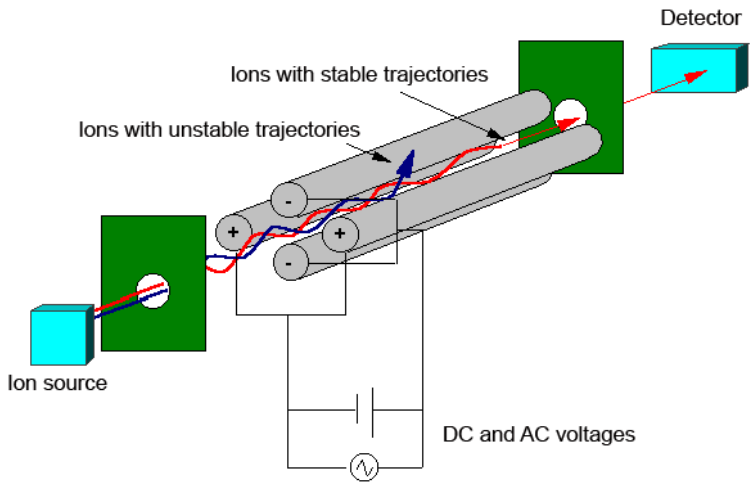

Figure 15. Structure of a quadrupole mass analyser (408). The 4 parallel rods conduct electricity. DC and AC voltages are switched to the rods in an alternating manner. Two opposite rods have a certain applied potential, while the other two rods have the same potential with negative sign. As a result of the AC voltage the relative charge of the rods is changing from time to time, thus the ions oscillate as determined by their charge while passing through the rods with a speed defined by their mass. For given DC and AC voltages, only ions of a certain mass-to-charge ratio pass through the quadrupole and all other ions are thrown out of their original path.

The linear ion trap part of the instrument is an independent MS detector, thus able not just to store and isolate, but fragment and then send ions through one of the three exit slots either to the Orbitrap for further analysis or to a secondary electron multiplyer (SEM) detector. Fragmentation occurs in the LTQ by collision-induced dissociation (CID). The precursor ions are accelerated by electric potential to high kinetic energy and then collide with helium. The kinetic energy is partly converted into internal energy which results in breakage of bonds and the molecular ion falls apart into smaller fragments. These fragment ions can then be analysed by a mass spectrometer.

Mass analysis (**Figure 16.**) is achieved by making ion trajectories unstable in a mass-selective manner. The main radio frequency voltage is ramped and simultaneously AC voltage is applied to the exit rods to facilitate ejection. As the main radio frequency voltage is increased, ions of greater and greater *m/z* values become unstable and are ejected through the exit slots.

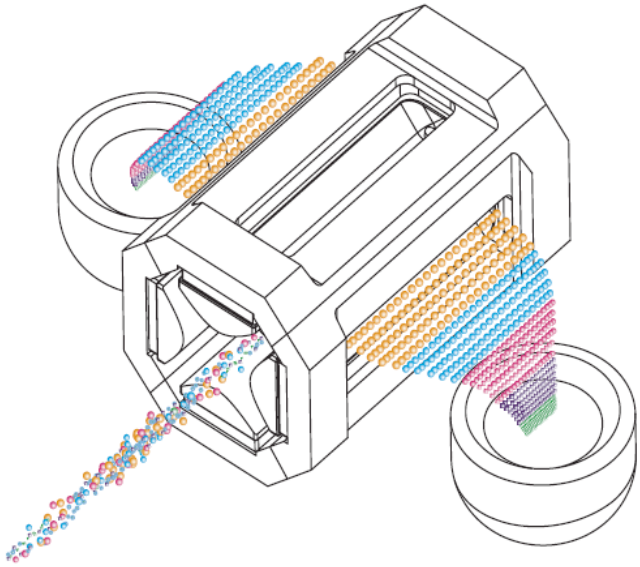

Figure 16. Operation of LTQ. Ions of different m/z values (represented by colored spheres) enter the linear ion trap. The ions are ejected from the trap in order of increasing *m/z* values. After exiting the trap through slots in the exit rods, the ions strike the conversion dynodes on each side of the trap (409).

These ions are focused toward the ion detection system where they are detected. If the linear ion trap functions as a mass detector as well, the ions strike the conversion dynodes in the off-axis ion detection systems upon ion ejection. This is located in both sides of the trap. Upon striking the surface of the conversion dynode by an ion, secondary particles are produced. These secondary particles are focused by the curved

surface of the conversion dynode and are accelerated by a voltage gradient into the electron multiplier. The current that leaves the electron multiplier via the anode is converted to a voltage and recorded by the data system.

If the detector is the orbitrap, ions move through the gas-free radio frequency octapole (Oct 1) into the gas-filled curved linear trap (C-Trap) on their way from the linear trap to the Orbitrap. Ions in the C-Trap are returned by a trap electrode. Upon their passage, using nitrogen collision gas the ions loose kinetic energy and cool down, thus preventing them from leaving the C-Trap through the gate. From the C-trap, ion packets are injected tangentially into the field of the Orbitrap.

The orbitrap (**Figure 17.**) is both a mass analyser and a detector, consisting of a spindle-shaped central electrode surrounded by a pair of bell-shaped outer electrodes (410).

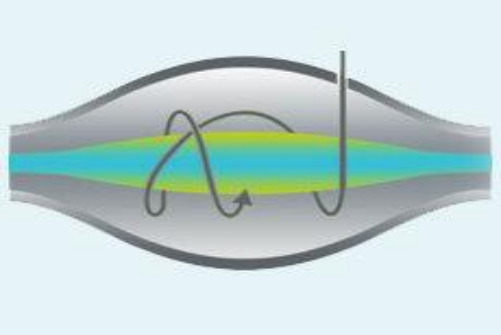

Figure 17. Orbitrap mass analyser (411), consisting of an outer bell-like electrode and an inner spindle-like electrode. Ions are trapped in an orbital motion around the spindle based on their *m/z* value. Image currents from the trapped ions are detected and converted into mass spectrum using Fourier transformation of the frequency signal.

Upon ions leaving the C-trap, the electric field in the orbitrap is increased by elevating voltage on the inner electrode. Thus, ions get squeezed towards the central electrode until they reach the desired orbit inside the trap. At that moment ramping of the voltage is stopped, the field becomes static and detection starts. Ions in the orbitrap move with different rotational frequencies based on their *m/z* ratio, but with the same axial frequency along the central electrode. The outer electrode is split in two symmetrical pick-up sensors connected to a differential amplifier. Axial oscillations of ion rings are detected by their image current induced on the outer electrode. This signal is converted into mass spectrum by Fourier-transformation (406).

From the linear ion trap ions are either sent to the orbitrap or to the high energy collisional dissociation (HCD) part of the instrument through the C-trap. The offset

between the C-Trap and HCD is used to accelerate the precursors into the gas-filled collision cell. It is supplied with a nitrogen collision gas providing increased gas pressure inside the multipole. HCD is specific to the orbitrap, in which fragmentation takes place outside the trap. After dissociation ions return to the C-trap before injection into the orbitrap for mass analysis. Despite the name, the collision energy of HCD is typically in the low regimen, thus fragmentation is not as efficient as in the linear ion trap, but as fragment ions of approx. 5%–10% *m/z* of the precursor ion mass can be observed, it may be used, when fragments are in a low *m/z* range (412).

Analysers are characterized by the following features:

Linear dynamic range is the concentration range in which signal intensity is in a linear correlation with the concentration.

Mass resolution defines how accurately two neighbouring m/z values can be distinguished. The border between the low and high mass accuracy instruments is 10^4. This means, that ions of a molecule of hundred mass numbers can be differentiated by 0.01 *m/z*. (R_s=100/0.01=10^4).

The mass range is the range between the *m/z* values the instrument can minimally and maximally detect.

The detection limit shows the minimal amount of the analyte molecule, the instrument can detect. This can be highly influenced by the ion transmission efficiency. If the distance between the ion source and the detector is long enough, the efficiency of ion transmission is high enough.

Appropriate temperature of the instrument is essential, as the sample must be kept in gas phase during the ionization process.

The speed of the mass analyser is expressed in the amount of spectrums generated in a certain amount of time. This is important so that the mass spectrum reflects the real mass intensity dispersion of each sampled spot.

The LTQ Orbitrap XL has the following measuring properties:

Resolution: 60 000 (Full Width Half Maximum) @ *m/z* 400 with a scan repetition rate of 1 second.

Cycle Time: 1 scan at 60 000 resolution @ *m/z* 400 per second.

Mass Range: *m/z* 50–2 000; m/z 200–4 000.

Mass Accuracy: <3 ppm root mean square for 2 h period with external calibration using defined conditions, <2 ppm root mean square with internal calibration.

Dynamic Range: >10 000 between mass spectra, >4 000 between highest and lowest detectable mass in one spectrum.

Three scan modes are defined in MS. The mass spectrometry scan mode is a single stage mass analysis (n = 1). In that scan mode no fragmentation of the precursor ion occurs. The MS/MS scan is a two stage mass analysis (n = 2). In an MS/MS scan, precursor ions are fragmented into product ions. An MS^n scan usually involves three to ten stages of mass analysis (n = 3-10), in which the precursor ion is first fragmented, and afterwards fragment ions are selected as precursor ions and fragmented again. This process can be repeated 10 times. The instrument has MS/MS and MS^n scan functions.

5.3.2 Compound characterization

Drugs were dissolved in 50% methanol (Sigma-Aldrich, Steinheim, Germany) at HPLC grade (99.8+%) at 0.5 mg/mL concentration. After the selection of the appropriate matrix molecule, 7.5 mg/mL CHCA (Sigma Aldrich, Steinheim, Germany) was dissolved in 50% ACN (Merck, Darmstadt, Germany) and 0.1% TFA (Sigma-Aldrich, Steinheim, Germany) was added. 1μL of the compound solution was applied with 1μL matrix solution to the MALDI plate.

Full scan was performed, to determine the *m/z* value of the RTKIs and their fragment ions. Full scan presents a full mass spectrum of the analyte. In that case, ions are scanned from the first mass to the last without interruption. To determine the precursor ion peak, single-stage full scan was done. In that analysis, ions formed in the ion source are stored in the mass analyser and afterwards they are sequentially scanned to produce a full mass spectrum. Fragment ions were determined in a two-stage full scan experiment. In the first stage of mass analysis, the ions formed in the ion source are stored in the mass analyser. Then, ions of one specific mass-to-charge ratio (the precursor ions) are selected and all other ones are ejected from the mass analyser. The precursor ions are excited and collide with background gas. This facilitates their fragmentation to create one or more product ions. In the second stage of mass analysis the product ions are first stored and then sequentially scanned out of the mass analyser to produce a full product ion mass spectrum.

Full mass spectra were obtained at 60,000 resolution by using positive polarity. The spots were sampled in survey mode (accidentially choosing sampled spots) collecting 20 experiments for a single run. The nitrogen laser was set to 10 μJ. The detected precursor ions were isolated with *m/z* 2.0 width isolation window, and were fragmentized by using 40% normalized collision energy (NCE) during a 30 ms activation time, while activation *Q* of 0.25 was applied. MS/MS spectra were collected at normal scan rate in centroid format.

5.3.3 Compound detection in the blood

Blood was removed from the canthus just before sacrificing the animals. After centrifugation plasma samples were stored in -80 ^{o}C until utilization. Acetonitrile precipitation was performed as the following: 20 μL of the plasma sample was removed and mixed with 40 μL ice cold 100% ACN to precipitate blood components. After vortexing and centrifugation at room temperature for 15000 rpm and 15 minutes, the supernatant was removed and dried with speed vac. Then the sample was diluted in 20 μL 0.1% TFA solvent. Pierce C18 Tips (Thermo Fisher Scientific, Rockford, IL, USA) were used to concentrate RTKIs from the precipitated plasma samples, following the manufacturer's instructions. 2 μL concentrate was eluted from the column, and 1μL of this was applied on the MALDI plate with 1μL matrix solution using the same instrument settings as used for compound characterization.

5.3.4 Tissue imaging of antiangiogenic RTKIs

10-μm frozen sections were cut using a cryotome and placed on glass slides. After drying of the tissue, 0.5 mL matrix solution was applied stepwise to avoid wetting of the sections by using an airbrush, while its position was kept constant. Full mass spectra were collected by performing a single stage full scan using the Orbitrap mass analyser at 60000 resolution (at *m/z* 400), in positive mode with a 150−800 Da mass range and 100 μm raster size. The nitrogen laser was operated at 10.0 μJ. For ensuring a known number of charges in the linear trap, in particular, in order to avoid overfilling the ion trap, automatic gain control (AGC) was used. AGC is a pre-scan event, which is performed before an analytical scan, for which the pre-scan serves as a prediction of the

number of charges, and the injection time. Depending on the result of the pre-scan event, the parameters of the live scan can be changed.

For obtaining MS/MS data two-stage full scan was performed. The observed peaks of the precursor drugs were isolated with *m/z* 2.0 width isolation window and fragmentized, using 40% NCE, 30 ms activation time and 0.25 activation *Q*. For MS/MS spectra generation the minimal signal required by the linear ion trap was 500 counts. The fragment ions were analysed in the linear ion trap at normal scan rate.

5.3.5 Quantification of the compounds

For tissue quantification of intratumoral drug concentration, calibration curves of each compound were established on untreated control C26 and C38 tumor tissue sections. After determining the detection limit of the instrument, drugs were dissolved and diluted in 50% methanol (concentration range: 0.001–0.5 μmol·mL−1), and 0.5 μL from each concentration was applied on a tissue section. Spraying and detection conditions were the same as those during the tissue sample analysis of the in vivo treated tumors. Average signal intensities of the applied concentrations were measured and normalized to total ion current (TIC) by Xcalibur v 2.0.7 and ImageQuest™ software packages.

Calibration curves were created, which were then used to estimate the tissue drug concentrations of in vivo treated tumor sections. Because of the possibility of generating nonspecific precursor ion peaks from the tissue itself, the average signal intensities and the corresponding concentrations obtained from RTKI-treated tumors were compared with that of non-treated control tumors.

Throughout our MS experiments drugs were considered to be detected if the precursor molecule and at least one fragment ion was discovered in the spectra.

Evaluation of all MS spectra was performed with Xcalibur v 2.0.7 software, while the visualization of the drugs and fragment ions in/on tissue was implemented with the ImageQuest™ software (both from Thermo Fisher Scientific, San José, CA).

5.4 Statistical analysis

Differences in parametric and non-parametric variables between multiple groups were analysed using one-way ANOVA and Dunnett's posthoc test or using the Kruskal–Wallis test followed by a posthoc Dunn’s multiple comparison test, respectively. For

comparing two groups, unpaired t-tests were applied to analyse parametric and Mann-Whitney U tests were used to analyse non-parametric data. Differences were considered statistically significant when $p<0.05$. All Statistical analyses were carried out using GraphPad Prism 5.0 software (GraphPad Inc., San Diego, CA, USA).

Figure 18. shows the flow chart of the experiments.

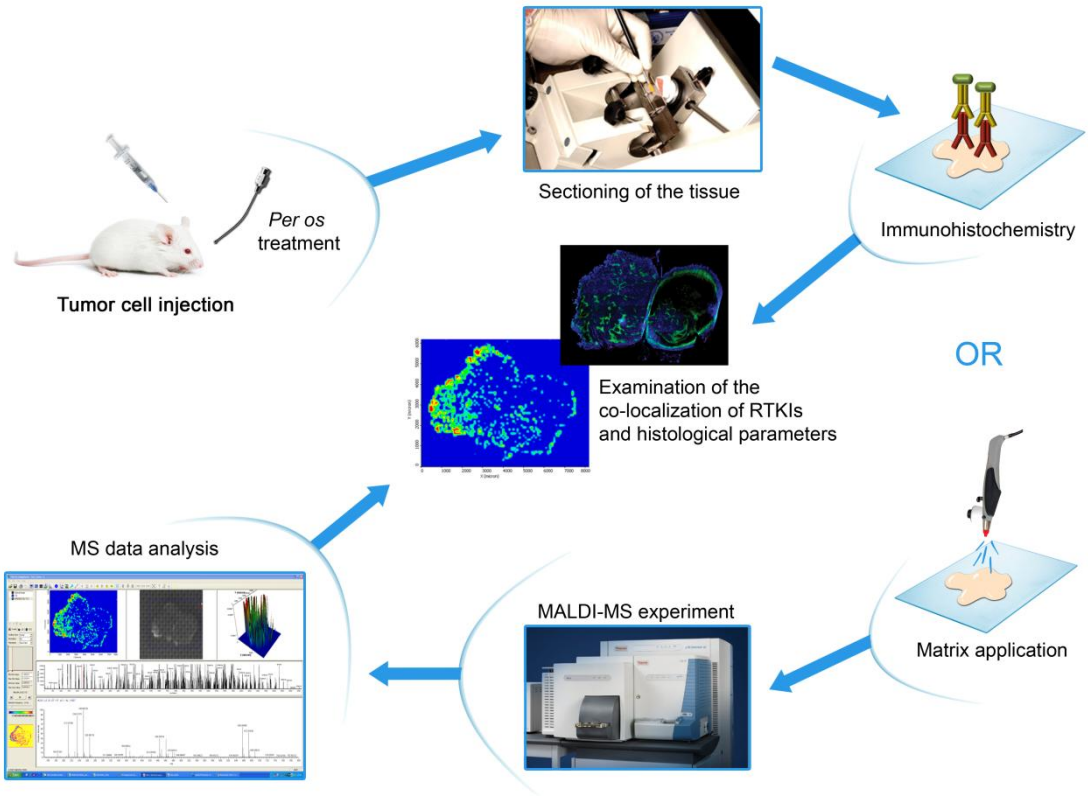

Figure 18. Flow chart of the study procedure. Nine serial frozen sections were cut from C26 or C38 mouse tumors treated with different antiangiogenic RTKIs. Sections were then used to analyse drug dispersal by MALDI-MSI, for subsequent HE staining and for immunolabeling with antibodies against CD31, laminin, desmin, αSMA and the target receptors of RTKIs. An additional slide was also used for hypoxia detection. After scanning the tissue sections, the antitumor and antivascular properties of RTKIs were correlated with their tumor tissue distribution data obtained by MALDI-MSI.

6. RESULTS

6.1 Tumor growth inhibititon

A significant (p=0.0194) relative tumor growth inhibitor effect was shown after two weeks of RTKI treatment, when comparing the % change in tumor volume in the C26 model. Sunitinib was the only drug affecting tumor growth in this experimental setting (**Figure 19A.**).

In the C38 model two weeks of vatalanib treatment significantly reduced (p=0.0173) tumor burden (**Figure 19B.**).

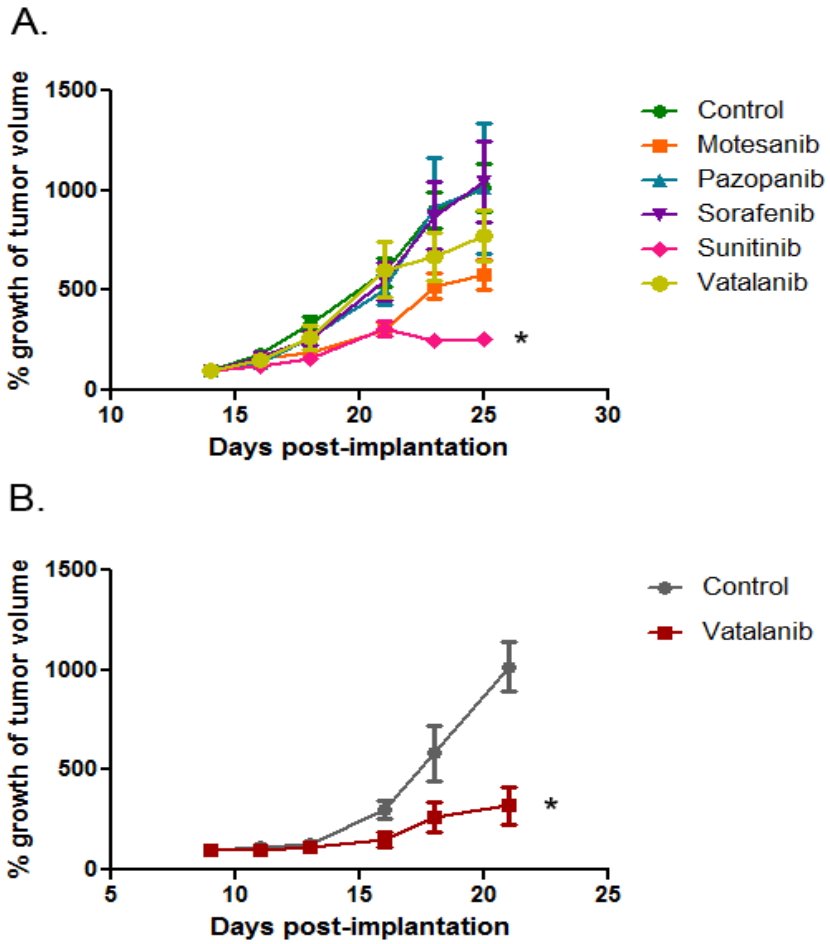

Figure 19. In vivo growth inhibition of different RTKIs in C26 and C38 tumors. **(A.)** Out of the five different antiangiogenic RTKIs (motesanib, pazopanib, sorafenib, sunitinib and vatalanib), only sunitinib reduced significantly the in vivo growth of C26 mouse colon adenocarcinoma cells in Balb/C mice, as shown by the one-way Anova test (p=0.0194) (**B.**) In contrast to the C26 model, vatalanib demonstrated a significant growth inhibitory effect in C57Bl/6 mice bearing C38 tumors, as shown by unpaired t-test (p=0.0173). Growth curves are means for six mice per group; bars, SEM.

In both models, control tumors weighted more than two times more than the ones treated with the effective compound (mean tumor weights 0.427g vs. 1.046g for sunitinib treated and control tumors, respectively in the C26 model and 0.811g vs. 2.146g for vatalanib treated and control mice, respectively in the C36 model, data not shown).

6.2 Immunohistochemical analysis

The growth of s.c. tumors in mice is known to be angiogenesis-dependent (413). Thus, in the next step of the experiment we tested, if the differences in tumor growth are in line with the effects of drugs on vascular parameters and the expression of target angiogenic receptors of the RTKIs. Therefore, we stained tissue sections for these parameters.

The expression level of antiangiogenic RTKs may significantly influence treatment response, and in turn, successful therapy can also regulate target receptor localization and function. In the C26 model expression of PDGFRα, -β and FGFR1 was observed not only on mural cells, but also on tumor cells. Expression patterns of PDGFRα, -β and FGFR-1 did not change in response to treatment with any of the compounds (p=0.8265 0.1261 and 0.2983, respectively) in the C26 model (**Figure 20-22**.).

The receptor distribution of the C38 model showed a different pattern compared to the C26 tumors. C38 tumor cells did not express the aforementioned receptors, but a definite cell population expressing PDGFRα, -β and FGFR1 was detectable on the mural cells. Similarly to the C26 model, no change in the expression of PDGFRα, -β and FGFR1 (p=0.7601, 0.7497

and 0.7178, respectively) was seen (**Figure 20-22**.).

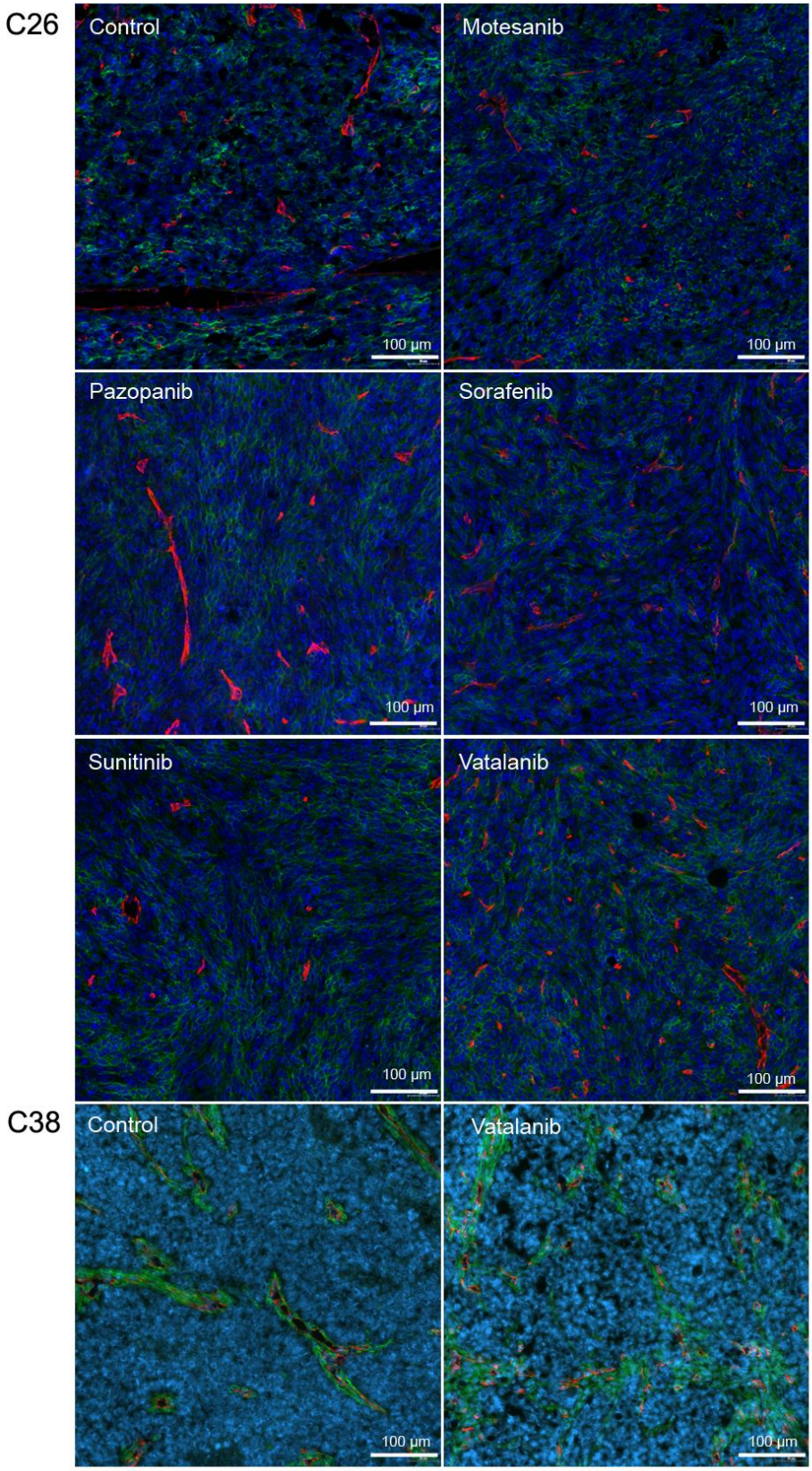

Figure 20. Low power views of C26 and C38 tumor sections stained for PDGFRα (green). Microvessels are labeled with anti-CD31 (red). Nuclei are stained with Hoechst 33342 (blue).

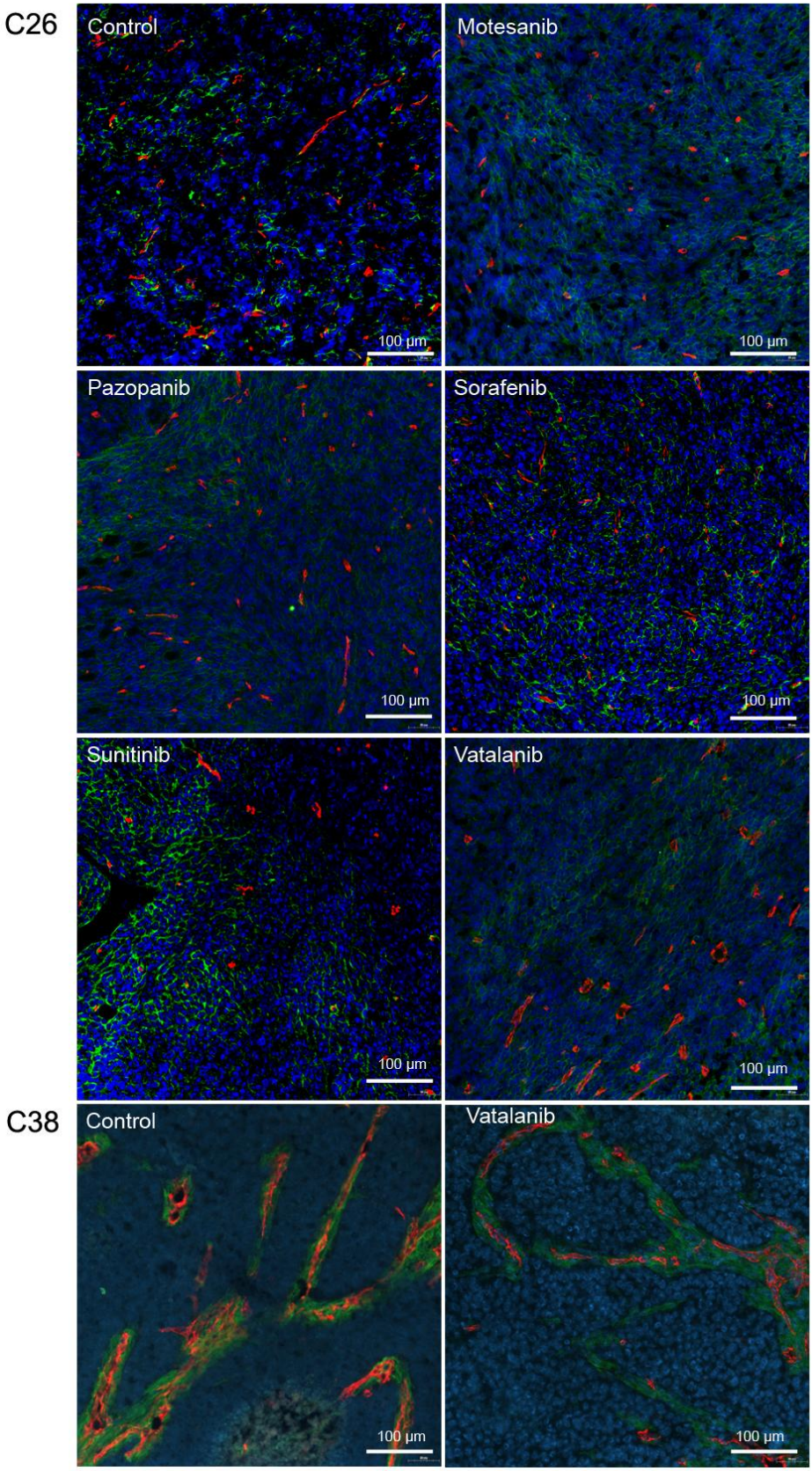

Figure 21. Low power views of C26 and C38 tumor sections stained for PDGFRβ (green). Microvessels are labeled with anti-CD31 (red). Nuclei are stained with Hoechst 33342 (blue).

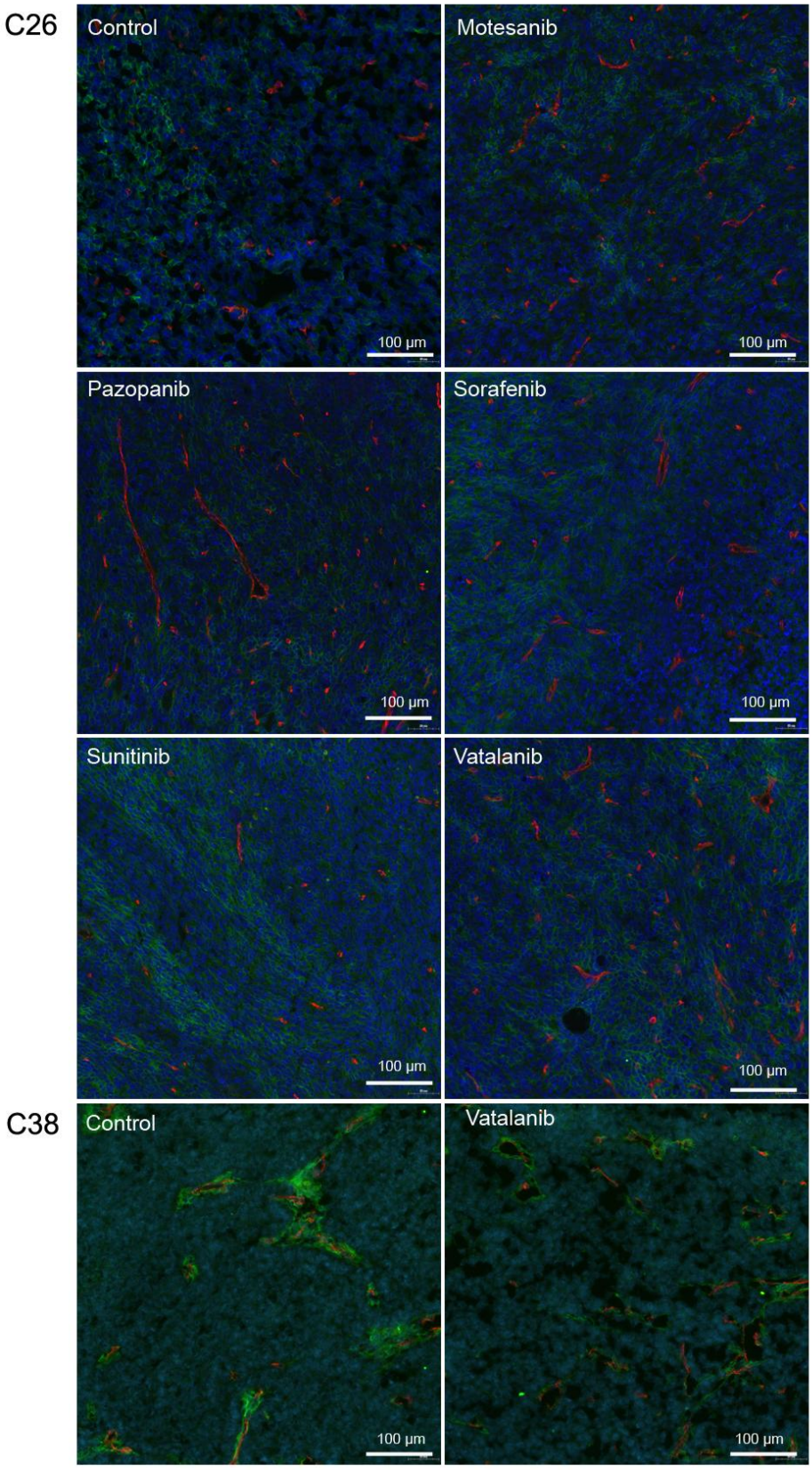

Figure 22. Low power views of C26 and C38 tumor sections stained for FGFR1 (green). Microvessels are labeled with anti-CD31 (red). Nuclei are stained with Hoechst 33342 (blue).

VEGFR2 expression was detected both on tumor and endothelial cells in the C26 model. Significant differences were shown both when counting the VEGFR2 signal and when measuring the area of VEGFR2+ cells in C26 tumors (p=0.0296 and 0.022 respectively; **Figure 23, 25)**. Post-hoc test showed that VEGFR2 expression was altered only in the sunitinib treated group.

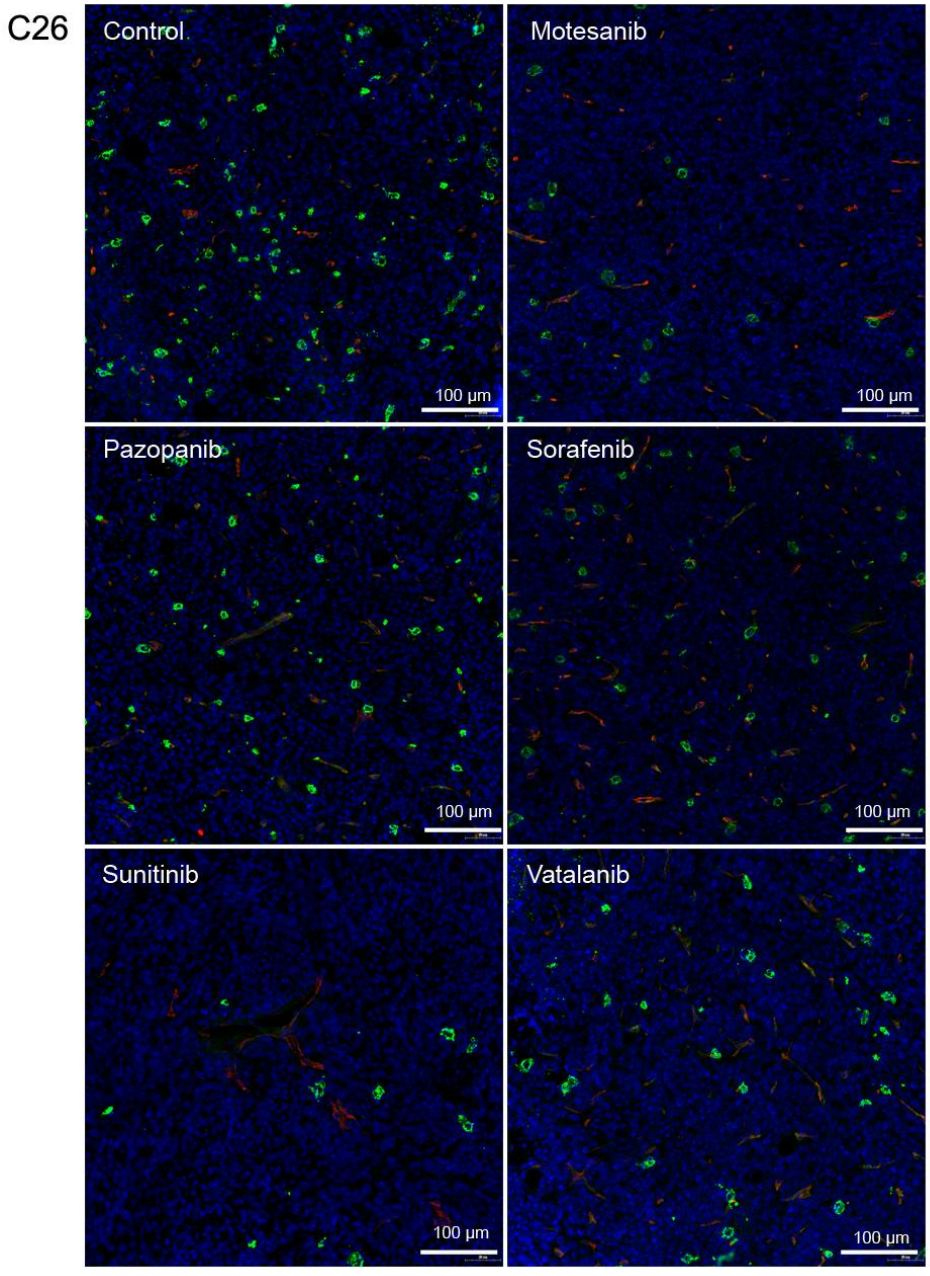

Figure 23. Low power views of C26 tumors stained for VEGFR2 (green). Microvessels are labeled with anti-CD31 (red). Nuclei are stained with Hoechst 33342 (blue).

C38 tumors were characterized by a weak VEGFR2 expression of the CD31+ endothelial layer, but no signal of the receptor on tumor cells was observed. No difference in the expression of VEGFR2 in the treated vs. non treated groups (p=0.6857 and 0.4857 for VEGFR2 density and area respectively) was detected (**Figure 24-25.**).

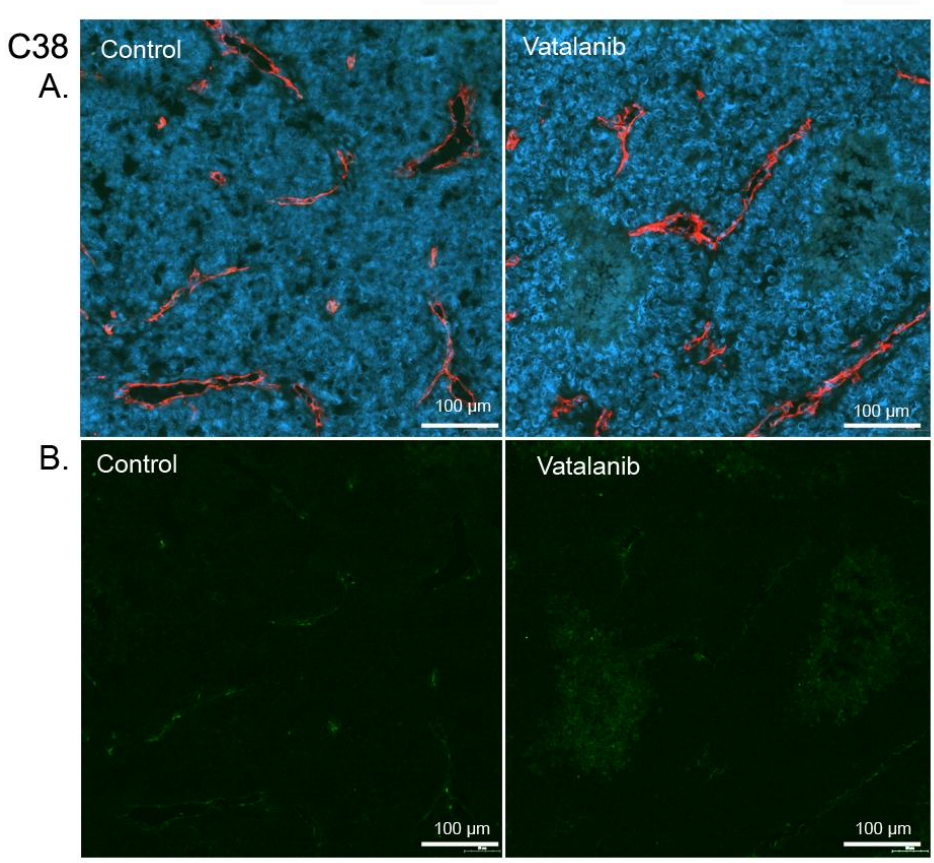

Figure 24. (**A**.) Low power views of C38 tumors stained for VEGFR2 (green). Microvessels are labeled with anti-CD31 (red). Nuclei are stained with Hoechst 33342 (blue). (**B.**) The same images without counterstain with anti-CD31 and Hoechst 33342.

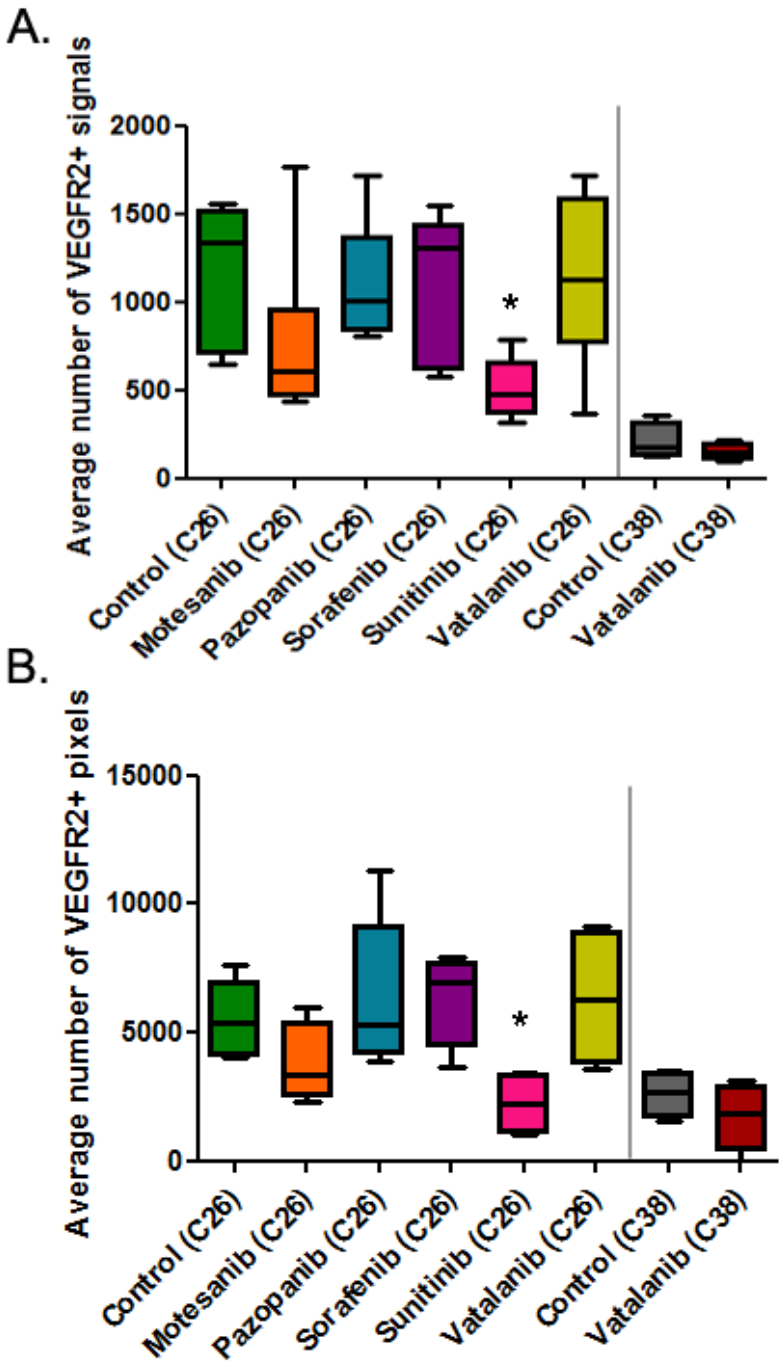

Figure 25. VEGFR2 (**A**.) densities and (**B**.) areas of C26 and C38 tumors. Data are shown as box (first and third quartiles) and whisker (maximum to minimum) plots with the mean (horizontal bar) from 6 animals per group. VEGFR2 densities were counted in ten viable intratumoral regions. VEGFR2 areas were calculated by counting the number of VEGFR2-positive pixels in ten viable intratumoral regions. p=0.0296 and 0.022 for VEGFR2 density and VEGFR2 area respectively in the C26 model as shown by the Kruskal-Wallis test, p=0.6857 and 0.4857 for VEGFR2 density and VEGFR2 area respectively in the C38 model as shown by the Mann Whitney U test.

We found a significant difference between the MVD of the C26 groups, $p<0.0001$. The post-hoc test showed a suppressed MVD by sunitinib, motesanib and minimally vatalanib in that model. Microvessel area was also decreased in the sunitinib, motesanib and less intensively in the sorafenib treated group, $p<0.0001$ (**Figure 26-27.**).

In the C38 model however, no difference in the vessel density ($p=0.235$), but in vessel area was detected, $p=0.0341$ (**Figure 26-27.**). It is also important to mention, that major differences in the vasculature of the two groups were observed. While C26 tumors had lots of small vessels, C38 tumors were characterized by only a few, but large and complex vascular structures.

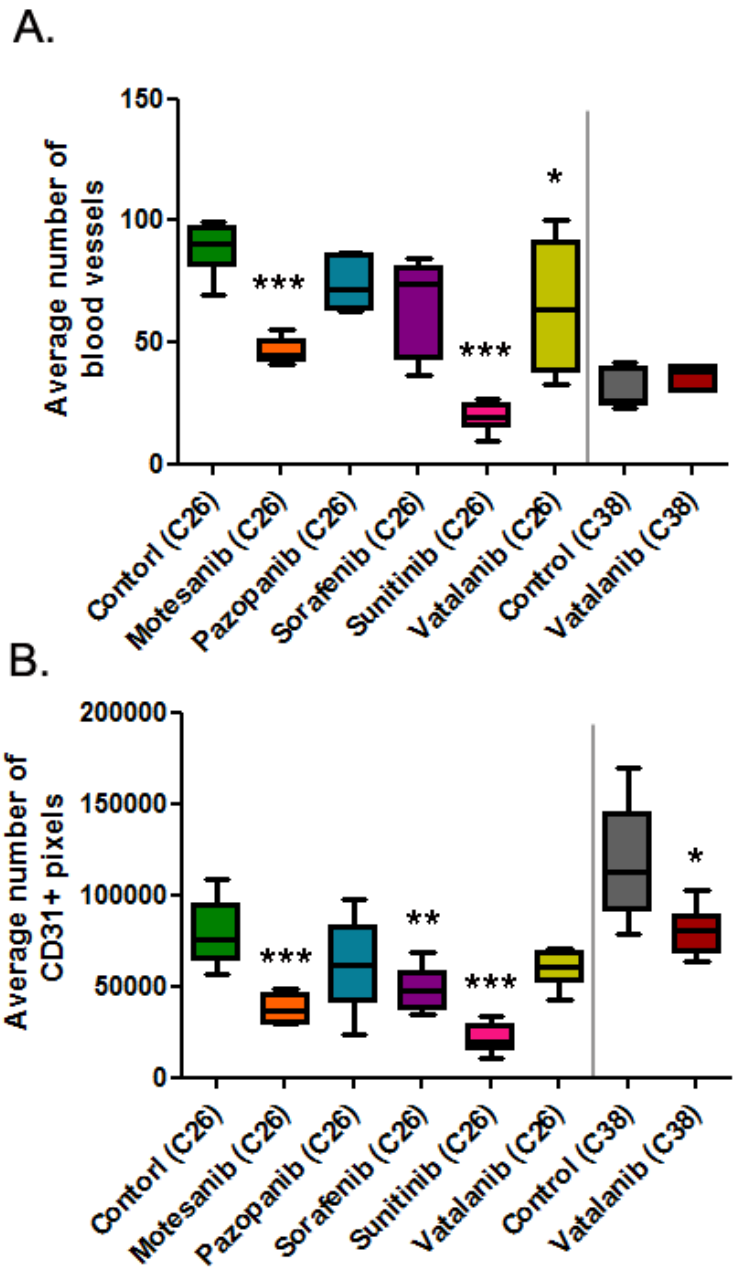

Figure 26. Microvessel density (**A.**) and microvessel area (**B.**) data of C26 and C38 tumors. Data are shown as box (first and third quartiles) and whisker (maximum to minimum) plots with the mean (horizontal bar) from 6 animals per group. Microvessel densities were counted in ten viable intratumoral regions. Microvessel areas were calculated by counting the number of CD31-positive pixels in ten viable intratumoral regions. $p<0.0001$ both for MVD and vessel area in the C26 model as shown by the one-way Anova test, $p=0.235$ and 0.0341 for vessel density and area respectively as shown by unpaired t-test in the C38 model.

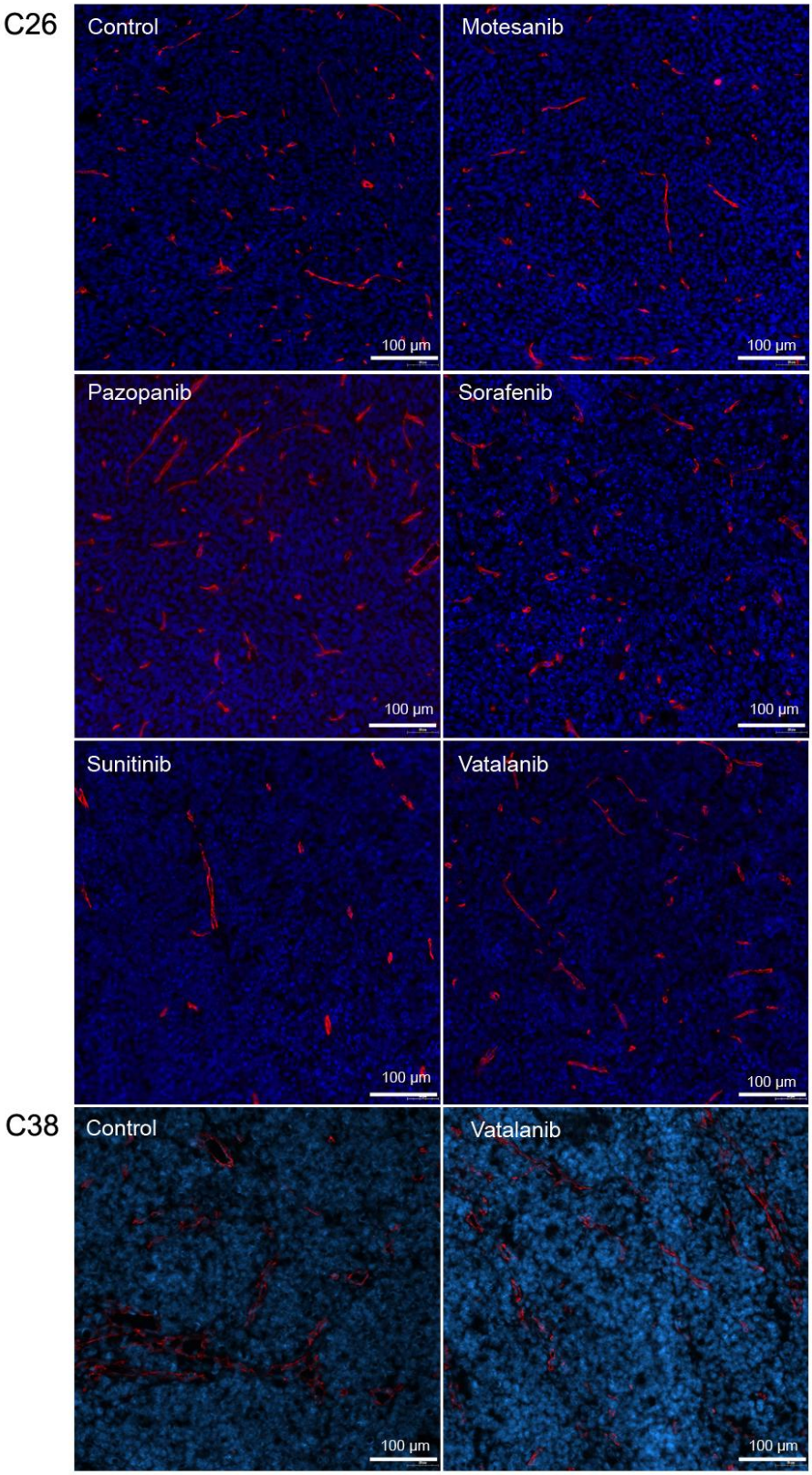

Figure 27. Microvessel density and area of C26 and C38 tumors. Tumors were labeled for the endothelial cell marker CD31 (red) and nuclei are stained with Hoechst 33342 (blue).

MVD clearly correlated with tumor oxygenation. Hypoxia was located in the less vascularized areas of the tumor. Accordingly, a significant increase (p=0.0152) in the intratumoral hypoxic areas was observed in the sunitinib treated group (**Figure 28-29.**). The ratio of hypoxic areas did not differ (p=0.9143) in the C38 model (**Figure 28-29.**).

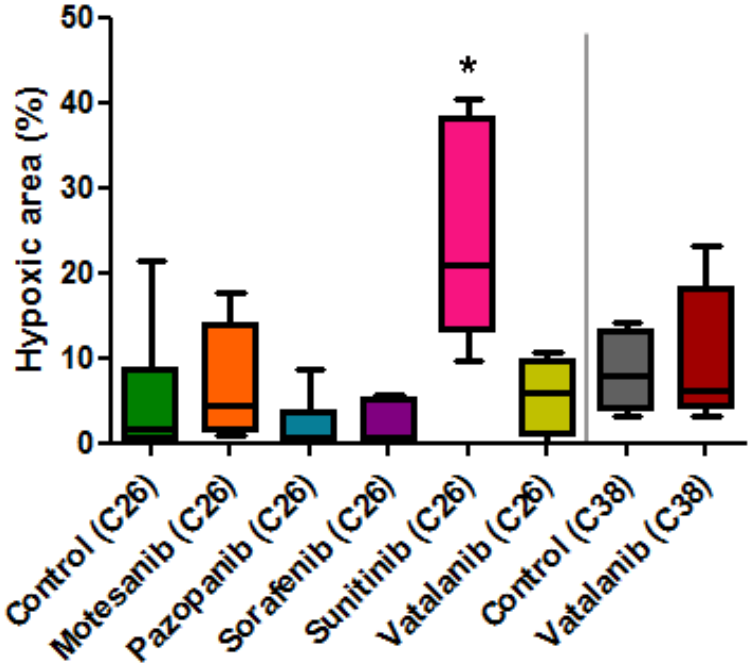

Figure 28. Hypoxic areas of C26 and C38 tumors. Data are shown as box (first and third quartiles) and whisker (maximum to minimum) plots with the mean (horizontal bar) from 6 animals per group. Hypoxic areas are shown in the percentage of the total tumor sections. p=0.0152 as shown by the Kruskal-Wallis test in the C26 model and 0.9143 as shown by the Mann-Whitney U test in the C38 model.

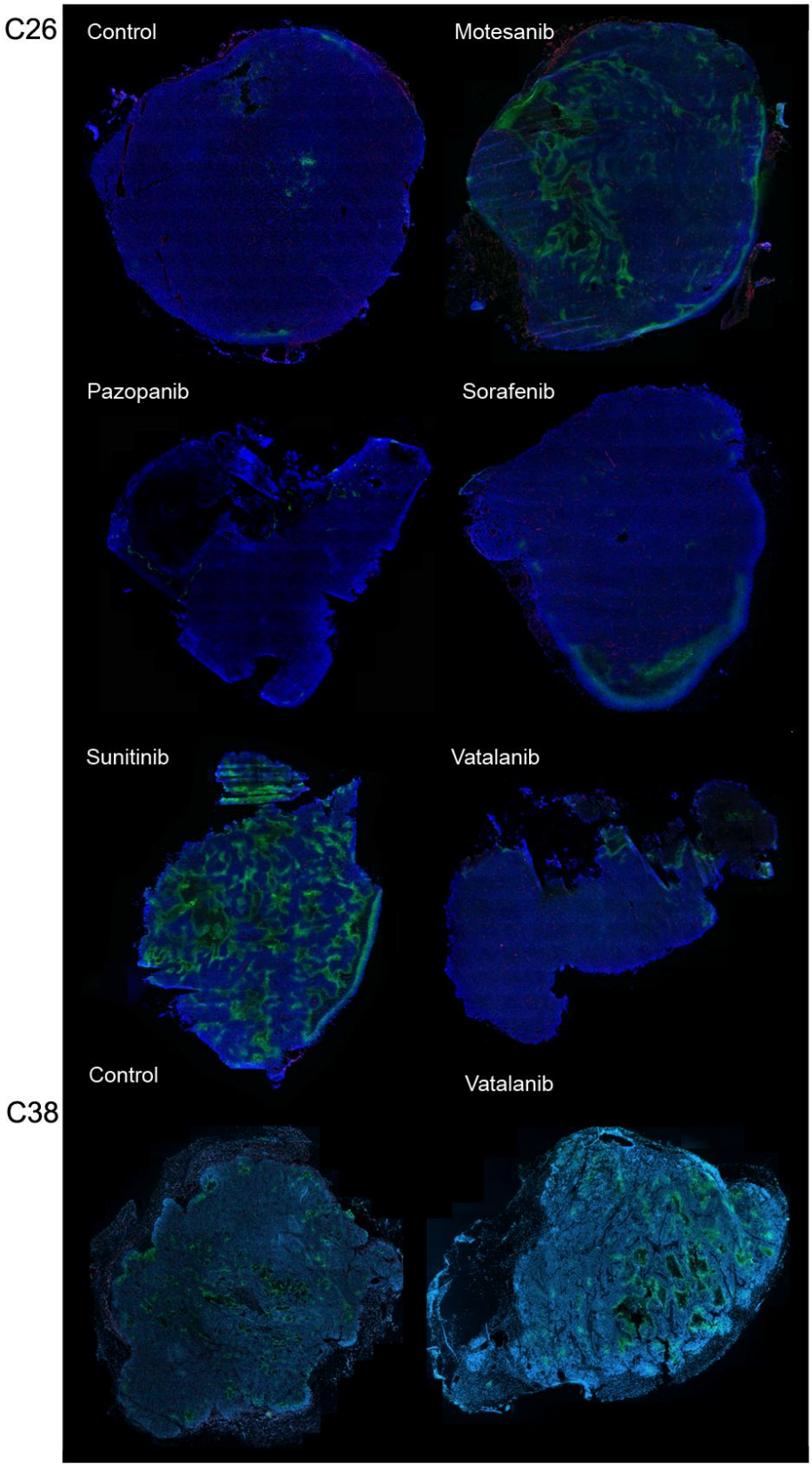

Figure 29. Representative images of hypoxic areas in the C26 and C38 tumors. Green: anti-pimonidazole staining for hypoxia; blue: nuclear staining with Hoechst 33342.

Beside the inhibition of endothelial cell proliferation, multi-target antiangiogenic RTKIs also influence PDGFR and FGFR positive pericyte and VSMC recruitment to tumor blood vessels. Therefore, the inhibition of these receptors may result in not only decreased MVD and consequently lower blood flow rate of tumors, but could also facilitate cancer cell metastatization. To observe the structural changes of the vasculature in response to treatment, we examined the expression of laminin, desmin and αSMA of tumor sections. While all vessels remained underlaid with a definite layer of laminin and covered with αSMA, desmin expression has decreased in response to sunitinib and motesanib treatment in the C26 model; p=0.0135 (**Figure 30-32.**).

Both laminin and αSMA expression were definite and did not change in response to treatment in the C38 model (**Figure 30-31.**), but unlike in C26, no difference in desmin expression was observed either p=0.9143 (**Figure 32-33.**).

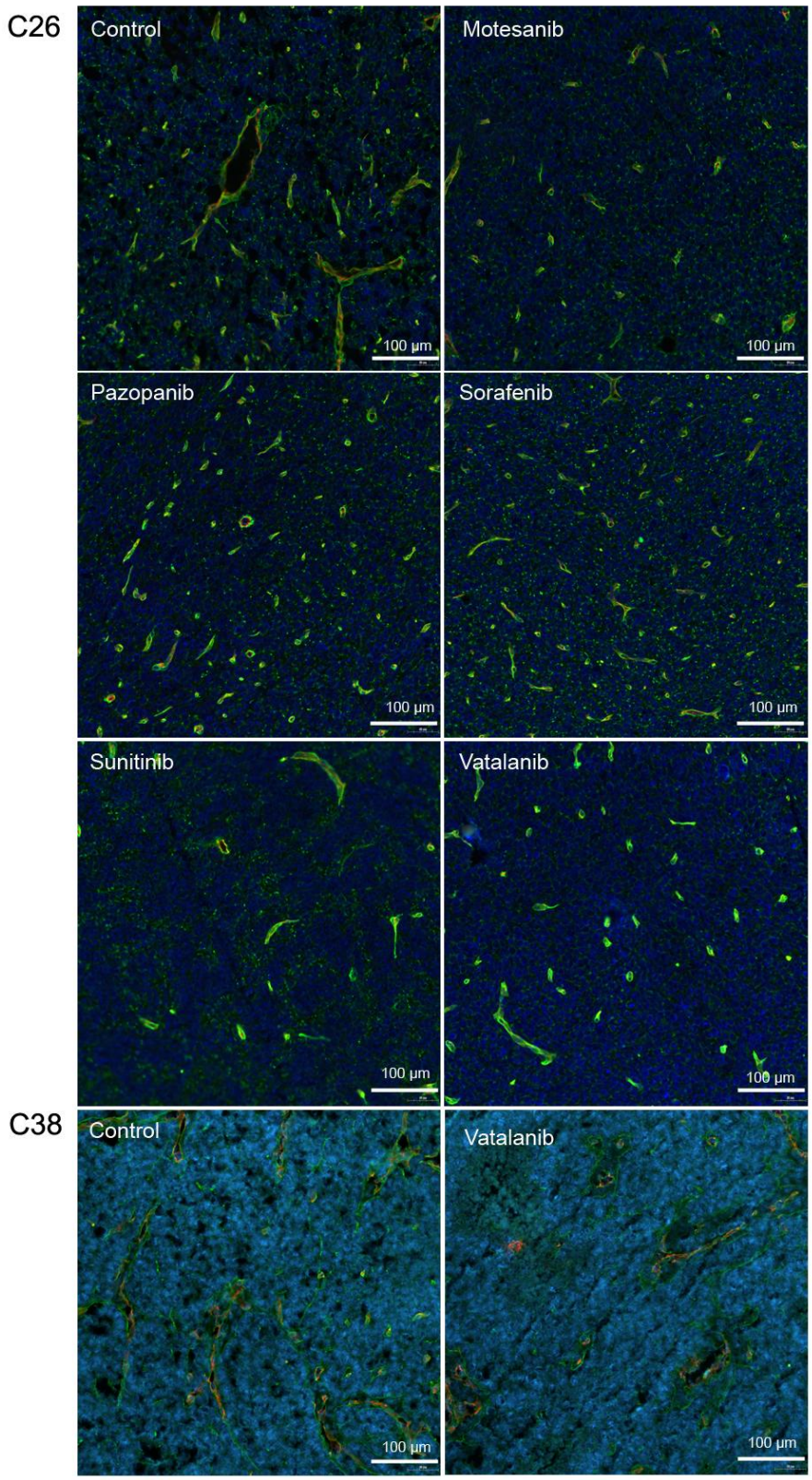

Figure 30. Low power views of C26 and C38 tumor sections stained for the capillary basement membrane component laminin (green) and CD31 (red). Nuclei are stained with Hoechst 33342 (blue). Note that tumor cells are also weakly positive for laminin.

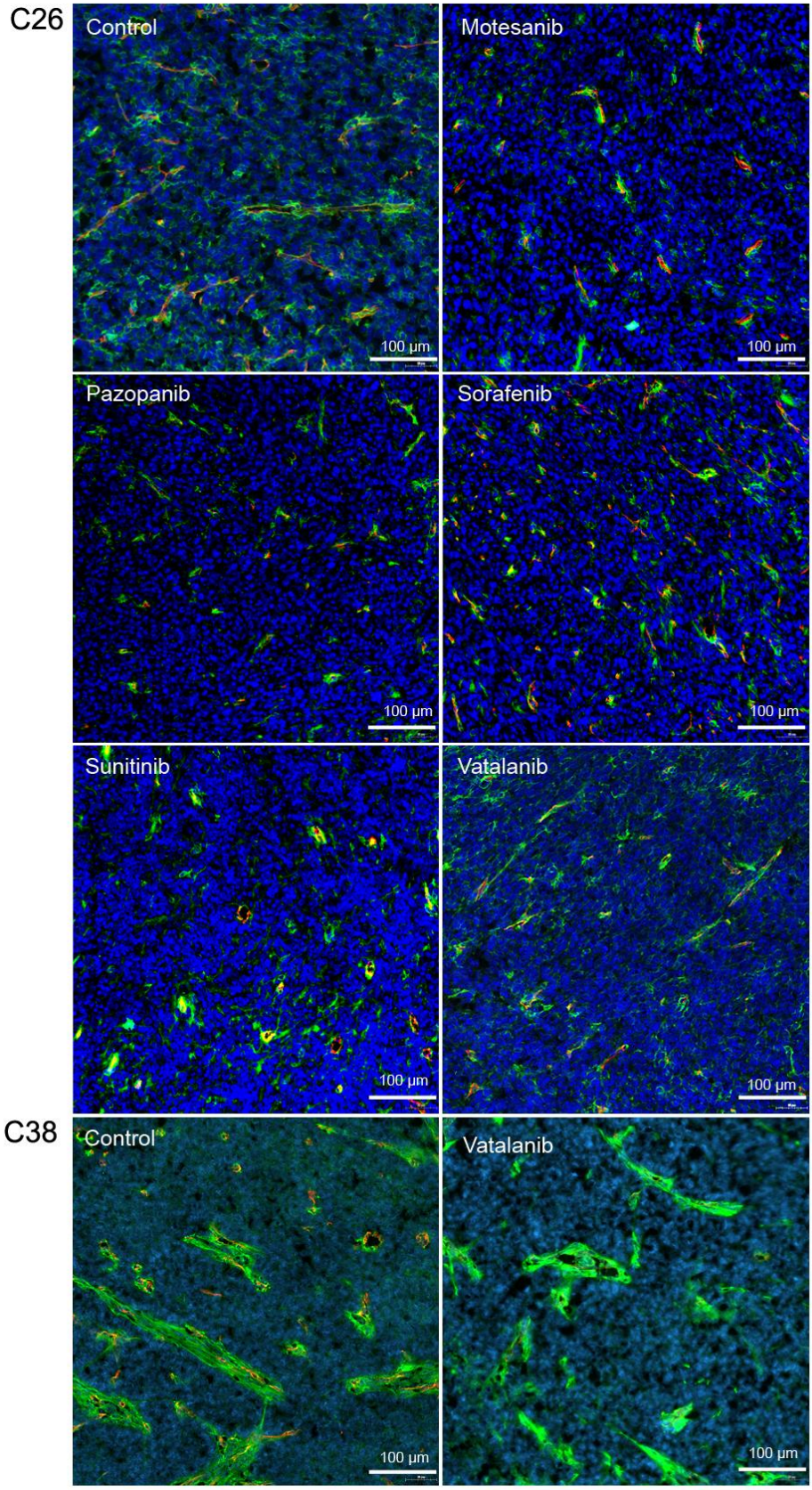

Figure 31. Low power views of C26 and C38 tumor sections stained for αSMA (green) and CD31 (red). Nuclei are stained with Hoechst 33342 (blue).

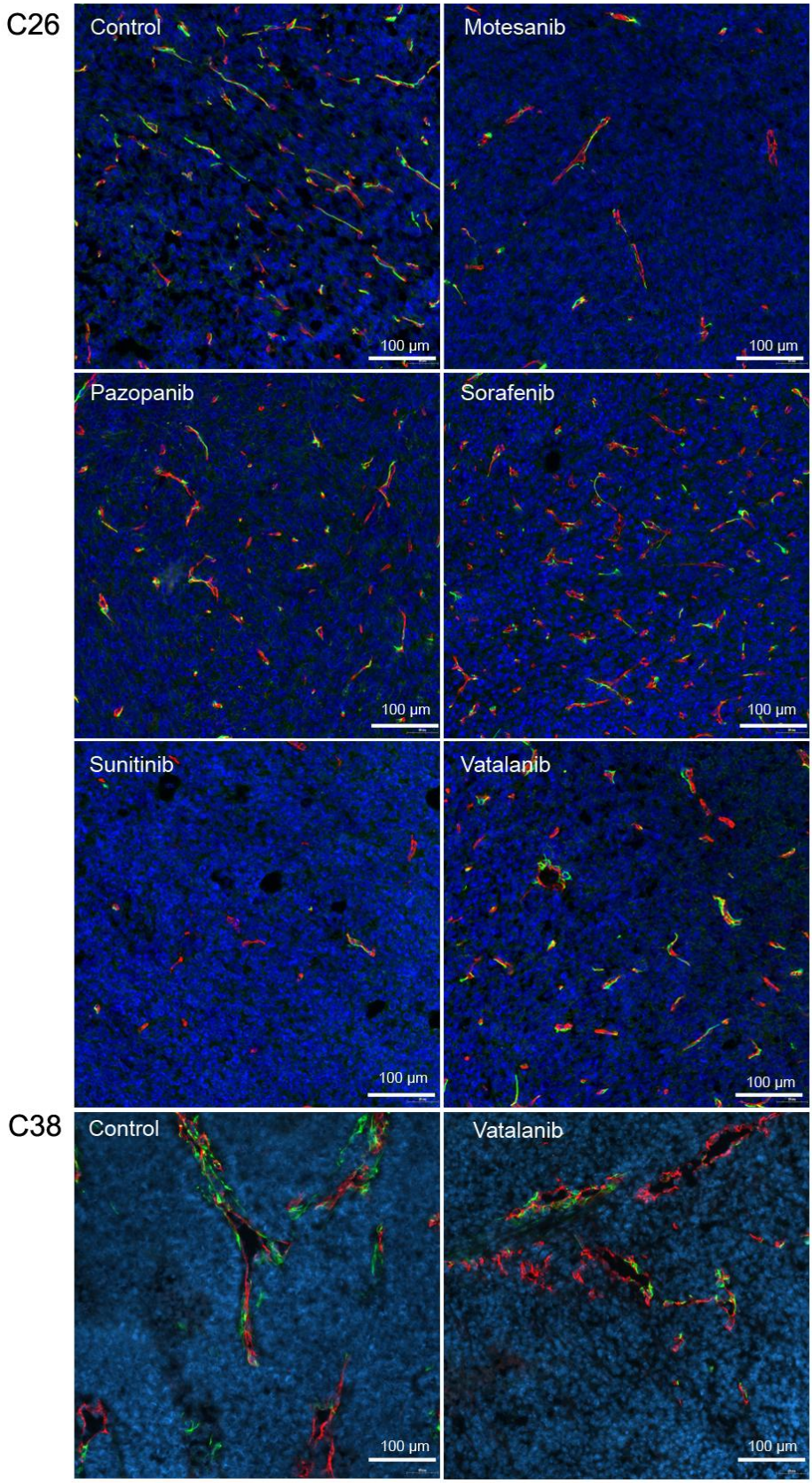

Figure 32. Desmin expression in C26 and C38 tumors. Tumor sections are immunolabeled for pericyte desmin (green) and CD31 (red). Nuclei are counterstained with Hoechst 33342 (blue).

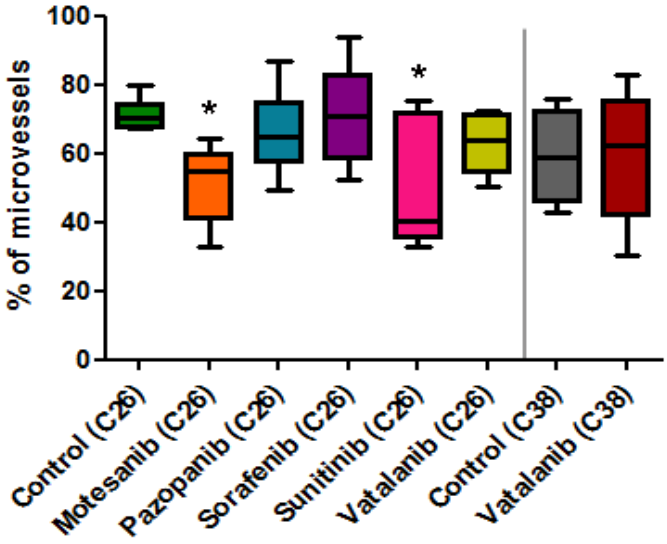

Figure 33. Desmin expression of C26 and C38 tumors. Data are shown as box (first and third quartiles) and whisker (maximum to minimum) plots with the mean (horizontal bar) from 6 animals per group. Desmin expression is expressed in the % of the microvessels covered by desmin expressing pericytes. p=0.0135 for the C26 model and 0.9143 for the C38 model as shown by the one-way Anova and the Mann-Whitney U tests respectively.

6.3 Mass spectrometric analysis

6.3.1 Compound characterization

To determine if these differences in the biological effects of the compounds arise from the differences in the intratumoral drug distribution, we have developed a method to characterize the antiangiogenic RTKIs in tissue samples.

First, the *m/z* value of the quasimolecular ion and fragmentation pattern of each drug compound were defined on a MALDI stainless steel target plate.

The quasimolecular ion of motesanib was detected at *m/z* 374.199. Fragmentation of the molecule resulted in ions at *m/z* 212.1, which corresponds to the split at the amide bond of nicotinamide. The fragment ions corresponding to the indoline formamide moiety were identified at *m/z* 189.1. Cleavage of the pyridine moiety and charge retention resulted fragment ions at *m/z* 163.1.

Pazopanib was detected with a quasimolecular ion at *m/z* 438.17. Subsequent MS/MS fragmentation of the precursor ions led to the loss of the amidogen group, generating fragment ions at *m/z* 421.1. Further loss of the sulfur dioxide eventuated fragment ions

at *m/z* 357.1, while the presence of fragment ions at *m/z* 342.1 indicated the loss of an additional methyl group.

The quasimolecular ion of sorafenib was found at *m/z* 465.093. Dehydroxylation of the formamide moiety and subsequent bond retention resulted in fragment ions at *m/z* 447.1, while cleavage of the pyridine ring eventuated fragment ions at *m/z* 425.1. Fragmentation of the molecule also led to detection of ions at *m/z* 270.2, corresponding to the loss of the chloro-trifluoromethyl-phenylamine group. Presence of fragment ions at *m/z* 252.2 indicated the cleavage of the chloro-trifluoromethyl-phenyl ring and the scission of the carboxamide group.

Sunitinib was identified with a quasimolecular ion at *m/z* 399.218. Subsequent MS/MS fragmentation of the precursor ions led to the loss of the terminal diethylamino group, generating fragment ions at *m/z* 326.1, while the presence of fragment ions at *m/z* 283.1 indicated a cleavage at the amide group.

The quasimolecular ion of vatalanib was seen at *m/z* 347.105. Scission of the benzene ring resulted in the generation of ions at *m/z* 320.2. Loss of the chloride eventuated fragment ions at *m/z* 311.2. Decomposition of the phthalazin-amine ring led to the detection of ions at *m/z* 294.2. Loss of the pyridine moiety resulted in fragment ions at *m/z* 268.1, whle cleavage of the methylpiridyne group indicated the detection of ions at *m/z* 254.1. Loss of the chlorophenil-amine group resulted in fragment ions at *m/z* 220.2.

When applied to the tissue surface, drug molecules showed similar ionization and fragmentation properties to those generated on the MALDI plate. The same quasimolecular ions and fragment ions detected on both surfaces are shown in **Table 4**.

Table 4. Chemical properties of the studied drugs

	Motesanib	**Pazopanib**	**Sorafenib**	**Sunitinib**	**Vatalanib**
Chemical formula	$C_{22}H_{23}N_5O$	$C_{21}H_{23}N_7O_2S$	$C_{21}H_{16}ClF_3N_4O_3$	$C_{22}H_{27}FN_4O_2$	$C_{20}H_{15}ClN_4$
Molecular weight (g/mol)	373.45	437.52	464.82	398.47	346.81
Quasimolecular ion $[M+H]^+$ (*m/z*)	374.199	438.170	465.093	399.218	347.105
Fragment ions (*m/z*)	212.1;189.1; 163.1	421.1; 357.1; 342.1	447.1; 425.1; 270.2; 252.2	326.1; 283.1	320.2; 311.2; 294.2; 268.1; 254.1; 220.2

6.3.2 Precursor compound and metabolite detection in the blood

Adsorption of the drugs was examined in the peripheral blood, drawn just before sacrificing the animals. In both models all applied drugs absorbed successfully with notable signal intensities being observed in the peripheral blood.

Moreover, all so far identified metabolites of motesanib (414) could also be characterized in blood samples, however, 2-amino nicotinamide metabolite (*m/z* 283.157), the lactam form of this metabolite (*m/z* 297.137), the carbinolamine metabolite (*m/z* 372.184), and the oxindole metabolite (*m/z* 388.179) were found with high signal intensities, reaching 5-90% of the signal intensitiy of the precursor compound (**Figure 34.**).

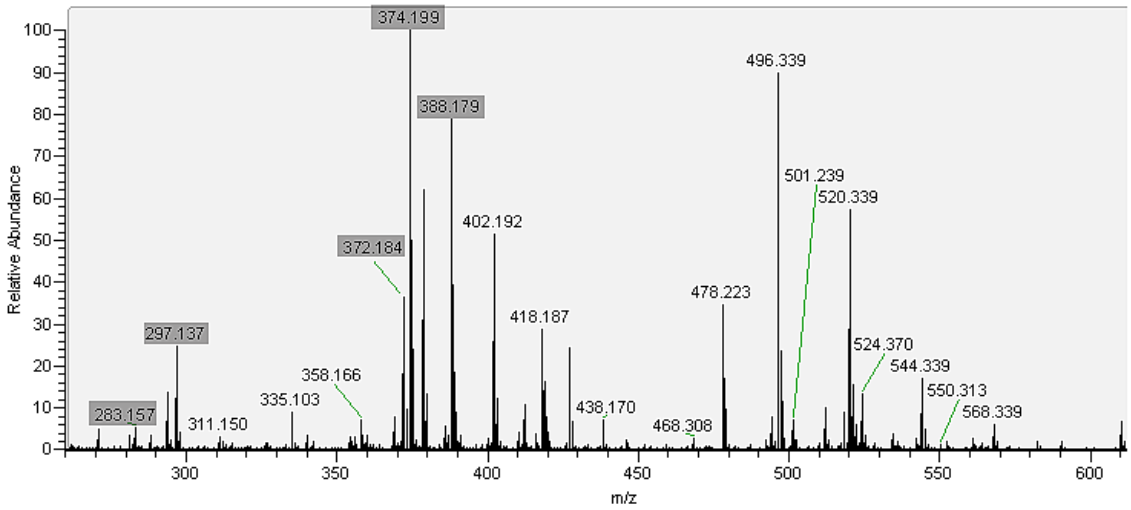

Figure 34. A representative mass spectrum of a blood sample taken from a motesanib-treated mouse. Marked are peaks of motesanib and its main metabolites.

Metabolization of pazopanib is less remarkable. Indeed, although all so far detected (415) metabolites of pazopanib were traceable, but none of them reached 5% of the signal intensity of the precursor pazopanib (**Figure 35.**).

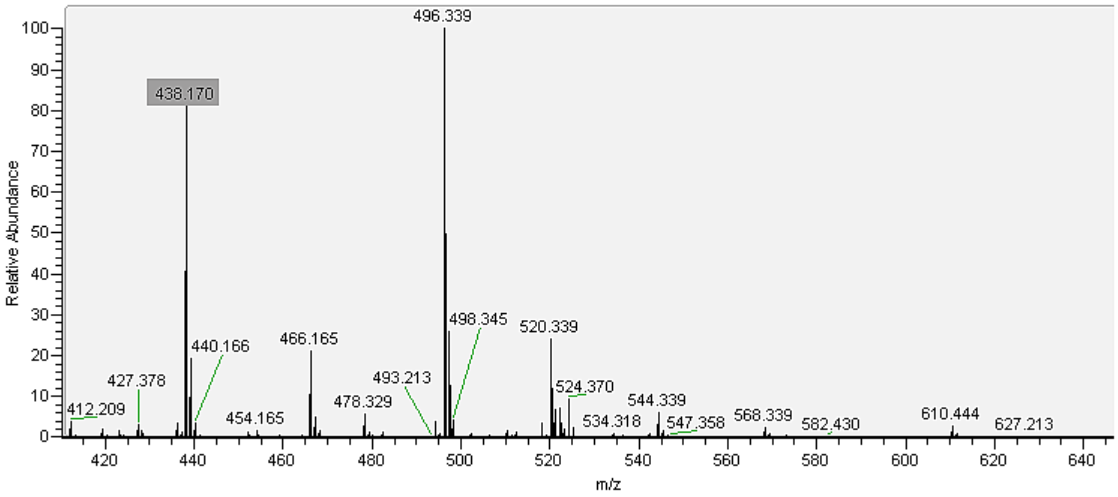

Figure 35. A representative mass spectrum of a blood sample taken from a pazopanib-treated mouse. Peak of pazopanib is marked.

Sorafenib was present with the lowest signal intensity in the blood samples. Moreover, metabolization of sorafenib is even less known than that of pazopanib. Neither the N-oxide, nor the glucuronide metabolite of sorafenib was reliably detected, but the desmethylated metabolite (*m/z* 451.078) was traceble (**Figure 36.**).

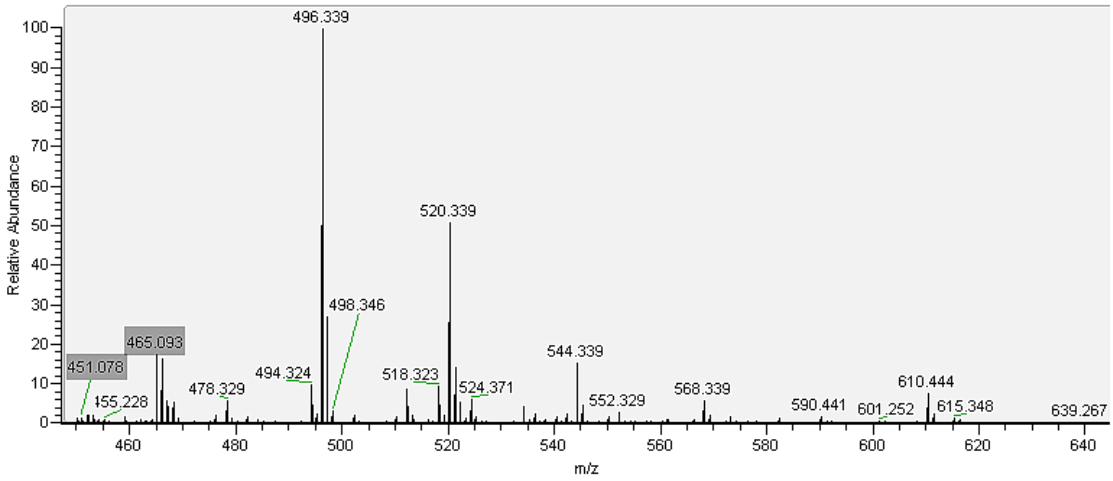

Figure 36. A representative mass spectrum of a blood sample taken from a sorafenib-treated mouse. Marked are peaks of sorafenib and its main metabolite.

Sunitinib was measured in all plasma samples, moreover, all metabolites of the precursor compound were also traceable and could be characterized. Presumed structures and MS/MS spectra of the precursor compound and its metabolites in blood plasma are presented in **Figure 37**.

The previously described bis-desethylated metabolite (M1) of sunitinib (349), with the quasimolecular ion at *m/z* 343.000 could be detected only in a few blood samples performing full mass scans. However, isolating and fragmenting the proposed peak of that metabolite resulted in fragment ions at *m/z* 326.2 and 283.1 in all samples. Stepwise elevation of the collision energy proved that the detected fragment ions are formed by the fragmentation of M1. The missing precursor ion in full mass spectra may be explained by the low concentration of M1 that appeared to be below the detection limit of the FT analyser compared to the linear ion trap.

The signal generated at *m/z* 358.126 of M2 indicates the loss of the terminal diethylamine group, with the oxidation of the molecule. This resulted in fragment ions at *m/z* 283.1 but not at *m/z* 326.1. The presence of fragment ions at *m/z* 340.2 refers to the terminal dehydroxilation of the molecule.

M3, an active metabolite of sunitinib (SU012662) (416) was formed by the mono-desethylation of the molecule, resulting a quasimolecular ion at *m/z* 371.188 and the same fragment ions as sunitinib.

Two mono-hydroxilated variations of the active metabolite were detected at *m/z* 387.182. M4 was modified at the indolylidene-dimethylpyrrole moiety, resulting fragment ions at *m/z* 342.2 and 299.1. M5 was hydroxilated at the carbon next to the amide nitrogen, which generated fragment ions at *m/z* 283.1. The detected fragment ion peak at *m/z* 369.2 could be derived from both molecules by dehydroxilation.

Loss of two hydrogen atoms of the terminal ethyl group of sunitinib eventuated in a metabolite (M6) at *m/z* 397.203 Fragmentation of the molecule generated ions at *m/z* 326.1 and 283.1.

Fragment ions of a previously described metabolite with the quasimolecular ion at *m/z* 397.224 (M7) could also be detected by MS/MS (349). Signals of fragments were generated at *m/z* 324.2 and 281.2, suggesting defluorination and subsequent dehydroxilation of the molecule. M7 was not traceable by full MS, probably because of the signal suppression of M6 at *m/z* 397.203.

Similarly to M1, the saturated metabolite of sunitinib, M8, was detected by Speed et al. at *m/z* 401.00 in rat and monkey feces (349). This could only rarely be measured in our mouse model by full MS. However, when isolating the presumed metabolite peak, the detected fragment ions at *m/z* 285.1 and 328.2 indicated the presence of the molecule, and that the saturation occurred at the indolylidene-dimethylpyrrole moiety.

Mono-hydroxylated metabolites of sunitinib were also measured at *m/z* 415.214. Fragmentation of the molecule indicated the oxidation on the indolylidene-dimethylpyrrole group (M9) with 16 Da higher fragments than the corresponding ions of sunitinib at *m/z* 342.2 and 299.2. Moreover, upon fragmentation of the detected metabolite peak, ions at *m/z* 326.1 and 283.1 were also formed, indicating that the oxidation occurred either at one of the terminal carbons of the diethylamine group (M10) or at the amine moiety (M11). M11 was previously synthesized as SU012487 (349). Dehydroxilation of any of the mono-hydroxilated metabolites could result in fragment ions at *m/z* 397.1.

M12 at *m/z* 495.283 was identified as a sulphate conjugate of M9. Desulphuration of the molecule eventuated in fragment ions at *m/z* 415.2, while dehydroxilation resulted in fragment ions at *m/z* 477.2.

The glucuronide metabolite, M13, was detected at *m/z* 575.252. The cleavage at the amide group and the loss of the terminal diethylamino moiety resulted in fragment ions at *m/z* 459.2 and 502.2, respectively.

The metabolite at *m/z* 591.243 (M14) was generated by both the oxidation and the glucuronidation of sunitinib. When the molecule fragmented as the unmodified compound, ions at *m/z* 518.2 and 475.1 were generated. Dehydroxilation eventuated in a signal at *m/z* 573.2, while fragment ions at *m/z* 415.2 were formed by the loss of the dehydrated glucuronic acid. Deglucuronidation and dehydroxilation of the molecule resulted in ions at *m/z* 342.2.

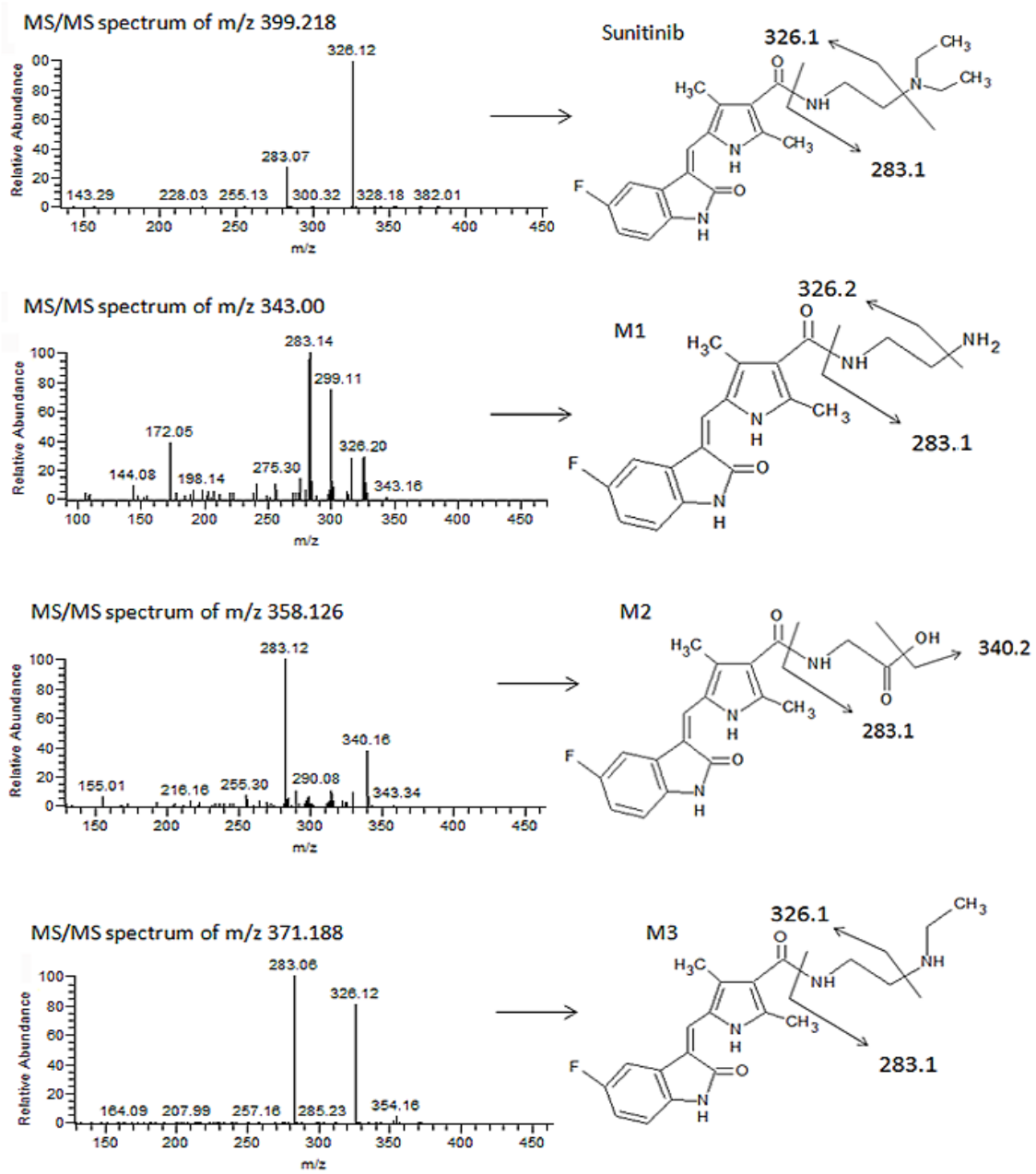

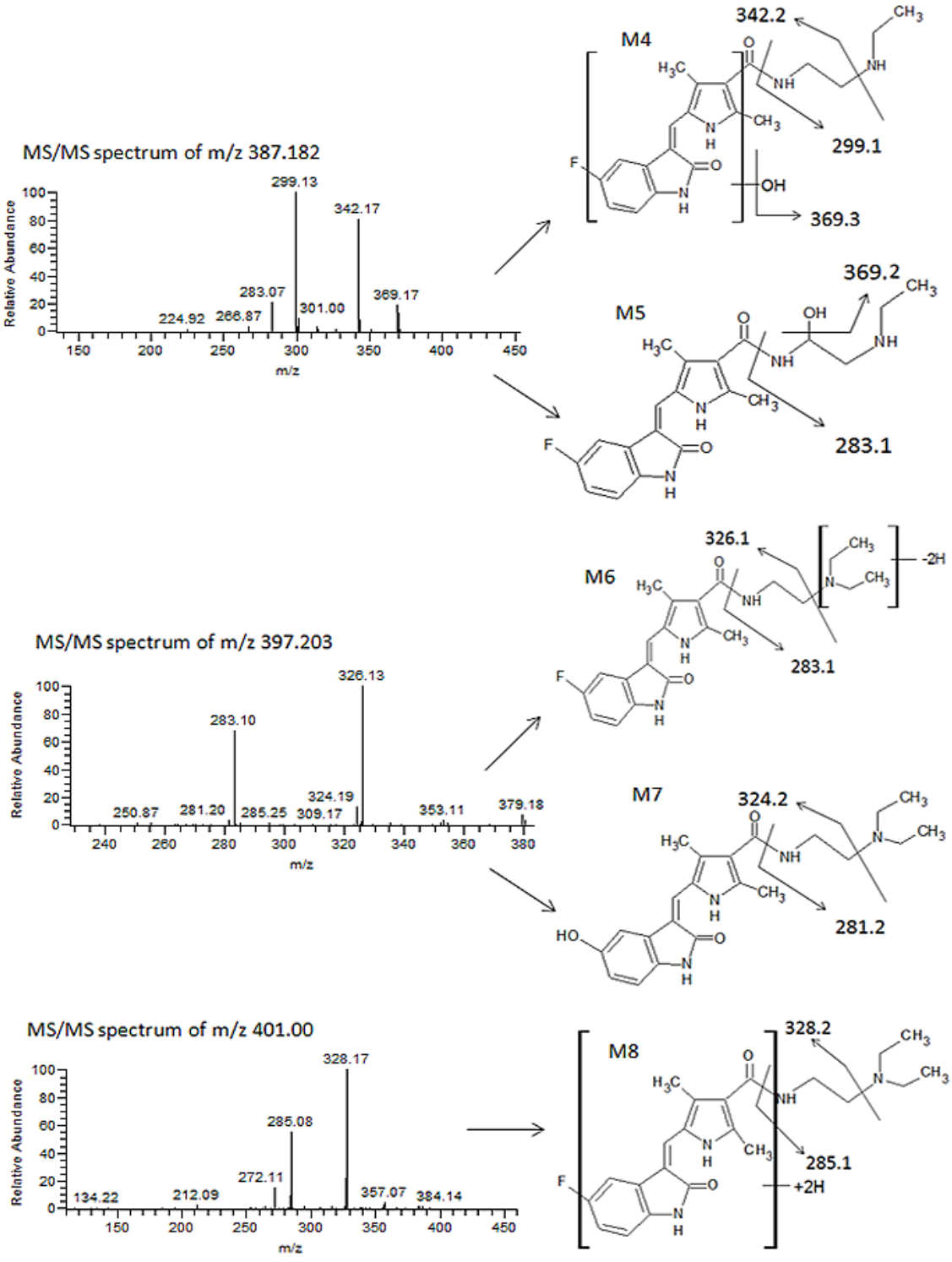
MS/MS spectrum of m/z 387.182
Relative Abundance
m/z
299.13
342.17
283.07
301.00
369.17
224.92
266.87
M4
342.2
299.1
369.3
M5
369.2
283.1
MS/MS spectrum of m/z 397.203
326.13
283.10
324.19
250.87
281.20
285.25
309.17
353.11
379.18
M6
326.1
-2H
283.1
M7
324.2
281.2
MS/MS spectrum of m/z 401.00
328.17
285.08
272.11
134.22
212.09
357.07
384.14
M8
328.2
285.1
+2H

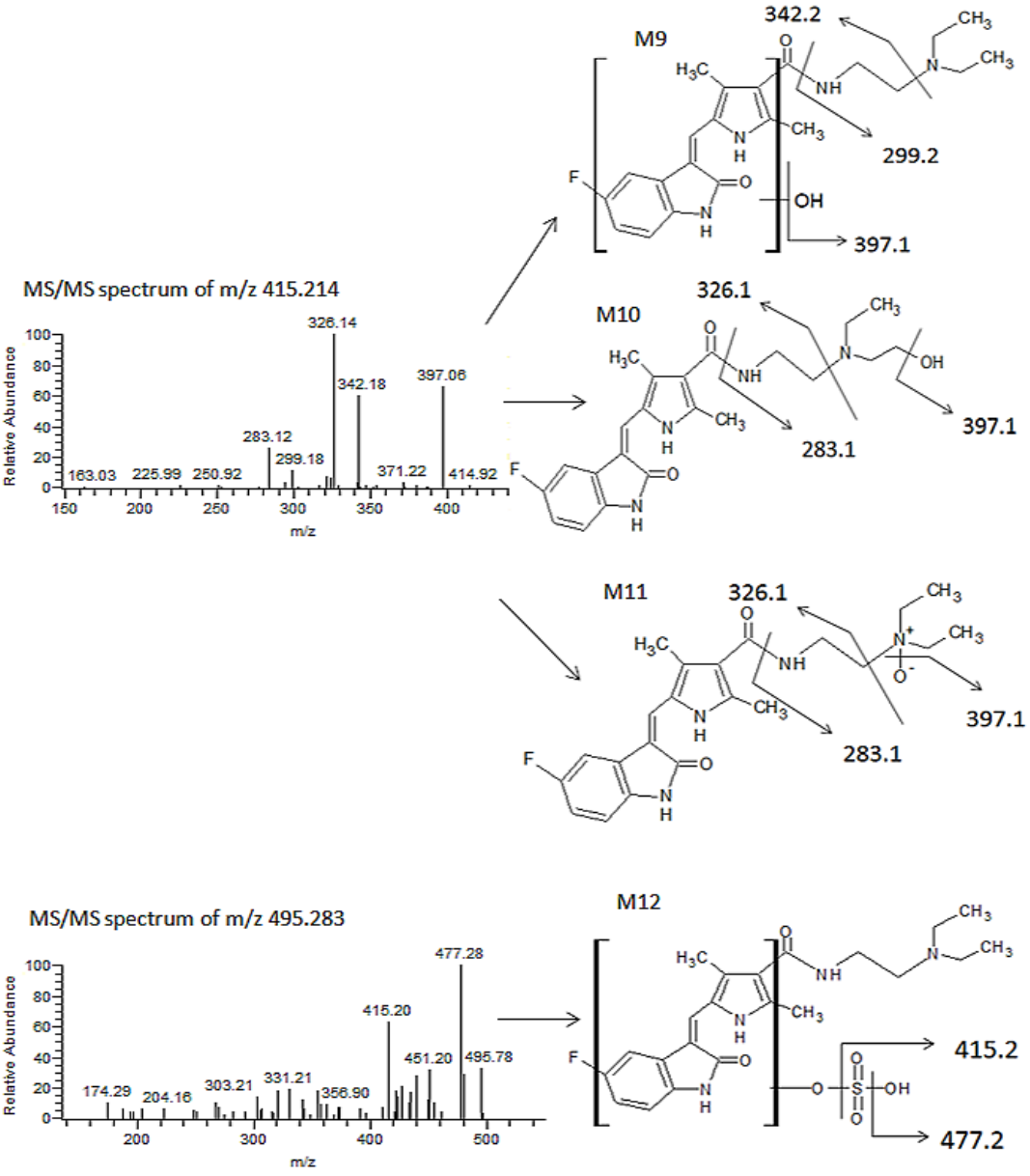
MS/MS spectrum of m/z 415.214
Relative Abundance
m/z
326.14
342.18
397.06
283.12
299.18
163.03
225.99
250.92
371.22
414.92
M9
342.2
299.2
397.1
OH
M10
326.1
283.1
397.1
M11
326.1
283.1
397.1
MS/MS spectrum of m/z 495.283
477.28
415.20
451.20
495.78
174.29
204.16
303.21
331.21
356.90
M12
415.2
477.2

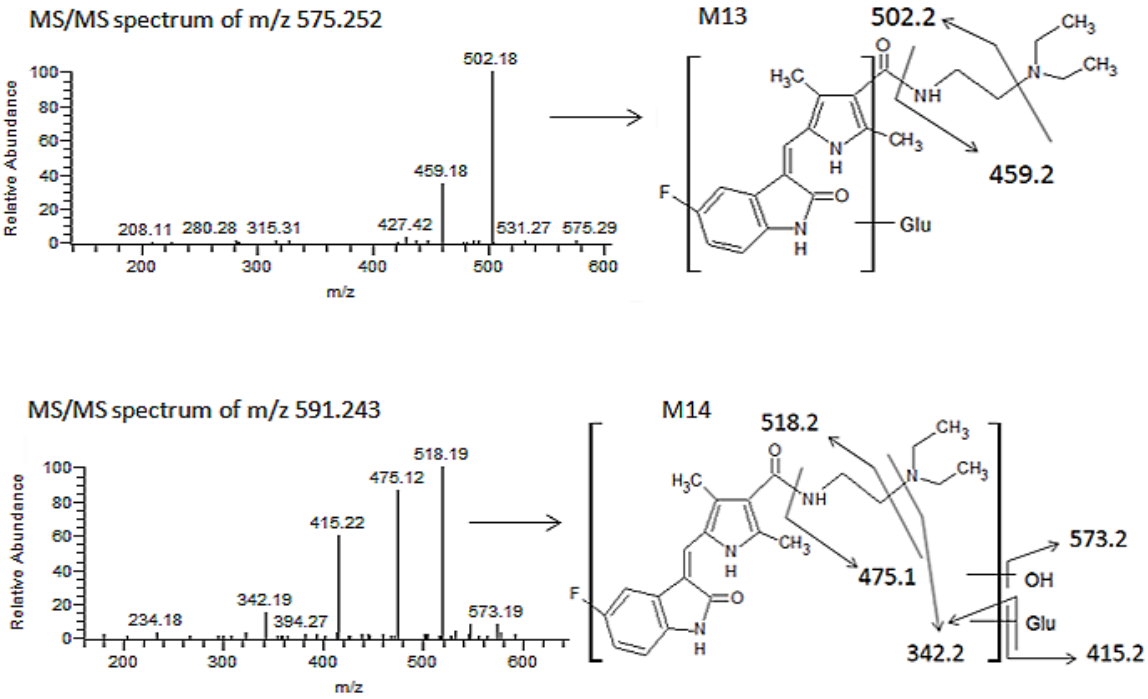

Figure 37. Detection of sunitinib and its metabolites in blood samples. MS/MS spectra of sunitinib and its metabolites with the proposed structure and fragmentation properties.

M3, the active metabolite generated 2-3-fold less intensive signal than the precursor molecule in blood samples. All the other metabolites were only traceable, with less than 5% of the signal intensity of the unmodified compound (data not shown).

Vatalanib also highly metabolized as observed in the blood samples, however, metabolites were mainly traceable, and the signal intensity of only the main oxydative metabolite (*m/z* 363.1) reached the 30% of the precursor compound. No difference in the signal intensities and metabolization pattern of vatalanib in the blood samples taken from the Balb/C and the C57black/6 mice was detected (**Figure 38.**).

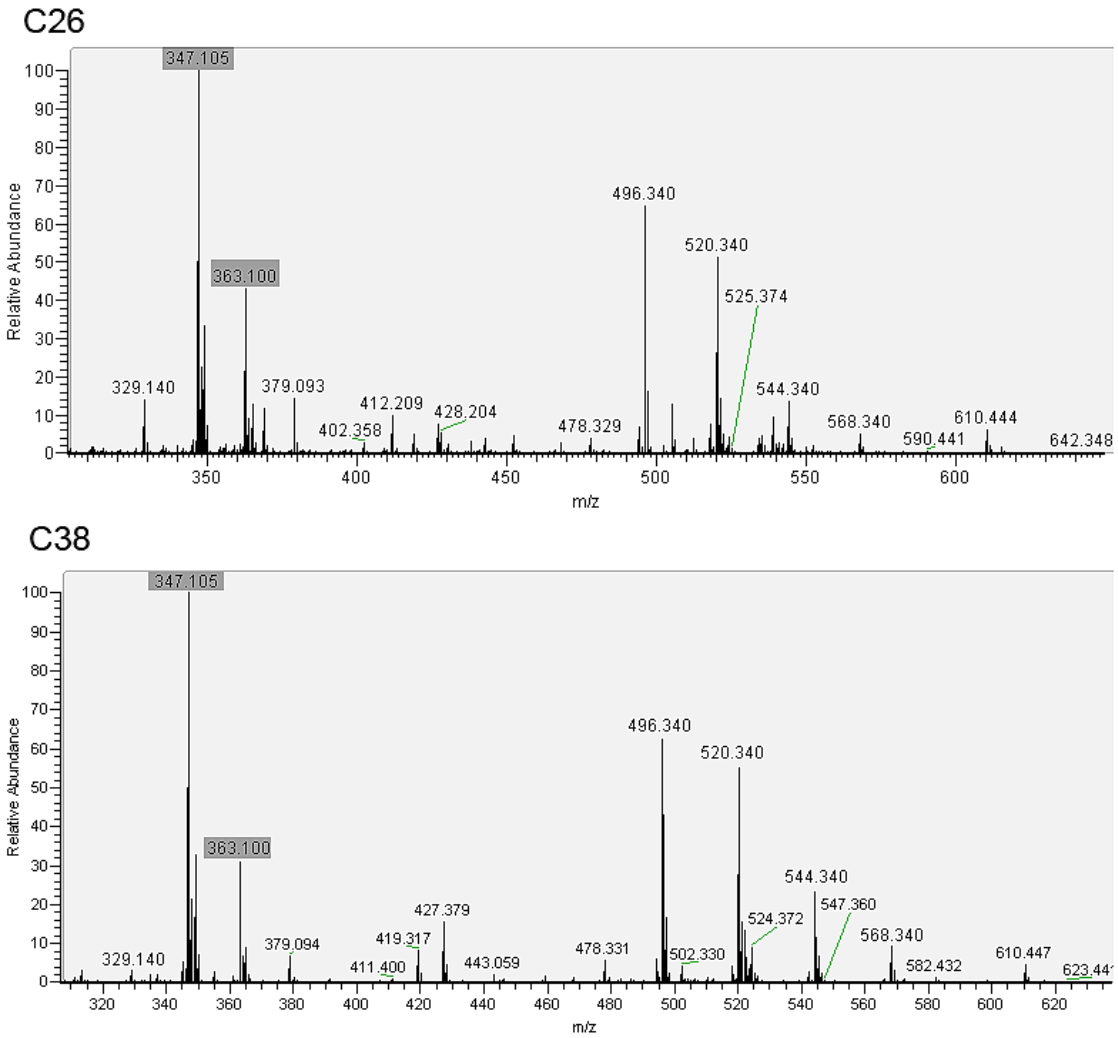

Figure 38. Representative mass spectra of blood samples of mice bearing C26 or C38 tumors, and treated with vatalanib. Marked are peaks of vatalanib and its main metabolite.

6.3.3 Tissue imaging of antiangiogenic RTKIs

Calibration of the drug molecules resulted in linear correlation between concentration and normalized average signal intensity for all compounds in the examined concentration range (**Figure 39.**).

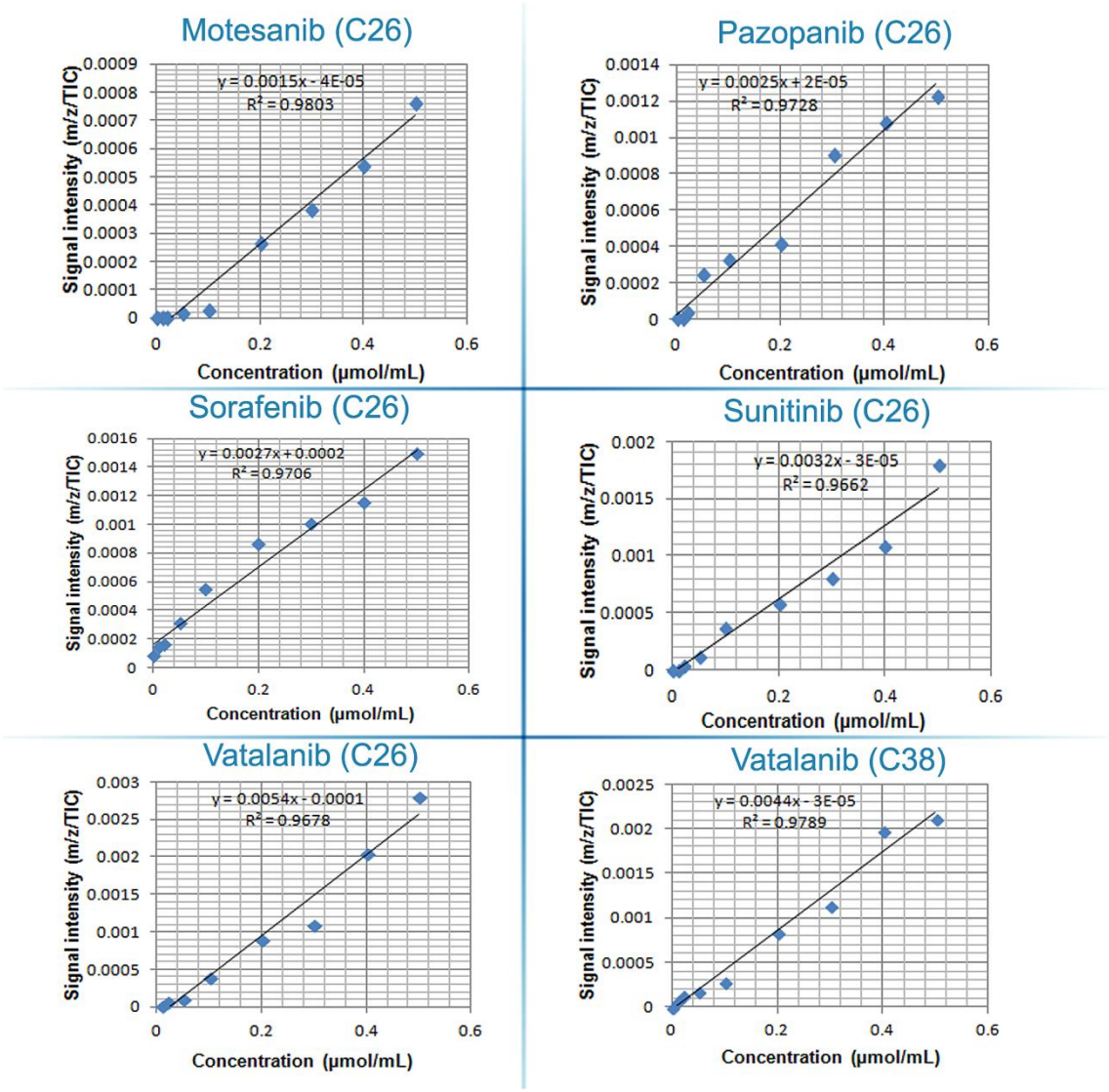

Figure 39. Calibration curves of antiangiogenic RTKIs. Drugs were dissolved and diluted in 50% methanol in the concentration range of 0.001–0.5 µmol·mL−1. One microliters of the compound solutions were applied on control tumor tissue surfaces. Spraying and detection conditions were the same as those during the analysis of in vivo-treated tumors. Average signal intensities of the applied concentrations were measured and normalized to TIC by using Xcalibur v 2.0.7. and ImageQuest™ softwares.

Based on the calibration curves, average signal intensities were translated into drug concentration (µmol/mL) data of C26 and C38 tumors. While intratumoral sorafenib and vatalanib levels did not differ between drug-treated and control C26 tumors (p=1), the concentrations of motesanib, pazopanib and sunitinib were significantly elevated (vs. control), with the highest values detected in the sunitinib-treated animals (0.0083, 0.148, 0.2372 µmol/mL, respectively; **Figure 40.**).

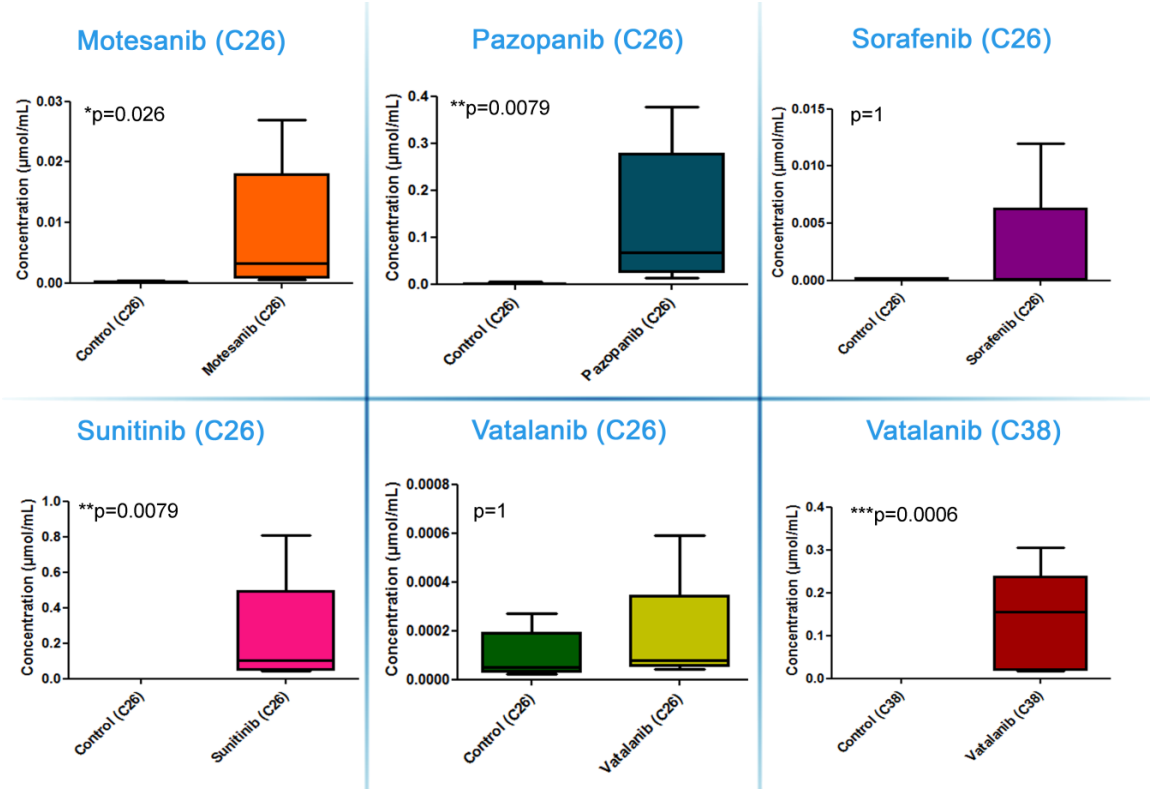

Figure 40. Tumor tissue concentrations of antiangiogenic RTKIs. Signal intensities (normalized to TIC) of the appropriate RTKIs in treated tumors and the same non-specific normalized m/z values measured in control tumors were used to calculate intratumoral drug concentrations. Data are shown as box (first and third quartiles) and whisker (maximum to minimum) plots with the mean (horizontal bar) from 6 animals per group.

Importantly, the above described drug concentrations refer to the entire tumor section and striking differences in the drug distribution were observable within the in vivo-treated C26 tumors. As for sunitinib, the drug was quite homogeneously distributed within the viable C26 tumor areas and apoptotic regions showed notably lower signal intensities (**Figures 41 and 42.**). In contrast, motesanib was seen only in one third of the C26 tumors at relatively high levels in connected areas and the intratumoral distributions of this RTKI and pazopanib (both of which were also present at relatively high average tumor tissue levels; **Figure 40.**) were inhomogeneous with the highest signal intensities observed in non-viable areas (**Figure 41.**). Only traces of sorafenib and vatalanib were detected in the C26 model. Representative images of intratumoral drug distributions are shown in **Figure 41**.

In a previously published study, we found significantly decreased C38 tumor burdens in C57Bl/6 mice treated with vatalanib (267). Accordingly, in order to determine why

mice bearing C26 tumors respond notably poorer to vatalanib than those with C38 tumors, we also utilized MALDI-MSI of C38 tumors and addressed whether there are animal model-specific variations in the tumor tissue penetration and distribution of antiangiogenic RTKIs. In contrast to the C26 model, vatalanib was well-distributed with notable signal intensities in the C38 tumors (**Figure 41.).** In line with this, in vatalanib-treated mice bearing C38 tumors, the intratumoral drug concentration was significantly higher than that in the group of untreated controls (p=0.0006, **Figure 40.**). It is also important to mention that we found significantly higher vatalanib concentrations in C38 than in C26 tumors (0.142 μmol/mL vs 0.174 nmol/mL, p=0.0025, **Figures 40 and 41**.). No correlation between drug signal intensities in the blood and in the corresponding tumor tissue was detected.

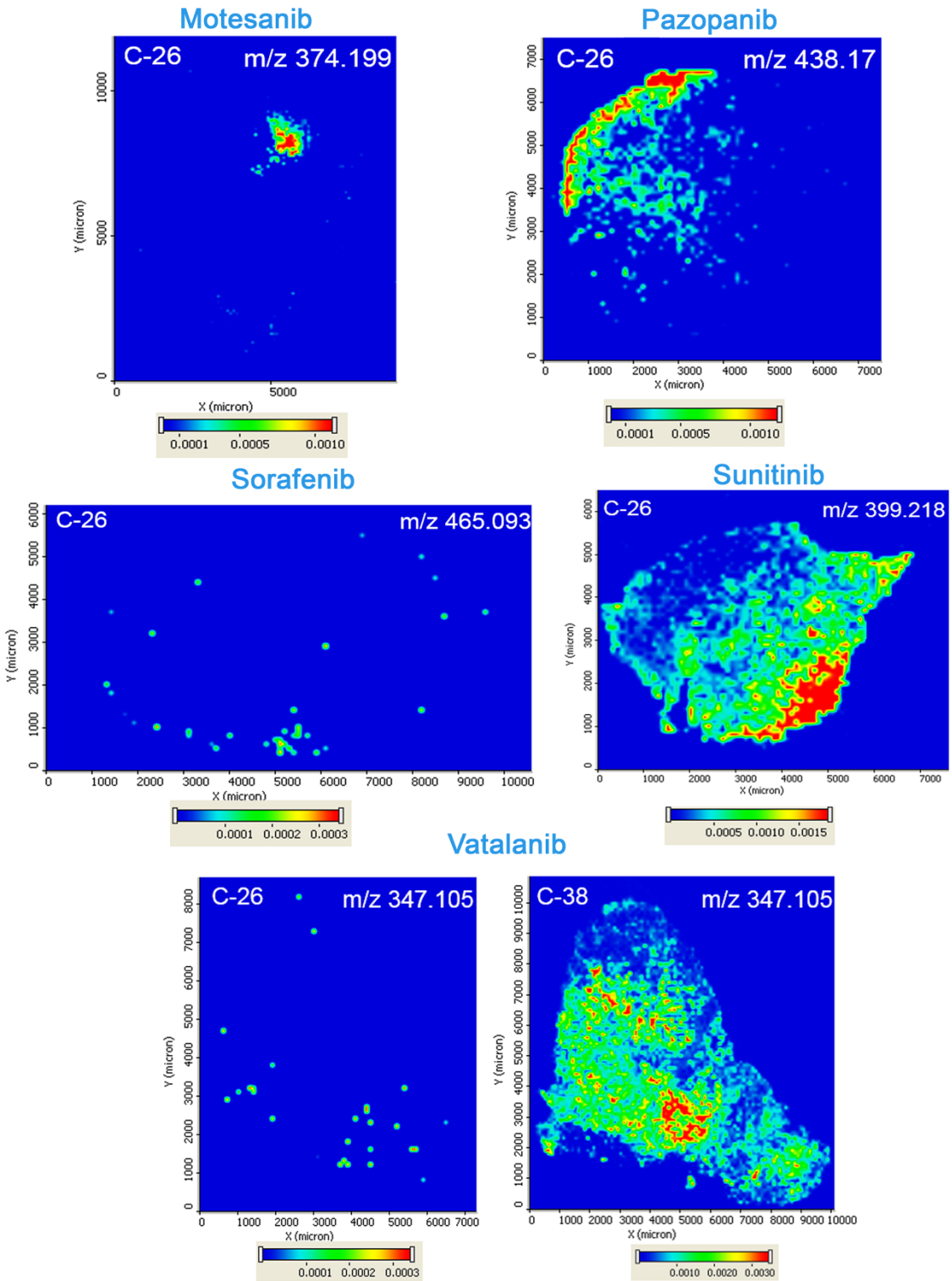

Figure 41. Representative images of drug distribution in C26 and C38 tumors after two weeks of treatment with different antiangiogenic RTKIs. Precursor ion signals of RTKIs were normalized to TIC.

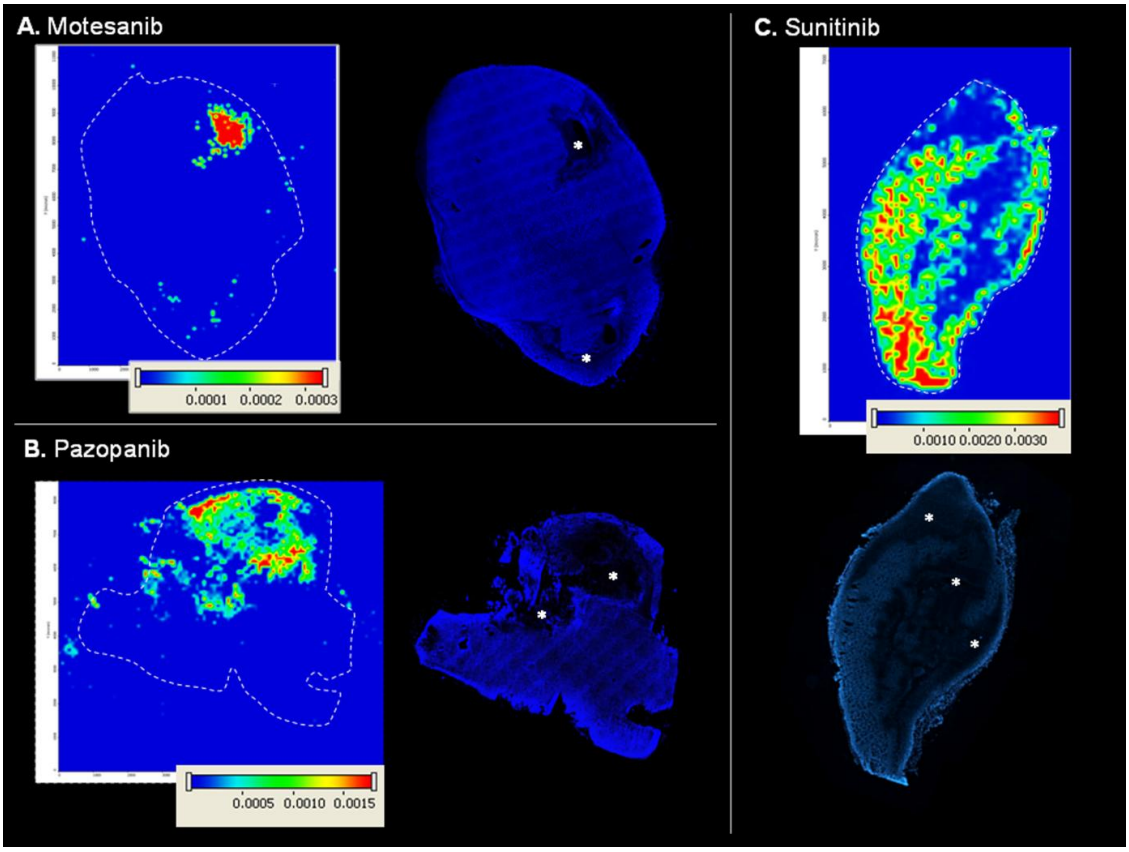

Figure 42. Co-localization of drug compounds (as visualized by MALDI-MSI) and non-viable areas in C26 tumors treated with motesanib (**A.**), pazopanib (**B.**) and sunitinib (**C.**). Asterisks mark non-viable intratumoral areas that appear black due to lack of nuclear counterstain (Hoechst 33342, blue). Tumor boundaries are delineated with dashed line in MALDI-MS images.

All detected RTKIs and their fragment ions showed co-localization within the tissues. This co-localization can be interpreted as a molecular fingerprint that confirms the identity of RTKIs. Representative examples showing the distribution of sunitinib and its fragment ions in tumor, liver and kidney samples are shown in **Figure 43**.

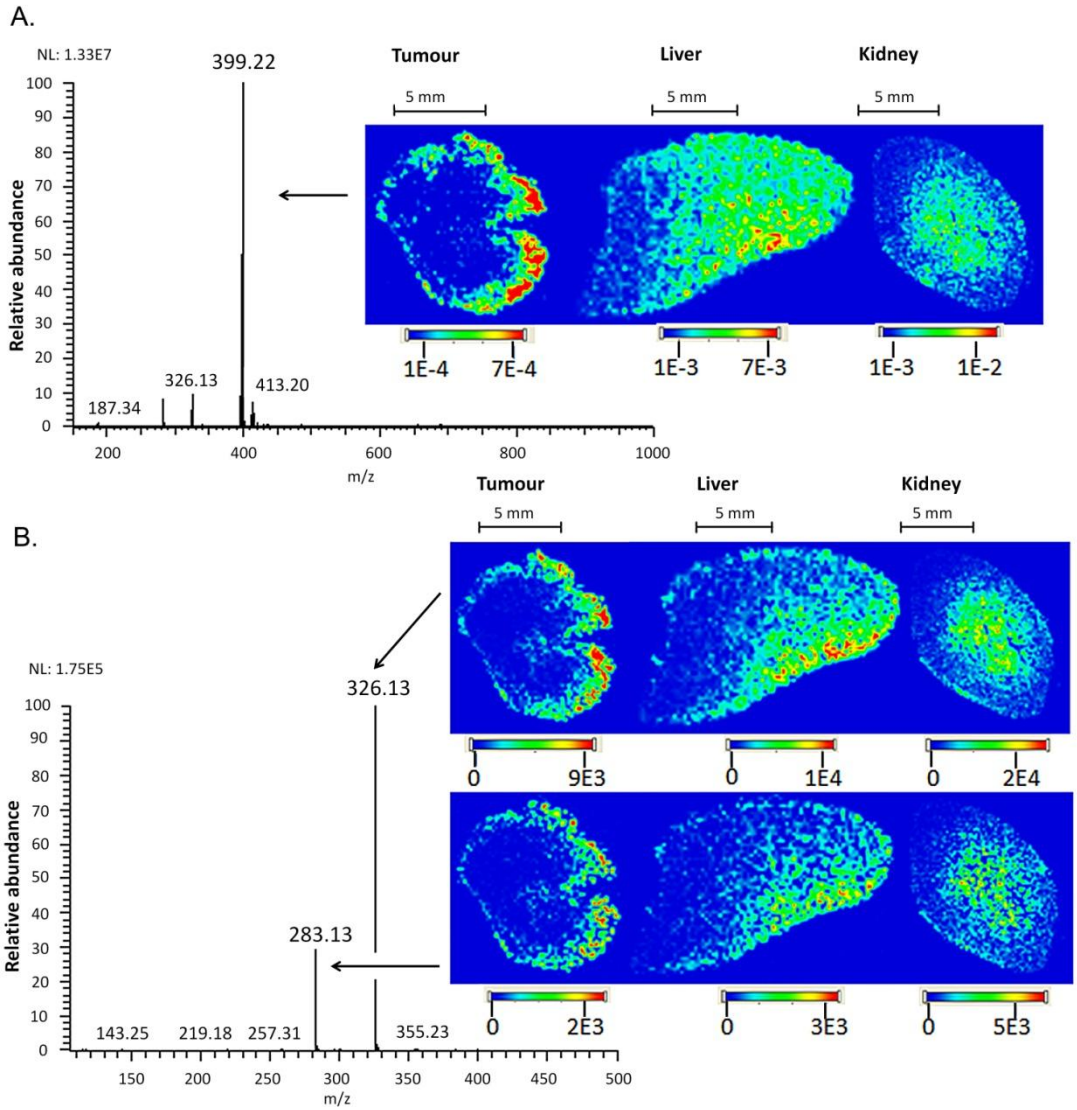

Figure 43. (**A.**) Full mass spectrum of sunitinib (399.218) and images of the distribution of the precursor molecule in tumor, liver and kidney tissues after 2 weeks of treatment. Signal of sunitinib is normalized to TIC. (**B.**) MS/MS spectrum of sunitinib and images of the distribution of the fragment ions (m/z 326.1 and 283.1) in tumor, liver and kidney tissues.

We also identified several sunitinib metabolites within the different tissues. In particular, the mono-desethylated (*m/z* 371.188), the desaturated (*m/z* 397.203), and the monohydroxylated (*m/z* 415.215) metabolites were observable by imaging (**Figure 44.**).

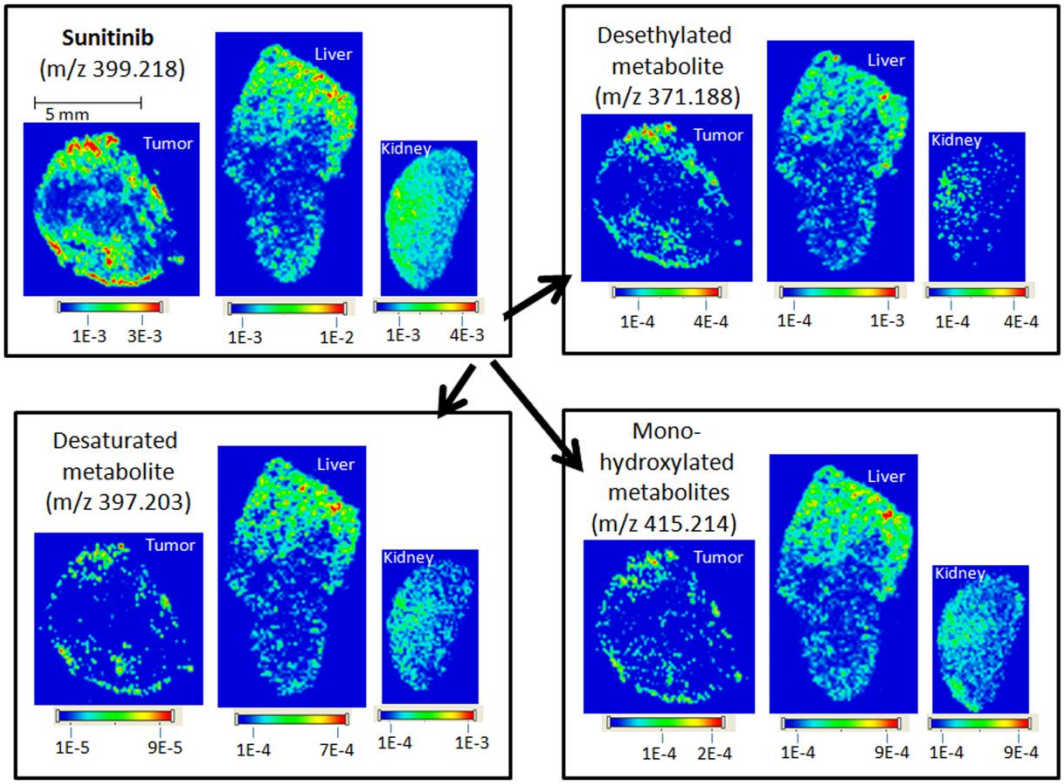

Figure 44. Distribution properties of sunitinib and its metabolites. Precursor molecule, desethylated metabolite (SU012662, M3), desaturated metabolite (M6) and mono-hydroxylated metabolites (M9, M10 and/or M11) in tumor, liver and kidney tissue sections.

Similarly, the carbinolamine (*m/z* 372.184) and the oxindole metabolite (*m/z* 388.179) of motesanib could also be shown in tissue (data not shown). Moreover, the main oxydative metabolite (*m/z* 363.1) of vatalanib was also identified in tissue sections, however, only in the C38 model (data not shown).

The precursor compoundsand all the measured metabolites showed an overlapping tissue pattern.

7. DISCUSSION

Angiogenesis research has led to the identification of several regulators of the process, some of which represent therapeutic targets. However, results of trials with antiangiogenic agents have been both encouraging and disappointing. The most important problem in the clinical application of these drugs is assessing the tumor response that can be inadequate. Tumor shrinkages characterized by cavitation have been observed and these do not meet the usual standard radiologic criteria for response. A relevant clinical challenge is therefore to find the best techniques for monitoring the effects of antivascular drugs. Especially antiangiogenic RTKI treatment raises a lot of questions. As the main receptors being involved in the angiogenic process have high structural similarities in the kinase domain, and thus activate similar signaling cascades, a relevant attempt is to develop drugs with a broad specifity, blocking not only the VEGF pathway, but PDGF and FGF signaling as well (417). Indeed, all of the approved antiangiogenic RTKIs are multi-target inhibitors, which beside the better efficacy caused by hitting multiple targets on one hand, can lead to increased toxicities on the other hand. Moreover, by blocking mural cell recruitment, treatment can affect vessel integrity as well, emerging the metastatizing potential of the tumor. However, by destructing the tumor vasculature, it is also questionable, whether the drug can reach the place of action in an effective level. Nevertheless, although the combination of antiangiogenic agents with conventional chemotherapy is highly problematic and should be carefully designed, there had been no studies that focused directly on the exact intratumoral distribution of these agents during and after their delivery.

In our study, the combination of the tolerability of the ionization mode, the resolving power of the Orbitrap with the sensitivity of the linear ion trap made MALDI-MS an ideal technique for both drug and metabolite detection in different tissue compartments (**Figures 37 and 44.**). Besides detecting non labeled compounds, another advantage of MALDI-MSI compared to other previously used methods is that these techniques require either fluid samples (such as urine, blood or sweat) or the homogenization of the tissue (418-420). Therefore, they are not capable of analyzing the spatial tissue distribution of a compound in an organ or in a solid tumor.

The current study is the first describing the tissue distribution of unlabelled antiangiogenic RTKIs and their metabolites by MSI and provides the first direct evidence that antiangiogenic drugs given orally are transported to, taken up and metabolized within the targeted compartment, the adenocarcinoma tumor. Moreover, the presented results are the first demonstrating that MALDI-MSI is a versatile and simple method of conducting ADME studies on antiangiogenic RTKIs.

The observed overlap in the distribution pattern of the RTKIs and their fragment ions confirms the identity of the drugs (**Figure 43.**). Co-localization of the RTKIs and their metabolites (**Figure 44.**) suggests that the chemical properties responsible for drug dispersion remain similar in case of the metabolites, and accordingly, they may contribute to the tumor growth inhibitory activity of the precursor compound as well. Alternatively, the co-localization may indicate that the drug is being taken up and metabolized locally rather than being transported from other sites of metabolism, such as the liver, back to the same location as the precursor compound. Further studies are warranted to confirm or rule out these assumptions.

To the best of our knowledge, this is the first study reporting the head-to-head comparison of the intratumoral concentrations and distributions of various unlabeled antiangiogenic RTKIs by MSI. We found that oral administration of motesanib, pazopanib, sorafenib, sunitinib or vatalanib resulted in the absorption of all the five drugs with notable signal intensities being observed in the circulation. Surprisingly, only motesanib, pazopanib and sunitinib treatments resulted in significantly elevated intratumoral drug levels in the C26 model with the highest concentrations and the most homogeneous tumor tissue distributions observed in sunitinib-treated animals (**Figure 41.**). The intratumoral distributions of motesanib and pazopanib were inhomogeneous and notable signal intensities were confined to non-viable areas (**Figure 42.**). We also found, that both sorafenib and vatalanib was only traceable in the C26 tumors. In contrast, vatalanib was always detectable at homogeneously high concentrations throughout the malignant tissue in the C38 model (**Figure 41.**). Chances, therefore, are that besides their dose, schedule and direct antivascular activity, the phenotype of the host vasculature and/or the tumor type are also likely to influence the tumor tissue levels and distribution of antiangiogenic RTKIs. The possible mechanisms linking inadequate antiangiogenic RTKI tumor concentration and endothelial- or tumor-specific

characteristics involve lysosomal degradation of RTKIs (421) and increased RTKI efflux by the tumor (422) or the endothelial (423) cells or both.

Importantly, high viable intratumoral drug concentrations were linked with tumor growth inhibition both in the C26 model (sunitinib) and C38 model (vatalanib) (**Figure 19.**). Moreover, suppressed vascular supply was also observable in these treatment groups. Although decreased MVD and/or microvessel area could also sporadically be observed in other treatment groups in the C26 model (**Figure 26-27.**). However, the low number of microvessels in case of vatalanib was accompanied by a relatively high microvessel area, while decreased microvessel area in case of sorafenib was linked with a relatively high MVD (**Figure 26.**). These opposing parameters of the vasculature could keep tumor blood flow levels, and consequently tumor burden high in these treatment groups. The suppressed MVD was linked with decreased microvessel area in case of motesanib, while both parameters were high in the pazopanib treated group (**Figure 26.**), both of which were present in the tumor in realtively high concentrations (**Figure 40.**), although in the non-viable tumor areas. A number of possible explanations of these opposing results exist, of which probably the most adequate is the difference in the efflux of the drugs by ECs and tumor cells. However, further experiments are needed to examine these parameters.

Hypoxic area ratios clearly correlated with decreased MVD (**Figures 26, 28-29.**).

We observed that VEGFR2 expression was significantly reduced only in sunitinib treated C26 tumors, while no difference in the expression pattern of the other receptors, or that of VEGFR2 in the C38 model were observed (**Figures 20-25.**). While no evidence exists that the expression profile of PDGFRs or FGFRs should change in response to receptor blockade, Domingues et al. documented, that successful therapy downregulates VEGFR2 expression (424). The lack of the decrease in VEGFR2 expression in the vatalanib treated C38 tumors may be explained by the different receptor expression profile of the two models, and probably by the fact, that vatalanib treatment induces a swich from sprouting angiogenesis to intussuception, which in contrast to sprouting, is not dependent on VEGFR signaling (267). However, it is also important to mention, that the intensity of VEGFR2 signal was not analysed.

Furthermore, one could also assume that since PDGFB is a key survival factor for the pericyte population and pericytes have a crucial role in the maintenance of vascular

stability (425), RTKIs with potent anti-PDGFRβ activity may not promote normalization but, instead, might destabilize the vasculature and thus interfere with drug delivery. Our actual findings, however, do not support this assumption. In Balb/C mice bearing C26 tumors, treatment with sunitinib (the tested RTKI with the lowest IC50 value against PDGFRβ, (386)) significantly decreased the pericyte coverage of tumor capillaries, as assessed by desmin expression (**Figures 32-33.**), and was also found in the highest intratumoral concentration (**Figures 40-41.**). However, how much this high concentration is the result of drug accumulation is still an open question. No difference in the desmin expression of C38 tumors was expected, as the IC50 value of vatalanib against PDGFRβ is less remarkable (**Table 2.**).

In our study also no changes in the structure of the vasculature, as examined by laminin and αSMA expression was observed in any group (**Figures 30-31.**).

Although antiangiogenic drugs also have direct effects against autocrine tumor cell signaling, the main effect of antivascular agents is exerted on the tumor vasculature itself and, consequently, they influence the efficacy of their own delivery. Additionally, recent clinical data raised serious concern that bevacizumab can significantly reduce the uptake of chemotherapy by human tumors (426). Of note, this is in contrast to the "vessel normalization theory" proposed by Jain and colleagues whereby treatment with an antiangiogenic agent such as bevacizumab (427) normalizes the chaotic tumor blood vessel network thus increasing chemotherapeutic drug delivery. It is also unclear whether antiangiogenic RTKIs - which are typically used as monotherapies in the indications for which they are so far approved - after a long time of treatment, can efficiently penetrate tumor tissues. As the tumor mass grows and the given antiangiogenic RTKI exerts its antivasular effects, blood capillaries may become nonfunctional or separated by longer distances resulting in limited drug delivery to RTK expressing tumor cells located distally from functional blood capillaries. Thus, the net result of antiangiogenic RTKI treatment in solid tumors might be tightly balanced by the (potentially opposing) antivascular and direct antitumor effects of these drugs.

Our current findings demonstrate the potential of MALDI-MSI to help in optimizing the dose and schedule of RTKIs, which is of crucial importance, because there is a pressing need for biomarkers of antiangiogenic therapy in the clinics (428).

8. CONCLUSIONS

1. Our results provide the first evidence that MALDI-MSI can be used to conduct ADME studies on low molecular weight antiangiogenic drugs.

2. Limited tumor tissue drug penetration contributes to primary resistance against angiogenesis inhibitors.

3. Drug concentration detected in the viable regions of the tumor is related to the antitumor and antivascular effects of the applied compounds.

4. The effects of antiangiogenic RTKIs are dependent on the tumor model used.

5. Effective treatment in the C26 model, but not the C38 model resulted in a decreased expression of VEGFR2 and desmin, and an increase in the intratumoral hypoxia.

9. SUMMARY

Since Judah Folkman postulated that tumor growth is angiogenesis dependent, several agents have been developed to inhibit the progress of new vessel formation. Despite the considerable progress made with antiangiogenic cancer therapies, the overall survival benefit with these drugs is still frustratingly limited for most patients and the mechanisms of primary and acquired resistances are unclear.

To find the potential causes of the observed ineffectiveness, we elaborated a method for the detection of antiangiogenic RTKIs and their metabolites in different tissue compartments. We correlated the antitumor and antivascular properties, as well as target receptor expressions of five different antiangiogenic RTKIs (motesanib, pazopanib, sorafenib, sunitinib, vatalanib) with their tumor tissue drug distribution data.

In Balb/C mice bearing C26 tumors, all five RTKIs absorbed efficiently, but only sunitinib exhibited broad-spectrum antivascular and antitumor activities by significantly inhibiting both tumor growth and vascularisation, while simultaneously suppressing VEGFR2, desmin expression, and increasing intratumoral hypoxia. Importantly, the highest tumor tissue drug concentrations and the most homogeneous intratumoral drug distributions have been found in sunitinib-treated animals. Motesanib and pazopanib were also present intratumorally in relatively high concentrations in connected areas, but their expression co-localized with non-viable tissue areas. Meanwhile sorafenib and vatalanib was detected only in traces in the tumor tissue. In another animal model, where - in contrast to the C26 model - vatalanib was detectable at homogenously high concentrations throughout the malignant tissue, the drug significantly reduced the growth and microvessel area of C38 tumors in C57Bl/6 mice.

Our results suggest, that the tumor tissue penetration and thus the antiangiogenic and antitumor potential of small molecule angiogenesis inhibitors varies among the tumor models and demonstrates the potential of MALDI-MSI to predict the efficacy of unlabelled small molecule antiangiogenic drugs in malignant tissues. Our approach is thus a major technical and preclinical advance demonstrating that primary resistance to angiogenesis inhibitors involves limited tumor tissue drug penetration. We also conclude that MALDI-MSI can significantly aid in the improvement of antivascular cancer therapies.

10. ÖSSZEFOGLALÁS

Mióta Judah Folkman felvetette, hogy a tumornövekedésben az angiogenezis fontos szerepet tölt be, számos, az új erek képződésének gátlását célzó szer került kifejlesztésre. Az antiangiogén rákterápia területén elért jelentős haladás ellenére azonban a teljes túlélés meghosszabítására tett kísérletek ezen gyógyszercsoporttal korlátozottak és az elsődleges, és szerzett rezisztencia mechanizmusai tisztázatlanok.

Ezen hatástalanság okainak felkutatására kidolgoztunk egy módszert az antiangiogén receptor tirozinkináz-inhibitorok (RTKI-k) és metabolitjaik különböző szöveti környezetben való detektálására. Összevetettük öt különböző RTKI (motesanib, pazopanib, sorafenib, sunitinib, vatalanib) tumorellenes és angiogenezist gátló hatását, valamint célreceptor expresszióját a gyógyszerek intratumorális denzitásával.

C26 tumort hordozó Balb/C egereknél mind az öt RTKI sikeresen felszívódott, de egyedül a sunitinib mutatott széles körű antivaszkuláris és antitumorális hatást szignifikánsan gátolva a tumornövekedést, és csökkentve mind az erek mennyiségét, mind a VEGFR2- és a dezmin kifejeződést, valamint növelve a hipoxiát. A legmagasabb intratumorális gyógyszerkoncentráció és leghomogénebb gyógyszereloszlás a sunitinib esetén volt megfigyelhető. Ezzel szemben, a motesanib és a pazopanib szintén relatív magas koncentrációban és összefüggő területeken volt detektálható, de jelenlétük a tumor elhalt területein volt jellemző. A sorafenib és a vatalanib csak nyomokban volt megtalálható a tumorszövetben. Egy másik állatmodellben, ahol a vatalanib homogénen magas koncentrációban volt jelen a tumorszövetben, ez a gyógyszer is szignifikánsan csökkentette a tumornövekedést és az intratumorális erek területét C57Bl/6 egerekben növő C38 tumorokban.

Eredményeink bizonyítják, hogy a kis molekulasúlyú angiogenezis inhibitorok tumorszövetbe való eljutása és az ennek következtében kialakuló növekedésgátló és antiangiogén hatás függ az alkalmazott tumormodelltől, valamint hogy a MALDI képalkotó tömegspektrometria alkalmas ezen jelöletlen gyógyszercsoport hatásának előrejelzésére, így segíthet az antivaszkuláris rákterápiák hatékonyságának növelésében. Az általunk alkalmazott módszer ezért egy egy fontos technikai és preklinikai újítás, mely bizonyítja, hogy az antiangiogén kezeléssel szembeni primer rezisztencia egyik oka az elégtelen intratumorális penetráció.

11. REFERENCES

1. V. Vinoth Prabhu NC, V. Gopal. (2011) A Historical Review on Current Medication and Therapies for Inducing and Inhibiting Angiogenesis. J Chem Pharm Res, 3:526-533

2. Wang GL, Jiang BH, Rue EA, Semenza GL. (1995) Hypoxia-inducible factor 1 is a basic-helix-loop-helix-PAS heterodimer regulated by cellular O2 tension. Proc Natl Acad Sci USA, 92:5510-5514

3. Tian H, McKnight SL, Russell DW. (1997) Endothelial PAS domain protein 1 (EPAS1), a transcription factor selectively expressed in endothelial cells. Genes Dev, 11:72-82

4. Gu YZ, Moran SM, Hogenesch JB, Wartman L, Bradfield CA. (1998) Molecular characterization and chromosomal localization of a third alpha-class hypoxia inducible factor subunit, HIF3alpha. Gene Expr, 7:205-213

5. Hirose K, Morita M, Ema M, Mimura J, Hamada H, Fujii H, Saijo Y, Gotoh O, Sogawa K, Fujii-Kuriyama Y. (1996) cDNA cloning and tissue-specific expression of a novel basic helix-loop-helix/PAS factor (Arnt2) with close sequence similarity to the aryl hydrocarbon receptor nuclear translocator (Arnt). Mol Cell Biol, 16:1706-1713

6. Makino Y, Kanopka A, Wilson WJ, Tanaka H, Poellinger L. (2002) Inhibitory PAS domain protein (IPAS) is a hypoxia-inducible splicing variant of the hypoxia-inducible factor-3alpha locus. J Biol Chem, 277:32405-32408

7. Heikkila M, Pasanen A, Kivirikko KI, Myllyharju J. (2011) Roles of the human hypoxia-inducible factor (HIF)-3alpha variants in the hypoxia response. Cell Mol Life Sci, 68:3885-3901

8. Huang LE, Gu J, Schau M, Bunn HF. (1998) Regulation of hypoxia-inducible factor 1alpha is mediated by an O2-dependent degradation domain via the ubiquitin-proteasome pathway. Proc Natl Acad Sci USA, 95:7987-7992

9. Ivan M, Kondo K, Yang H, Kim W, Valiando J, Ohh M, Salic A, Asara JM, Lane WS, Kaelin WG, Jr. (2001) HIFalpha targeted for VHL-mediated destruction by proline hydroxylation: implications for O2 sensing. Science, 292:464-468

10. Moroz E, Carlin S, Dyomina K, Burke S, Thaler HT, Blasberg R, Serganova I. (2009) Real-time imaging of HIF-1alpha stabilization and degradation. PloS One, 4:e5077

11. Ravi R, Mookerjee B, Bhujwalla ZM, Sutter CH, Artemov D, Zeng Q, Dillehay LE, Madan A, Semenza GL, Bedi A. (2000) Regulation of tumor angiogenesis by p53-induced degradation of hypoxia-inducible factor 1alpha. Genes Dev, 14:34-44

12. Arany Z, Huang LE, Eckner R, Bhattacharya S, Jiang C, Goldberg MA, Bunn HF, Livingston DM. (1996) An essential role for p300/CBP in the cellular response to hypoxia. Proc Natl Acad Sci USA, 93:12969-12973

13. Feldser D, Agani F, Iyer NV, Pak B, Ferreira G, Semenza GL. (1999) Reciprocal positive regulation of hypoxia-inducible factor 1alpha and insulin-like growth factor 2. Cancer Res, 59:3915-3918

14. Fink T, Kazlauskas A, Poellinger L, Ebbesen P, Zachar V. (2002) Identification of a tightly regulated hypoxia-response element in the promoter of human plasminogen activator inhibitor-1. Blood, 99:2077-2083

15. Garayoa M, Martinez A, Lee S, Pio R, An WG, Neckers L, Trepel J, Montuenga LM, Ryan H, Johnson R, Gassmann M, Cuttitta F. (2000) Hypoxia-inducible factor-1 (HIF-1) up-regulates adrenomedullin expression in human tumor cell lines during oxygen deprivation: a possible promotion mechanism of carcinogenesis. Mol Endocrinol, 14:848-862

16. Hayashi M, Sakata M, Takeda T, Tahara M, Yamamoto T, Okamoto Y, Minekawa R, Isobe A, Ohmichi M, Tasaka K, Murata Y. (2005) Up-regulation of c-met protooncogene product expression through hypoxia-inducible factor-1alpha is involved in trophoblast invasion under low-oxygen tension. Endocrinology, 146:4682-4689

17. Nishi H, Nakada T, Hokamura M, Osakabe Y, Itokazu O, Huang LE, Isaka K. (2004) Hypoxia-inducible factor-1 transactivates transforming growth factor-beta3 in trophoblast. Endocrinology, 145:4113-4118

18. Palmer LA, Semenza GL, Stoler MH, Johns RA. (1998) Hypoxia induces type II NOS gene expression in pulmonary artery endothelial cells via HIF-1. Am J Physiol, 274:L212-219

19. Simon MP, Tournaire R, Pouyssegur J. (2008) The angiopoietin-2 gene of endothelial cells is up-regulated in hypoxia by a HIF binding site located in its first intron and by the central factors GATA-2 and Ets-1. J Cell Physiol, 217:809-818

20. Takeda N, Maemura K, Imai Y, Harada T, Kawanami D, Nojiri T, Manabe I, Nagai R. (2004) Endothelial PAS domain protein 1 gene promotes angiogenesis through the transactivation of both vascular endothelial growth factor and its receptor, Flt-1. Circ Res, 95:146-153

21. Wang GL, Semenza GL. (1996) Molecular basis of hypoxia-induced erythropoietin expression. Curr Opin Hematol, 3:156-162

22. Rahimi N. (2012) The ubiquitin-proteasome system meets angiogenesis. Mol Cancer Ther, 11:538-548

23. Carmeliet P. (2005) VEGF as a key mediator of angiogenesis in cancer. Oncology, 69 Suppl 3:4-10

24. Risau W, Drexler H, Mironov V, Smits A, Siegbahn A, Funa K, Heldin CH. (1992) Platelet-derived growth factor is angiogenic in vivo. Growth Factors, 7:261-266

25. Cao R, Brakenhielm E, Li X, Pietras K, Widenfalk J, Ostman A, Eriksson U, Cao Y. (2002) Angiogenesis stimulated by PDGF-CC, a novel member in the PDGF family, involves activation of PDGFR-alphaalpha and -alphabeta receptors. FASEB J, 16:1575-1583

26. Li H, Fredriksson L, Li X, Eriksson U. (2003) PDGF-D is a potent transforming and angiogenic growth factor. Oncogene, 22:1501-1510

27. Lindner V, Majack RA, Reidy MA. (1990) Basic fibroblast growth factor stimulates endothelial regrowth and proliferation in denuded arteries. J Clin Invest, 85:2004-2008

28. Carmeliet P. (2000) Fibroblast growth factor-1 stimulates branching and survival of myocardial arteries: a goal for therapeutic angiogenesis? Circ Res, 87:176-178

29. De Falco S. (2012) The discovery of placenta growth factor and its biological activity. Exp Mol Med, 44:1-9

30. Saharinen P, Eklund L, Pulkki K, Bono P, Alitalo K. (2011) VEGF and angiopoietin signaling in tumor angiogenesis and metastasis. Trends Mol Med, 17:347-362

31. Garcia A, Kandel JJ. (2012) Notch: a key regulator of tumor angiogenesis and metastasis. Histol Histopathol, 27:151-156

32. Ellis LM. (2004) Epidermal growth factor receptor in tumor angiogenesis. Hematol Oncol Clin North Am, 18:1007-1021, viii

33. You WK, McDonald DM. (2008) The hepatocyte growth factor/c-Met signaling pathway as a therapeutic target to inhibit angiogenesis. BMB Rep, 41:833-839

34. Waugh DJ, Wilson C. (2008) The interleukin-8 pathway in cancer. Clin Cancer Res, 14:6735-6741

35. Li D, Zhang C, Song F, Lubenec I, Tian Y, Song QH. (2009) VEGF regulates FGF-2 and TGF-beta1 expression in injury endothelial cells and mediates smooth muscle cells proliferation and migration. Microvasc Res, 77:134-142

36. Zhang J, Cao R, Zhang Y, Jia T, Cao Y, Wahlberg E. (2009) Differential roles of PDGFR-alpha and PDGFR-beta in angiogenesis and vessel stability. FASEB J, 23:153-163

37. Rundhaug JE. (2005) Matrix metalloproteinases and angiogenesis. J Cell Mol Med, 9:267-285

38. Serini G, Valdembri D, Bussolino F. (2006) Integrins and angiogenesis: a sticky business. Exp Cell Res, 312:651-658

39. Lindahl P, Johansson BR, Leveen P, Betsholtz C. (1997) Pericyte loss and microaneurysm formation in PDGF-B-deficient mice. Science, 277:242-245

40. Hall AP. (2006) Review of the pericyte during angiogenesis and its role in cancer and diabetic retinopathy. Toxicol Pathol, 34:763-775

41. Goumans MJ, Valdimarsdottir G, Itoh S, Rosendahl A, Sideras P, ten Dijke P. (2002) Balancing the activation state of the endothelium via two distinct TGF-beta type I receptors. EMBO J, 21:1743-1753

42. Thurston G, Rudge JS, Ioffe E, Zhou H, Ross L, Croll SD, Glazer N, Holash J, McDonald DM, Yancopoulos GD. (2000) Angiopoietin-1 protects the adult vasculature against plasma leakage. Nat Med, 6:460-463

43. Allende ML, Proia RL. (2002) Sphingosine-1-phosphate receptors and the development of the vascular system. Biochim Biophys Acta, 1582:222-227

44. Timar J, Dome B, Fazekas K, Janovics A, Paku S. (2001) Angiogenesis-dependent diseases and angiogenesis therapy. Pathol Oncol Res, 7:85-94

45. Ferrara N. (2002) VEGF and the quest for tumour angiogenesis factors. Nat Rev Cancer, 2:795-803

46. Folkman J, Merler E, Abernathy C, Williams G. (1971) Isolation of a tumor factor responsible for angiogenesis. J Exp Med, 133:275-288

47. Gao N, Ding M, Zheng JZ, Zhang Z, Leonard SS, Liu KJ, Shi X, Jiang BH. (2002) Vanadate-induced expression of hypoxia-inducible factor 1 alpha and vascular endothelial growth factor through phosphatidylinositol 3-kinase/Akt pathway and reactive oxygen species. J Biol Chem, 277:31963-31971

48. Gao N, Jiang BH, Leonard SS, Corum L, Zhang Z, Roberts JR, Antonini J, Zheng JZ, Flynn DC, Castranova V, Shi X. (2002) p38 Signaling-mediated hypoxia-inducible factor 1alpha and vascular endothelial growth factor induction by Cr(VI) in DU145 human prostate carcinoma cells. J Biol Chem, 277:45041-45048

49. Peng XH, Karna P, Cao Z, Jiang BH, Zhou M, Yang L. (2006) Cross-talk between epidermal growth factor receptor and hypoxia-inducible factor-1alpha signal pathways increases resistance to apoptosis by up-regulating survivin gene expression. J Biol Chem, 281:25903-25914

50. Laughner E, Taghavi P, Chiles K, Mahon PC, Semenza GL. (2001) HER2 (neu) signaling increases the rate of hypoxia-inducible factor 1alpha (HIF-1alpha) synthesis: novel mechanism for HIF-1-mediated vascular endothelial growth factor expression. Mol Cell Biol, 21:3995-4004

51. Blancher C, Moore JW, Robertson N, Harris AL. (2001) Effects of ras and von Hippel-Lindau (VHL) gene mutations on hypoxia-inducible factor (HIF)-1alpha, HIF-2alpha, and vascular endothelial growth factor expression and their regulation by the phosphatidylinositol 3'-kinase/Akt signaling pathway. Cancer Res, 61:7349-7355

52. Hudson CC, Liu M, Chiang GG, Otterness DM, Loomis DC, Kaper F, Giaccia AJ, Abraham RT. (2002) Regulation of hypoxia-inducible factor 1alpha expression and function by the mammalian target of rapamycin. Mol Cell Biol, 22:7004-7014

53. Lee HY, Lee T, Lee N, Yang EG, Lee C, Lee J, Moon EY, Ha J, Park H. (2011) Src activates HIF-1alpha not through direct phosphorylation of HIF-1alpha specific prolyl-4 hydroxylase 2 but through activation of the NADPH oxidase/Rac pathway. Carcinogenesis, 32:703-712

54. Zundel W, Schindler C, Haas-Kogan D, Koong A, Kaper F, Chen E, Gottschalk AR, Ryan HE, Johnson RS, Jefferson AB, Stokoe D, Giaccia AJ. (2000) Loss of PTEN facilitates HIF-1-mediated gene expression. Genes Dev, 14:391-396

55. Rivera CG, Mellberg S, Claesson-Welsh L, Bader JS, Popel AS. (2011) Analysis of VEGF--a regulated gene expression in endothelial cells to identify genes linked to angiogenesis. PLoS One, 6:e24887

56. Stiehl DP, Jelkmann W, Wenger RH, Hellwig-Burgel T. (2002) Normoxic induction of the hypoxia-inducible factor 1alpha by insulin and interleukin-1beta involves the phosphatidylinositol 3-kinase pathway. FEBS Lett, 512:157-162

57. Zhong H, Chiles K, Feldser D, Laughner E, Hanrahan C, Georgescu MM, Simons JW, Semenza GL. (2000) Modulation of hypoxia-inducible factor 1alpha expression by the epidermal growth factor/phosphatidylinositol 3-kinase/PTEN/AKT/FRAP pathway in human prostate cancer cells: implications for tumor angiogenesis and therapeutics. Cancer Res, 60:1541-1545

58. Watanabe T, Yasue A, Tanaka E. (2006) Inhibition of Transforming Growth Factor beta1 (TGF-beta1)/ Smad3 Signaling Decreases Hypoxia-Inducible Factor 1alpha (HIF-1alpha) Protein Stability by Inducing Prolyl Hydroxylase 2 (PHD2) Expression in Human Periodontal Ligament Cells. J Periodontol, 281(34):24171-81.

59. Haddad JJ, Land SC. (2001) A non-hypoxic, ROS-sensitive pathway mediates TNF-alpha-dependent regulation of HIF-1alpha. FEBS Lett, 505:269-274

60. Fleming RY, Ellis LM, Parikh NU, Liu W, Staley CA, Gallick GE. (1997) Regulation of vascular endothelial growth factor expression in human colon carcinoma cells by activity of src kinase. Surgery 122:501-507

61. Mayerhofer M, Valent P, Sperr WR, Griffin JD, Sillaber C. (2002) BCR/ABL induces expression of vascular endothelial growth factor and its transcriptional activator, hypoxia inducible factor-1alpha, through a pathway involving phosphoinositide 3-kinase and the mammalian target of rapamycin. Blood, 100:3767-3775

62. Konishi T, Huang CL, Adachi M, Taki T, Inufusa H, Kodama K, Kohno N, Miyake M. (2000) The K-ras gene regulates vascular endothelial growth factor gene expression in non-small cell lung cancers. Int J Oncol, 16:501-511

63. Fujisawa T, Watanabe J, Kamata Y, Hamano M, Hata H, Kuramoto H. (20039 Effect of p53 gene transfection on vascular endothelial growth factor expression in endometrial cancer cells. Exp Mol Pathol, 74:276-281

64. Maity A, Pore N, Lee J, Solomon D, O'Rourke DM. (2000) Epidermal growth factor receptor transcriptionally up-regulates vascular endothelial growth factor expression in human glioblastoma cells via a pathway involving phosphatidylinositol 3'-kinase and distinct from that induced by hypoxia. Cancer Res, 60:5879-5886

65. Warren RS, Yuan H, Matli MR, Ferrara N, Donner DB. (1996) Induction of vascular endothelial growth factor by insulin-like growth factor 1 in colorectal carcinoma. J Biol Chem, 271:29483-29488

66. Kumar R, Yarmand-Bagheri R. (2001) The role of HER2 in angiogenesis. Semin Oncol, 28:27-32

67. Joo YE, Rew JS, Seo YH, Choi SK, Kim YJ, Park CS, Kim SJ. (2003) Cyclooxygenase-2 overexpression correlates with vascular endothelial growth factor expression and tumor angiogenesis in gastric cancer. J Clin Gastroenterol, 37:28-33

68. Dong J, Grunstein J, Tejada M, Peale F, Frantz G, Liang WC, Bai W, Yu L, Kowalski J, Liang X, Fuh G, Gerber HP, Ferrara N. (2004) VEGF-null cells require PDGFR alpha signaling-mediated stromal fibroblast recruitment for tumorigenesis. EMBO J, 23:2800-2810

69. Folkman J. (2007) Angiogenesis: an organizing principle for drug discovery? Nat Rev Drug Discov, 6:273-286

70. Paul MK, Mukhopadhyay AK. (2004) Tyrosine kinase - Role and significance in Cancer. Int J Med Sci, 1:101-115

71. Blume-Jensen P, Hunter T. (2001) Oncogenic kinase signalling. Nature, 411:355-365

72. Muller YA, Christinger HW, Keyt BA, de Vos AM. (1997) The crystal structure of vascular endothelial growth factor (VEGF) refined to 1.93 A resolution: multiple copy flexibility and receptor binding. Structure, 5:1325-1338

73. DiSalvo J, Bayne ML, Conn G, Kwok PW, Trivedi PG, Soderman DD, Palisi TM, Sullivan KA, Thomas KA. (1995) Purification and characterization of a naturally

occurring vascular endothelial growth factor.placenta growth factor heterodimer. J Biol Chem, 270:7717-7723

74. Koch S, Tugues S, Li X, Gualandi L, Claesson-Welsh L. (2011) Signal transduction by vascular endothelial growth factor receptors. Biochem, J 437:169-183

75. Stuttfeld E, Ballmer-Hofer K. (2009) Structure and function of VEGF receptors. IUBMB Life, 61:915-922

76. Stringer SE. (2006) The role of heparan sulphate proteoglycans in angiogenesis. Biochem Soc Trans, 34:451-453

77. Soker S, Takashima S, Miao HQ, Neufeld G, Klagsbrun M. (1998) Neuropilin-1 is expressed by endothelial and tumor cells as an isoform-specific receptor for vascular endothelial growth factor. Cell, 92:735-745

78. Favier B, Alam A, Barron P, Bonnin J, Laboudie P, Fons P, Mandron M, Herault JP, Neufeld G, Savi P, Herbert JM, Bono F. (2006) Neuropilin-2 interacts with VEGFR-2 and VEGFR-3 and promotes human endothelial cell survival and migration. Blood, 108:1243-1250

79. Waltenberger J, Claesson-Welsh L, Siegbahn A, Shibuya M, Heldin CH. (1994) Different signal transduction properties of KDR and Flt1, two receptors for vascular endothelial growth factor. J Biol Chem, 269:26988-26995

80. Barleon B, Sozzani S, Zhou D, Weich HA, Mantovani A, Marme D. (1996) Migration of human monocytes in response to vascular endothelial growth factor (VEGF) is mediated via the VEGF receptor flt-1. Blood, 87:3336-3343

81. Clark DE, Smith SK, Sharkey AM, Charnock-Jones DS. (1996) Localization of VEGF and expression of its receptors flt and KDR in human placenta throughout pregnancy. Hum Reprod, 11:1090-1098

82. Dikov MM, Ohm JE, Ray N, Tchekneva EE, Burlison J, Moghanaki D, Nadaf S, Carbone DP. (2005) Differential roles of vascular endothelial growth factor receptors 1 and 2 in dendritic cell differentiation. J Immunol, 174:215-222

83. Grosskreutz CL, Anand-Apte B, Duplaa C, Quinn TP, Terman BI, Zetter B, D'Amore PA. (1999) Vascular endothelial growth factor-induced migration of vascular smooth muscle cells in vitro. Microvasc Res, 58:128-136

84. Yao J, Wu X, Zhuang G, Kasman IM, Vogt T, Phan V, Shibuya M, Ferrara N, Bais C. (2011) Expression of a functional VEGFR-1 in tumor cells is a major

determinant of anti-PlGF antibodies efficacy. Proc Natl Acad Sci USA, 108:11590-11595

85. Kendall RL, Thomas KA. (1993) Inhibition of vascular endothelial cell growth factor activity by an endogenously encoded soluble receptor. Proc Natl Acad Sci USA, 90:10705-10709

86. Tanaka K, Yamaguchi S, Sawano A, Shibuya M. (1997) Characterization of the extracellular domain in vascular endothelial growth factor receptor-1 (Flt-1 tyrosine kinase). Jpn J Cancer Res, 88:867-876

87. Achen MG, Jeltsch M, Kukk E, Makinen T, Vitali A, Wilks AF, Alitalo K, Stacker SA. (1998) Vascular endothelial growth factor D (VEGF-D) is a ligand for the tyrosine kinases VEGF receptor 2 (Flk1) and VEGF receptor 3 (Flt4). Proc Natl Acad Sci USA, 95:548-553

88. Joukov V, Pajusola K, Kaipainen A, Chilov D, Lahtinen I, Kukk E, Saksela O, Kalkkinen N, Alitalo K. (1996) A novel vascular endothelial growth factor, VEGF-C, is a ligand for the Flt4 (VEGFR-3) and KDR (VEGFR-2) receptor tyrosine kinases. EMBO J, 15:1751

89. Takahashi T, Yamaguchi S, Chida K, Shibuya M. (2001) A single autophosphorylation site on KDR/Flk-1 is essential for VEGF-A-dependent activation of PLC-gamma and DNA synthesis in vascular endothelial cells. EMBO J, 20:2768-2778

90. Millauer B, Wizigmann-Voos S, Schnurch H, Martinez R, Moller NP, Risau W, Ullrich A. (1993) High affinity VEGF binding and developmental expression suggest Flk-1 as a major regulator of vasculogenesis and angiogenesis. Cell, 72:835-846

91. Graeven U, Fiedler W, Karpinski S, Ergun S, Kilic N, Rodeck U, Schmiegel W, Hossfeld DK. (1999) Melanoma-associated expression of vascular endothelial growth factor and its receptors FLT-1 and KDR. J Cancer Res Clin Oncol, 125:621-629

92. Neuchrist C, Erovic BM, Handisurya A, Steiner GE, Rockwell P, Gedlicka C, Burian M. (2001) Vascular endothelial growth factor receptor 2 (VEGFR2) expression in squamous cell carcinomas of the head and neck. Laryngoscope, 111:1834-1841

93. Dellinger MT, Meadows SM, Wynne K, Cleaver O, Brekken RA. (2013) Vascular endothelial growth factor receptor-2 promotes the development of the lymphatic vasculature. PLoS One, 8:e74686

94. Katoh O, Tauchi H, Kawaishi K, Kimura A, Satow Y. (1995) Expression of the vascular endothelial growth factor (VEGF) receptor gene, KDR, in hematopoietic cells and inhibitory effect of VEGF on apoptotic cell death caused by ionizing radiation. Cancer Res, 55:5687-5692

95. Ebos JM, Bocci G, Man S, Thorpe PE, Hicklin DJ, Zhou D, Jia X, Kerbel RS. (2004) A naturally occurring soluble form of vascular endothelial growth factor receptor 2 detected in mouse and human plasma. Mol Cancer Res, 2:315-326

96. Makinen T, Veikkola T, Mustjoki S, Karpanen T, Catimel B, Nice EC, Wise L, Mercer A, Kowalski H, Kerjaschki D, Stacker SA, Achen MG, Alitalo K. (2001) Isolated lymphatic endothelial cells transduce growth, survival and migratory signals via the VEGF-C/D receptor VEGFR-3. EMBO J, 20:4762-4773

97. Jeltsch M, Karpanen T, Strandin T, Aho K, Lankinen H, Alitalo K. (2006) Vascular endothelial growth factor (VEGF)/VEGF-C mosaic molecules reveal specificity determinants and feature novel receptor binding patterns. J Biol Chem, 281:12187-12195

98. Kaipainen A, Korhonen J, Mustonen T, van Hinsbergh VW, Fang GH, Dumont D, Breitman M, Alitalo K. (1995) Expression of the fms-like tyrosine kinase 4 gene becomes restricted to lymphatic endothelium during development. Proc Natl Acad Sci USA, 92:3566-3570

99. Petrova TV, Bono P, Holnthoner W, Chesnes J, Pytowski B, Sihto H, Laakkonen P, Heikkila P, Joensuu H, Alitalo K. (2008) VEGFR-3 expression is restricted to blood and lymphatic vessels in solid tumors. Cancer Cell, 13:554-556

100. He Y, Kozaki K, Karpanen T, Koshikawa K, Yla-Herttuala S, Takahashi T, Alitalo K. (2002) Suppression of tumor lymphangiogenesis and lymph node metastasis by blocking vascular endothelial growth factor receptor 3 signaling. J Nat Cancer Inst, 94:819-825

101. Yang H, Kim C, Kim MJ, Schwendener RA, Alitalo K, Heston W, Kim I, Kim WJ, Koh GY. (2011) Soluble vascular endothelial growth factor receptor-3 suppresses lymphangiogenesis and lymphatic metastasis in bladder cancer. Mol Cancer, 10:36

102. Robinson CJ, Stringer SE. (2001) The splice variants of vascular endothelial growth factor (VEGF) and their receptors. J Cell Sci, 114:853-865

103. Catena R, Larzabal L, Larrayoz M, Molina E, Hermida J, Agorreta J, Montes R, Pio R, Montuenga LM, Calvo A. (2010) VEGF(1)(2)(1)b and VEGF(1)(6)(5)b are weakly angiogenic isoforms of VEGF-A. Mol Cancer, 9:320

104. Varey AH, Rennel ES, Qiu Y, Bevan HS, Perrin RM, Raffy S, Dixon AR, Paraskeva C, Zaccheo O, Hassan AB, Harper SJ, Bates DO. (2008) VEGF 165 b, an antiangiogenic VEGF-A isoform, binds and inhibits bevacizumab treatment in experimental colorectal carcinoma: balance of pro- and antiangiogenic VEGF-A isoforms has implications for therapy. Br J Cancer, 98:1366-1379

105. Lemmon MA, Schlessinger J. (2010) Cell signaling by receptor tyrosine kinases. Cell, 141:1117-1134

106. Lee S, Chen TT, Barber CL, Jordan MC, Murdock J, Desai S, Ferrara N, Nagy A, Roos KP, Iruela-Arispe ML. (2007) Autocrine VEGF signaling is required for vascular homeostasis. Cell, 130:691-703

107. Fujio Y, Walsh K. (1999) Akt mediates cytoprotection of endothelial cells by vascular endothelial growth factor in an anchorage-dependent manner. J Biol Chem, 274:16349-16354

108. Gelinas DS, Bernatchez PN, Rollin S, Bazan NG, Sirois MG. (2002) Immediate and delayed VEGF-mediated NO synthesis in endothelial cells: role of PI3K, PKC and PLC pathways. Br J Pharmacol, 137:1021-1030

109. Lamalice L, Houle F, Huot J. (2006) Phosphorylation of Tyr1214 within VEGFR-2 triggers the recruitment of Nck and activation of Fyn leading to SAPK2/p38 activation and endothelial cell migration in response to VEGF. J Biol Chem, 281:34009-34020

110. Koch S, Tugues S, Li X, Gualandi L, Claesson-Welsh L. (2011) Signal transduction by vascular endothelial growth factor receptors. Biochem J, 437:169-183

111. Padro T, Bieker R, Ruiz S, Steins M, Retzlaff S, Burger H, Buchner T, Kessler T, Herrera F, Kienast J, Muller-Tidow C, Serve H, Berdel WE, Mesters RM. (2002) Overexpression of vascular endothelial growth factor (VEGF) and its cellular receptor KDR (VEGFR-2) in the bone marrow of patients with acute myeloid leukemia. Leukemia, 16:1302-1310

112. Tsourlakis MC, Khosrawi P, Weigand P, Kluth M, Hube-Magg C, Minner S, Koop C, Graefen M, Heinzer H, Wittmer C, Sauter G, Krech T, Wilczak W, Huland H, Simon R, Schlomm T, Steurer S. (2015) VEGFR-1 overexpression identifies a small subgroup of aggressive prostate cancers in patients treated by prostatectomy. Int J Mol Sci, 16:8591-8606

113. Uthoff SM, Duchrow M, Schmidt MH, Broll R, Bruch HP, Strik MW, Galandiuk S. (2002) VEGF isoforms and mutations in human colorectal cancer. IntJ Cancer, 101:32-36

114. Heldin CH, Eriksson U, Ostman A. (2002) New members of the platelet-derived growth factor family of mitogens. Arch Biochem Biophys, 398:284-290

115. Pietras K, Sjoblom T, Rubin K, Heldin CH, Ostman A. (2003) PDGF receptors as cancer drug targets. Cancer Cell, 3:439-443

116. Pellet-Many C, Frankel P, Evans IM, Herzog B, Junemann-Ramirez M, Zachary IC. (2011) Neuropilin-1 mediates PDGF stimulation of vascular smooth muscle cell migration and signalling via p130Cas. Biochem J, 435:609-618

117. Loukinova E, Ranganathan S, Kuznetsov S, Gorlatova N, Migliorini MM, Loukinov D, Ulery PG, Mikhailenko I, Lawrence DA, Strickland DK. (2002) Platelet-derived growth factor (PDGF)-induced tyrosine phosphorylation of the low density lipoprotein receptor-related protein (LRP). Evidence for integrated co-receptor function betwenn LRP and the PDGF. J Biol Chem, 277:15499-15506

118. Kourembanas S, Morita T, Liu Y, Christou H. (1997) Mechanisms by which oxygen regulates gene expression and cell-cell interaction in the vasculature. Kidney Int, 51:438-443

119. Daniel TO, Gibbs VC, Milfay DF, Garovoy MR, Williams LT. (1986) Thrombin stimulates c-sis gene expression in microvascular endothelial cells. J Biol Chem, 261:9579-9582

120. Nagineni CN, Kutty V, Detrick B, Hooks JJ. (2005) Expression of PDGF and their receptors in human retinal pigment epithelial cells and fibroblasts: regulation by TGF-beta. J Cell Physiol, 203:35-43

121. Boehm KD, Daimon M, Gorodeski IG, Sheean LA, Utian WH, Ilan J. (1990) Expression of the insulin-like and platelet-derived growth factor genes in human uterine tissues. Mol Reprod Dev, 27:93-101

122. Gnessi L, Emidi A, Jannini EA, Carosa E, Maroder M, Arizzi M, Ulisse S, Spera G. (1995) Testicular development involves the spatiotemporal control of PDGFs and PDGF receptors gene expression and action. J Cell Biol, 131:1105-1121

123. DiCorleto PE, Bowen-Pope DF. (1983) Cultured endothelial cells produce a platelet-derived growth factor-like protein. Proc Natl Acad Sci USA, 80:1919-1923

124. Nilsson J, Sjolund M, Palmberg L, Thyberg J, Heldin CH. (1985) Arterial smooth muscle cells in primary culture produce a platelet-derived growth factor-like protein. Proc Natl Acad Sci USA, 82:4418-4422

125. Campochiaro PA, Sugg R, Grotendorst G, Hjelmeland LM. (1989) Retinal pigment epithelial cells produce PDGF-like proteins and secrete them into their media. Exp Eye Res, 49:217-227

126. Noble M, Murray K, Stroobant P, Waterfield MD, Riddle P. (1988) Platelet-derived growth factor promotes division and motility and inhibits premature differentiation of the oligodendrocyte/type-2 astrocyte progenitor cell. Nature, 333:560-562

127. Richardson WD, Pringle N, Mosley MJ, Westermark B, Dubois-Dalcq M. (1988) A role for platelet-derived growth factor in normal gliogenesis in the central nervous system. Cell, 53:309-319

128. Shimokado K, Raines EW, Madtes DK, Barrett TB, Benditt EP, Ross R. (1985) A significant part of macrophage-derived growth factor consists of at least two forms of PDGF. Cell, 43:277-286

129. Alpers CE, Seifert RA, Hudkins KL, Johnson RJ, Bowen-Pope DF. (1992) Developmental patterns of PDGF B-chain, PDGF-receptor, and alpha-actin expression in human glomerulogenesis. Kidney Int, 42:390-399

130. Ansel JC, Tiesman JP, Olerud JE, Krueger JG, Krane JF, Tara DC, Shipley GD, Gilbertson D, Usui ML, Hart CE. (1993) Human keratinocytes are a major source of cutaneous platelet-derived growth factor. J Clin Invest, 92:671-678

131. Kohler N, Lipton A. (1974) Platelets as a source of fibroblast growth-promoting activity. Exp Cell Res, 87:297-301

132. Ross R, Glomset J, Kariya B, Harker L. (1974) A platelet-dependent serum factor that stimulates the proliferation of arterial smooth muscle cells in vitro. Proc Natl Acad Sci USA, 71:1207-1210

133. Westermark B, Wasteson A. (1976) A platelet factor stimulating human normal glial cells. Exp Cell Res, 98:170-174

134. Abramsson A, Lindblom P, Betsholtz C. (2003) Endothelial and nonendothelial sources of PDGF-B regulate pericyte recruitment and influence vascular pattern formation in tumors. J Clin Invest, 112:1142-1151

135. Abboud HE, Grandaliano G, Pinzani M, Knauss T, Pierce GF, Jaffer F. (1994) Actions of platelet-derived growth factor isoforms in mesangial cells. J Cell Physiol, 158:140-150

136. Tiesman J, Hart CE. (1993) Identification of a soluble receptor for platelet-derived growth factor in cell-conditioned medium and human plasma. J Biol Chem, 268:9621-9628

137. Duan DS, Pazin MJ, Fretto LJ, Williams LT. (1991) A functional soluble extracellular region of the platelet-derived growth factor (PDGF) beta-receptor antagonizes PDGF-stimulated responses. J Biol Chem, 266:413-418

138. Shim AH, Liu H, Focia PJ, Chen X, Lin PC, He X. (2010) Structures of a platelet-derived growth factor/propeptide complex and a platelet-derived growth factor/receptor complex. Proc Natl Acad Sci USA, 107:11307-11312

139. Kazlauskas A, Cooper JA. (1989) Autophosphorylation of the PDGF receptor in the kinase insert region regulates interactions with cell proteins. Cell, 58:1121-1133

140. Barrientos S, Stojadinovic O, Golinko MS, Brem H, Tomic-Canic M. (2008) Growth factors and cytokines in wound healing. Wound Repair Regen, 16:585-601

141. Funa K, Sasahara M. (2014) The roles of PDGF in development and during neurogenesis in the normal and diseased nervous system. J Neuroimmune Pharmacol, 9:168-181

142. Boucher P, Gotthardt M. (2004) LRP and PDGF signaling: a pathway to atherosclerosis. Trends Cardiovasc Med, 14:55-60

143. Bonner JC. (2004) Regulation of PDGF and its receptors in fibrotic diseases. Cytokine Growth Factor Rev, 15:255-273

144. Hermansson M, Nister M, Betsholtz C, Heldin CH, Westermark B, Funa K. (1988) Endothelial cell hyperplasia in human glioblastoma: coexpression of mRNA for platelet-derived growth factor (PDGF) B chain and PDGF receptor suggests autocrine growth stimulation. Proc Natl Acad Sci USA, 85:7748-7752

145. Sundberg C, Ljungstrom M, Lindmark G, Gerdin B, Rubin K. (1993) Microvascular pericytes express platelet-derived growth factor-beta receptors in human healing wounds and colorectal adenocarcinoma. Am J Pathol, 143:1377-1388

146. Fleming TP, Saxena A, Clark WC, Robertson JT, Oldfield EH, Aaronson SA, Ali IU. (1992) Amplification and/or overexpression of platelet-derived growth factor receptors and epidermal growth factor receptor in human glial tumors. Cancer Res, 52:4550-4553

147. Heinrich MC, Corless CL, Duensing A, McGreevey L, Chen CJ, Joseph N, Singer S, Griffith DJ, Haley A, Town A, Demetri GD, Fletcher CD, Fletcher JA. (2003) PDGFRA activating mutations in gastrointestinal stromal tumors. Science, 299:708-710

148. Shimizu A, O'Brien KP, Sjoblom T, Pietras K, Buchdunger E, Collins VP, Heldin CH, Dumanski JP, Ostman A. (1999) The dermatofibrosarcoma protuberans-associated collagen type Ialpha1/platelet-derived growth factor (PDGF) B-chain fusion gene generates a transforming protein that is processed to functional PDGF-BB. Cancer Res, 59:3719-3723

149. Hellberg C, Ostman A, Heldin CH. (2010) PDGF and vessel maturation. Recent Results Cancer Res, 180:103-114

150. Meisenhelder J, Suh PG, Rhee SG, Hunter T. (1989) Phospholipase C-gamma is a substrate for the PDGF and EGF receptor protein-tyrosine kinases in vivo and in vitro. Cell, 57:1109-1122

151. Falasca M, Logan SK, Lehto VP, Baccante G, Lemmon MA, Schlessinger J. (1998) Activation of phospholipase C gamma by PI 3-kinase-induced PH domain-mediated membrane targeting. EMBO J, 17:414-422

152. Hu Q, Klippel A, Muslin AJ, Fantl WJ, Williams LT. (1995) Ras-dependent induction of cellular responses by constitutively active phosphatidylinositol-3 kinase. Science, 268:100-102

153. Kauffmann-Zeh A, Rodriguez-Viciana P, Ulrich E, Gilbert C, Coffer P, Downward J, Evan G. (1997) Suppression of c-Myc-induced apoptosis by Ras signalling through PI(3)K and PKB. Nature, 385:544-548

154. Assefa Z, Valius M, Vantus T, Agostinis P, Merlevede W, Vandenheede JR. (1999) JNK/SAPK activation by platelet-derived growth factor in A431 cells requires both the phospholipase C-gamma and the phosphatidylinositol 3-kinase signaling pathways of the receptor. Biochem Biophys Res Commun, 261:641-645

155. Heldin CH. (2013) Targeting the PDGF signaling pathway in tumor treatment. Cell Commun Signal, 11:97

156. Wesche J, Haglund K, Haugsten EM. (2011) Fibroblast growth factors and their receptors in cancer. Biochem J 437:199-213

157. Beenken A, Mohammadi M. (2009) The FGF family: biology, pathophysiology and therapy. Nat Rev Drug Discov, 8:235-253

158. Itoh N. (2010) Hormone-like (endocrine) Fgfs: their evolutionary history and roles in development, metabolism, and disease. Cell Tissue Res, 342:1-11

159. Zhang JD, Cousens LS, Barr PJ, Sprang SR. (1991) Three-dimensional structure of human basic fibroblast growth factor, a structural homolog of interleukin 1 beta. Proc Natl Acad Sci USA, 88:3446-3450

160. Ago H, Kitagawa Y, Fujishima A, Matsuura Y, Katsube Y. (1991) Crystal structure of basic fibroblast growth factor at 1.6 A resolution. Jiochem, 110:360-363

161. Harmer NJ, Ilag LL, Mulloy B, Pellegrini L, Robinson CV, Blundell TL. (2004) Towards a resolution of the stoichiometry of the fibroblast growth factor (FGF)-FGF receptor-heparin complex. J Molecular Biol, 339:821-834

162. Padera R, Venkataraman G, Berry D, Godavarti R, Sasisekharan R. (1999) FGF-2/fibroblast growth factor receptor/heparin-like glycosaminoglycan interactions: a compensation model for FGF-2 signaling. FASEB J, 13:1677-1687

163. Zhang X, Ibrahimi OA, Olsen SK, Umemori H, Mohammadi M, Ornitz DM. (2006) Receptor specificity of the fibroblast growth factor family. The complete mammalian FGF family. J Biol Chem, 281:15694-15700

164. Ahmad I, Iwata T, Leung HY. (2012) Mechanisms of FGFR-mediated carcinogenesis. Biochim Biophys Acta, 1823:850-860

165. Gong SG. (2014) Isoforms of receptors of fibroblast growth factors. J Cell Physiol, 229:1887-1895

166. Turner N, Grose R. (2010) Fibroblast growth factor signalling: from development to cancer. Nat Rev Cancer, 10:116-129

167. Thomas A, Lee JH, Abdullaev Z, Park KS, Pineda M, Saidkhodjaeva L, Miettinen M, Wang Y, Pack SD, Giaccone G. (2014) Characterization of fibroblast growth factor receptor 1 in small-cell lung cancer. J Thorac Oncol, 9:567-571

168. Penault-Llorca F, Bertucci F, Adelaide J, Parc P, Coulier F, Jacquemier J, Birnbaum D, deLapeyriere O. (1995) Expression of FGF and FGF receptor genes in human breast cancer. Int J Cancer, 61:170-176

169. Armstrong E, Vainikka S, Partanen J, Korhonen J, Alitalo R. (1992) Expression of fibroblast growth factor receptors in human leukemia cells. Cancer Res, 52:2004-2007

170. Leung HY, Gullick WJ, Lemoine NR. (1994) Expression and functional activity of fibroblast growth factors and their receptors in human pancreatic cancer. Int J Cancer, 59:667-675

171. Krejci P, Dvorakova D, Krahulcova E, Pachernik J, Mayer J, Hampl A, Dvorak P. (2001) FGF-2 abnormalities in B cell chronic lymphocytic and chronic myeloid leukemias. Leukemia, 15:228-237

172. Rosen A, Sevelda P, Klein M, Dobianer K, Hruza C, Czerwenka K, Hanak H, Vavra N, Salzer H, Leodolter S. (1993) First experience with FGF-3 (INT-2) amplification in women with epithelial ovarian cancer. Br J Cancer, 67:1122-1125

173. Antoine M, Wirz W, Tag CG, Mavituna M, Emans N, Korff T, Stoldt V, Gressner AM, Kiefer P. (2005) Expression pattern of fibroblast growth factors (FGFs), their receptors and antagonists in primary endothelial cells and vascular smooth muscle cells. Growth Factors, 23:87-95

174. Klint P, Kanda S, Claesson-Welsh L. (1995) Shc and a novel 89-kDa component couple to the Grb2-Sos complex in fibroblast growth factor-2-stimulated cells. J Biol Chem, 270:23337-23344

175. Hu Y, Lu H, Zhang J, Chen J, Chai Z, Zhang J. (2014) Essential role of AKT in tumor cells addicted to FGFR. Anticancer Drugs, 25:183-188

176. Peters KG, Marie J, Wilson E, Ives HE, Escobedo J, Del Rosario M, Mirda D, Williams LT. (1992) Point mutation of an FGF receptor abolishes phosphatidylinositol turnover and Ca2+ flux but not mitogenesis. Nature, 358:678-681

177. Sorensen V, Zhen Y, Zakrzewska M, Haugsten EM, Walchli S, Nilsen T, Olsnes S, Wiedlocha A. (2008) Phosphorylation of fibroblast growth factor (FGF) receptor 1 at Ser777 by p38 mitogen-activated protein kinase regulates translocation of exogenous FGF1 to the cytosol and nucleus. Mol Cell Biol, 28:4129-4141

178. Carmo CR, Lyons-Lewis J, Seckl MJ, Costa-Pereira AP. (2011) A novel requirement for Janus kinases as mediators of drug resistance induced by fibroblast growth factor-2 in human cancer cells. PLoS One, 6:e19861

179. Kanda S, Hodgkin MN, Woodfield RJ, Wakelam MJ, Thomas G, Claesson-Welsh L. (1997) Phosphatidylinositol 3'-kinase-independent p70 S6 kinase activation by fibroblast growth factor receptor-1 is important for proliferation but not differentiation of endothelial cells. J Biol Chem, 272:23347-23353

180. Procopio WN, Pelavin PI, Lee WM, Yeilding NM. (1999) Angiopoietin-1 and -2 coiled coil domains mediate distinct homo-oligomerization patterns, but fibrinogen-like domains mediate ligand activity. J Biol Chem, 274:30196-30201

181. Kim KT, Choi HH, Steinmetz MO, Maco B, Kammerer RA, Ahn SY, Kim HZ, Lee GM, Koh GY. (2005) Oligomerization and multimerization are critical for angiopoietin-1 to bind and phosphorylate Tie2. J Biol Chem, 280:20126-20131

182. Macdonald PR, Progias P, Ciani B, Patel S, Mayer U, Steinmetz MO, Kammerer RA. (2006) Structure of the extracellular domain of Tie receptor tyrosine kinases and localization of the angiopoietin-binding epitope. J Biol Chem, 281:28408-28414

183. Fagiani E, Christofori G. (2013) Angiopoietins in angiogenesis. Cancer Lett, 328:18-26

184. Park YS, Kim G, Jin YM, Lee JY, Shin JW, Jo I. (2016) Expression of angiopoietin-1 in hypoxic pericytes: Regulation by hypoxia-inducible factor-2alpha and participation in endothelial cell migration and tube formation. Biochem Biophys Res Commun, 469:263-269

185. Nishishita T, Lin PC. (2004) Angiopoietin 1, PDGF-B, and TGF-beta gene regulation in endothelial cell and smooth muscle cell interaction. J Cell Biochem, 91:584-593

186. Pichiule P, Chavez JC, LaManna JC. (2004) Hypoxic regulation of angiopoietin-2 expression in endothelial cells. J Biol Chem, 279:12171-12180

187. Hackett SF, Ozaki H, Strauss RW, Wahlin K, Suri C, Maisonpierre P, Yancopoulos G, Campochiaro PA. (2000) Angiopoietin 2 expression in the retina: upregulation during physiologic and pathologic neovascularization. J Cell Physiol, 184:275-284

188. Fiedler U, Scharpfenecker M, Koidl S, Hegen A, Grunow V, Schmidt JM, Kriz W, Thurston G, Augustin HG. (2004) The Tie-2 ligand angiopoietin-2 is stored in and rapidly released upon stimulation from endothelial cell Weibel-Palade bodies. Blood, 103:4150-4156

189. Suri C, Jones PF, Patan S, Bartunkova S, Maisonpierre PC, Davis S, Sato TN, Yancopoulos GD. (1996) Requisite role of angiopoietin-1, a ligand for the TIE2 receptor, during embryonic angiogenesis. Cell, 87:1171-1180

190. Yuan HT, Khankin EV, Karumanchi SA, Parikh SM. (2009) Angiopoietin 2 is a partial agonist/antagonist of Tie2 signaling in the endothelium. Mol Cell Biol, 29:2011-2022

191. Song SH, Kim KL, Lee KA, Suh W. (2012) Tie1 regulates the Tie2 agonistic role of angiopoietin-2 in human lymphatic endothelial cells. Biochem Biophys Res Commun, 419:281-286

192. De Spiegelaere W, Cornillie P, Van den Broeck W, Plendl J, Bahramsoltani M. (2011) Angiopoietins differentially influence in vitro angiogenesis by endothelial cells of different origin. Clin Hemorheol Microcirc, 48:15-27

193. Hammes HP, Lin J, Wagner P, Feng Y, Vom Hagen F, Krzizok T, Renner O, Breier G, Brownlee M, Deutsch U. (2004) Angiopoietin-2 causes pericyte dropout in the normal retina: evidence for involvement in diabetic retinopathy. Diabetes, 53:1104-1110

194. Lobov IB, Brooks PC, Lang RA. (2002) Angiopoietin-2 displays VEGF-dependent modulation of capillary structure and endothelial cell survival in vivo. Proc Natl Acad Sci USA, 99:11205-11210

195. Valenzuela DM, Griffiths JA, Rojas J, Aldrich TH, Jones PF, Zhou H, McClain J, Copeland NG, Gilbert DJ, Jenkins NA, Huang T, Papadopoulos N, Maisonpierre PC, Davis S, Yancopoulos GD. (1999) Angiopoietins 3 and 4: diverging gene counterparts in mice and humans. Proc Natl Acad Sci USA, 96:1904-1909

196. Marron MB, Hughes DP, Edge MD, Forder CL, Brindle NP. (2000) Evidence for heterotypic interaction between the receptor tyrosine kinases TIE-1 and TIE-2. J Biol Chem, 275:39741-39746

197. Savant S, La Porta S, Budnik A, Busch K, Hu J, Tisch N, Korn C, Valls AF, Benest AV, Terhardt D, Qu X, Adams RH, Baldwin HS, Ruiz de Almodovar C, Rodewald HR, Augustin HG. (2015) The Orphan Receptor Tie1 Controls Angiogenesis and Vascular Remodeling by Differentially Regulating Tie2 in Tip and Stalk Cells. Cell Rep, 12:1761-1773

198. Qu X, Zhou B, Scott Baldwin H. (2015) Tie1 is required for lymphatic valve and collecting vessel development. Dev Biol, 399:117-128

199. Dumont DJ, Yamaguchi TP, Conlon RA, Rossant J, Breitman ML. (1992) tek, a novel tyrosine kinase gene located on mouse chromosome 4, is expressed in endothelial cells and their presumptive precursors. Oncogene, 7:1471-1480

200. Yuasa H, Takakura N, Shimomura T, Suenobu S, Yamada T, Nagayama H, Oike Y, Suda T. (2002) Analysis of human TIE2 function on hematopoietic stem cells in umbilical cord blood. Biochem Biophys Res Commun, 298:731-737

201. Felcht M, Luck R, Schering A, Seidel P, Srivastava K, Hu J, Bartol A, Kienast Y, Vettel C, Loos EK, Kutschera S, Bartels S, Appak S, Besemfelder E, Terhardt D, Chavakis E, Wieland T, Klein C, Thomas M, Uemura A, Goerdt S, Augustin HG. (2012) Angiopoietin-2 differentially regulates angiogenesis through TIE2 and integrin signaling. J Clin Invest, 122:1991-2005

202. Niu Q, Perruzzi C, Voskas D, Lawler J, Dumont DJ, Benjamin LE. (2004) Inhibition of Tie-2 signaling induces endothelial cell apoptosis, decreases Akt signaling, and induces endothelial cell expression of the endogenous anti-angiogenic molecule, thrombospondin-1. Cancer Biol Ther, 3:402-405

203. Saharinen P, Eklund L, Miettinen J, Wirkkala R, Anisimov A, Winderlich M, Nottebaum A, Vestweber D, Deutsch U, Koh GY, Olsen BR, Alitalo K. (2008) Angiopoietins assemble distinct Tie2 signalling complexes in endothelial cell-cell and cell-matrix contacts. Nat Cell Biol, 10:527-537

204. Iivanainen E, Nelimarkka L, Elenius V, Heikkinen SM, Junttila TT, Sihombing L, Sundvall M, Maatta JA, Laine VJ, Yla-Herttuala S, Higashiyama S, Alitalo K, Elenius K. (2003) Angiopoietin-regulated recruitment of vascular smooth muscle

cells by endothelial-derived heparin binding EGF-like growth factor. FASEB J, 17:1609-1621

205. Audero E, Cascone I, Zanon I, Previtali SC, Piva R, Schiffer D, Bussolino F. (2001) Expression of angiopoietin-1 in human glioblastomas regulates tumor-induced angiogenesis: in vivo and in vitro studies. Arterioscler Thromb Vasc Biol, 21:536-541

206. Tian S, Hayes AJ, Metheny-Barlow LJ, Li LY. (2002) Stabilization of breast cancer xenograft tumour neovasculature by angiopoietin-1. Br J Cancer, 86:645-651

207. Holopainen T, Huang H, Chen C, Kim KE, Zhang L, Zhou F, Han W, Li C, Yu J, Wu J, Koh GY, Alitalo K, He Y. (2009) Angiopoietin-1 overexpression modulates vascular endothelium to facilitate tumor cell dissemination and metastasis establishment. Cancer Res, 69:4656-4664

208. Cai M, Zhang H, Hui R. (2003) Single chain Fv antibody against angiopoietin-2 inhibits VEGF-induced endothelial cell proliferation and migration in vitro. Biochem Biophys Res Commun, 309:946-951

209. Brown LF, Dezube BJ, Tognazzi K, Dvorak HF, Yancopoulos GD. (2000) Expression of Tie1, Tie2, and angiopoietins 1, 2, and 4 in Kaposi's sarcoma and cutaneous angiosarcoma. Am J Pathol, 156:2179-2183

210. McCarthy MJ, Crowther M, Bell PR, Brindle NP. (1998) The endothelial receptor tyrosine kinase tie-1 is upregulated by hypoxia and vascular endothelial growth factor. FEBS Lett, 423:334-338

211. Wong AL, Haroon ZA, Werner S, Dewhirst MW, Greenberg CS, Peters KG. (1997) Tie2 expression and phosphorylation in angiogenic and quiescent adult tissues. Circ Res, 81:567-574

212. Robson H, Anderson E, James RD, Schofield PF. (1996) Transforming growth factor beta 1 expression in human colorectal tumours: an independent prognostic marker in a subgroup of poor prognosis patients. Br J Cancer, 74:753-758

213. de Caestecker M. (2004) The transforming growth factor-beta superfamily of receptors. Cytokine Growth Factor Rev, 15:1-11

214. Kyprianou N. (1999) Activation of TGF-beta signalling in human prostate cancer cells suppresses tumorigenicity via deregulation of cell cycle progression and

induction of caspase-1 mediated apoptosis: significance in prostate tumorigenesis. Prostate Cancer Prostatic Dis, 2:S18

215. Hirte H, Clark DA. (1991) Generation of lymphokine-activated killer cells in human ovarian carcinoma ascitic fluid: identification of transforming growth factor-beta as a suppressive factor. Cancer Immunol Immunother, 32:296-302

216. Xiong B, Yuan HY, Hu MB, Zhang F, Wei ZZ, Gong LL, Yang GL. (2002) Transforming growth factor-beta1 in invasion and metastasis in colorectal cancer. World J Gastroenterol, 8:674-678

217. Yi JY, Hur KC, Lee E, Jin YJ, Arteaga CL, Son YS. (2002) TGFbeta1 -mediated epithelial to mesenchymal transition is accompanied by invasion in the SiHa cell line. Eur J Cell Biol, 81:457-468

218. Malaponte G, Zacchia A, Bevelacqua Y, Marconi A, Perrotta R, Mazzarino MC, Cardile V, Stivala F. (2010) Co-regulated expression of matrix metalloproteinase-2 and transforming growth factor-beta in melanoma development and progression. Oncol Rep, 24:81-87

219. Yang SD, Sun RC, Mu HJ, Xu ZQ, Zhou ZY. (2010) The expression and clinical significance of TGF-beta1 and MMP2 in human renal clear cell carcinoma. Int J Surg Pathol, 18:85-93

220. Farina AR, Coppa A, Tiberio A, Tacconelli A, Turco A, Colletta G, Gulino A, Mackay AR. (1998) Transforming growth factor-beta1 enhances the invasiveness of human MDA-MB-231 breast cancer cells by up-regulating urokinase activity. Int J Cancer, 75:721-730

221. De Strooper B, Annaert W, Cupers P, Saftig P, Craessaerts K, Mumm JS, Schroeter EH, Schrijvers V, Wolfe MS, Ray WJ, Goate A, Kopan R. (1999) A presenilin-1-dependent gamma-secretase-like protease mediates release of Notch intracellular domain. Nature, 398:518-522

222. Wu L, Sun T, Kobayashi K, Gao P, Griffin JD. (2002) Identification of a family of mastermind-like transcriptional coactivators for mammalian notch receptors. Mol Cell Biol, 22:7688-7700

223. Weng AP, Millholland JM, Yashiro-Ohtani Y, Arcangeli ML, Lau A, Wai C, Del Bianco C, Rodriguez CG, Sai H, Tobias J, Li Y, Wolfe MS, Shachaf C, Felsher D, Blacklow SC, Pear WS, Aster JC. (2006) c-Myc is an important direct target of

Notch1 in T-cell acute lymphoblastic leukemia/lymphoma. Genes Dev, 20:2096-2109

224. Oswald F, Liptay S, Adler G, Schmid RM. (1998) NF-kappaB2 is a putative target gene of activated Notch-1 via RBP-Jkappa. Mol Cell Biol, 18:2077-2088

225. Chen Y, Fischer WH, Gill GN. (1997) Regulation of the ERBB-2 promoter by RBPJkappa and NOTCH. J Biol Chem, 272:14110-14114

226. Eliasz S, Liang S, Chen Y, De Marco MA, Machek O, Skucha S, Miele L, Bocchetta M. (2010) Notch-1 stimulates survival of lung adenocarcinoma cells during hypoxia by activating the IGF-1R pathway. Oncogene, 29:2488-2498

227. Noseda M, Chang L, McLean G, Grim JE, Clurman BE, Smith LL, Karsan A. (2004) Notch activation induces endothelial cell cycle arrest and participates in contact inhibition: role of p21Cip1 repression. Mol Cell Biol, 24:8813-8822

228. Joshi I, Minter LM, Telfer J, Demarest RM, Capobianco AJ, Aster JC, Sicinski P, Fauq A, Golde TE, Osborne BA. (2009) Notch signaling mediates G1/S cell-cycle progression in T cells via cyclin D3 and its dependent kinases. Blood, 113:1689-1698

229. Chen Y, Li D, Liu H, Xu H, Zheng H, Qian F, Li W, Zhao C, Wang Z, Wang X. (2011) Notch-1 signaling facilitates survivin expression in human non-small cell lung cancer cells. Cancer Biol Ther, 11:14-21

230. Jin S, Mutvei AP, Chivukula IV, Andersson ER, Ramskold D, Sandberg R, Lee KL, Kronqvist P, Mamaeva V, Ostling P, Mpindi JP, Kallioniemi O, Screpanti I, Poellinger L, Sahlgren C, Lendahl U. (2013) Non-canonical Notch signaling activates IL-6/JAK/STAT signaling in breast tumor cells and is controlled by p53 and IKKalpha/IKKbeta. Oncogene, 32:4892-4902

231. Aljedai A, Buckle AM, Hiwarkar P, Syed F. (2015) Potential role of Notch signalling in CD34+ chronic myeloid leukaemia cells: cross-talk between Notch and BCR-ABL. PLoS One, 10:e0123016

232. Fre S, Pallavi SK, Huyghe M, Lae M, Janssen KP, Robine S, Artavanis-Tsakonas S, Louvard D. (2009) Notch and Wnt signals cooperatively control cell proliferation and tumorigenesis in the intestine. Proc Natl Acad Sci USA, 106:6309-6314

233. Shimizu M, Cohen B, Goldvasser P, Berman H, Virtanen C, Reedijk M. (2011) Plasminogen activator uPA is a direct transcriptional target of the JAG1-Notch receptor signaling pathway in breast cancer. Cancer Res, 71:277-286

234. Gu Y, Masiero M, Banham AH. (2016) Notch signaling: its roles and therapeutic potential in hematological malignancies. Oncotarget, 7:29804-29823

235. Mazzone M, Selfors LM, Albeck J, Overholtzer M, Sale S, Carroll DL, Pandya D, Lu Y, Mills GB, Aster JC, Artavanis-Tsakonas S, Brugge JS. (2010) Dose-dependent induction of distinct phenotypic responses to Notch pathway activation in mammary epithelial cells. Proc Natl Acad Sci USA, 107:5012-5017

236. Wang Z, Li Y, Banerjee S, Sarkar FH. (2009) Emerging role of Notch in stem cells and cancer. Cancer Lett, 279:8-12

237. Zhao Y, Qiao X, Wang L, Tan TK, Zhao H, Zhang Y, Zhang J, Rao P, Cao Q, Wang Y, Wang Y, Wang YM, Lee VW, Alexander SI, Harris DC, Zheng G. (2016) Matrix metalloproteinase 9 induces endothelial-mesenchymal transition via Notch activation in human kidney glomerular endothelial cells. BMC Cell Biol, 17:21

238. Sieiro D, Rios AC, Hirst CE, Marcelle C. (2016) Cytoplasmic NOTCH and membrane-derived beta-catenin link cell fate choice to epithelial-mesenchymal transition during myogenesis. Elife, 5

239. Rizzo P, Osipo C, Foreman K, Golde T, Osborne B, Miele L. (2008) Rational targeting of Notch signaling in cancer. Oncogene, 27:5124-5131

240. Phng LK, Gerhardt H. (2009) Angiogenesis: a team effort coordinated by notch. Dev Cell, 16:196-208

241. Louvi A, Arboleda-Velasquez JF, Artavanis-Tsakonas S. (2006) CADASIL: a critical look at a Notch disease. Dev Neurosci, 28:5-12

242. Kamath BM, Spinner NB, Emerick KM, Chudley AE, Booth C, Piccoli DA, Krantz ID. (2004) Vascular anomalies in Alagille syndrome: a significant cause of morbidity and mortality. Circulation, 109:1354-1358

243. High FA, Lu MM, Pear WS, Loomes KM, Kaestner KH, Epstein JA. (2008) Endothelial expression of the Notch ligand Jagged1 is required for vascular smooth muscle development. Proc Natl Acad Sci USA, 105:1955-1959

244. Hofmann JJ, Luisa Iruela-Arispe M. (2007) Notch expression patterns in the retina: An eye on receptor-ligand distribution during angiogenesis. Gene Expr Patterns, 7:461-470

245. Liu ZJ, Shirakawa T, Li Y, Soma A, Oka M, Dotto GP, Fairman RM, Velazquez OC, Herlyn M. (2003) Regulation of Notch1 and Dll4 by vascular endothelial growth factor in arterial endothelial cells: implications for modulating arteriogenesis and angiogenesis. Mol Cell Biol, 23:14-25

246. Sorensen I, Adams RH, Gossler A. (2009) DLL1-mediated Notch activation regulates endothelial identity in mouse fetal arteries. Blood, 113:5680-5688

247. Sweeney C, Morrow D, Birney YA, Coyle S, Hennessy C, Scheller A, Cummins PM, Walls D, Redmond EM, Cahill PA. (2004) Notch 1 and 3 receptor signaling modulates vascular smooth muscle cell growth, apoptosis, and migration via a CBF-1/RBP-Jk dependent pathway. FASEB J, 18:1421-1423

248. Tsai S, Fero J, Bartelmez S. (2000) Mouse Jagged2 is differentially expressed in hematopoietic progenitors and endothelial cells and promotes the survival and proliferation of hematopoietic progenitors by direct cell-to-cell contact. Blood, 96:950-957

249. Wu J, Iwata F, Grass JA, Osborne CS, Elnitski L, Fraser P, Ohneda O, Yamamoto M, Bresnick EH. (2005) Molecular determinants of NOTCH4 transcription in vascular endothelium. Mol Cell Biol, 25:1458-1474

250. ZhuGe Q, Wu Z, Huang L, Zhao B, Zhong M, Zheng W, GouRong C, Mao X, Xie L, Wang X, Jin K. (2013) Notch4 is activated in endothelial and smooth muscle cells in human brain arteriovenous malformations. J Cell Mol Med, 17:1458-1464

251. Mailhos C, Modlich U, Lewis J, Harris A, Bicknell R, Ish-Horowicz D. (2001) Delta4, an endothelial specific notch ligand expressed at sites of physiological and tumor angiogenesis. Differentiation, 69:135-144

252. Noguera-Troise I, Daly C, Papadopoulos NJ, Coetzee S, Boland P, Gale NW, Lin HC, Yancopoulos GD, Thurston G. (2006) Blockade of Dll4 inhibits tumour growth by promoting non-productive angiogenesis. Nature, 444:1032-1037

253. Tammela T, Zarkada G, Wallgard E, Murtomaki A, Suchting S, Wirzenius M, Waltari M, Hellstrom M, Schomber T, Peltonen R, Freitas C, Duarte A, Isoniemi H, Laakkonen P, Christofori G, Yla-Herttuala S, Shibuya M, Pytowski B,

Eichmann A, Betsholtz C, Alitalo K. (2008) Blocking VEGFR-3 suppresses angiogenic sprouting and vascular network formation. Nature, 454:656-660

254. Gerhardt H, Golding M, Fruttiger M, Ruhrberg C, Lundkvist A, Abramsson A, Jeltsch M, Mitchell C, Alitalo K, Shima D, Betsholtz C. (2003) VEGF guides angiogenic sprouting utilizing endothelial tip cell filopodia. J Cell Biol, 161:1163-1177

255. Potente M, Gerhardt H, Carmeliet P. (2011) Basic and therapeutic aspects of angiogenesis. Cell, 146:873-887

256. Hellstrom M, Phng LK, Hofmann JJ, Wallgard E, Coultas L, Lindblom P, Alva J, Nilsson AK, Karlsson L, Gaiano N, Yoon K, Rossant J, Iruela-Arispe ML, Kalen M, Gerhardt H, Betsholtz C. (2007) Dll4 signalling through Notch1 regulates formation of tip cells during angiogenesis. Nature, 445:776-780

257. Suchting S, Freitas C, le Noble F, Benedito R, Breant C, Duarte A, Eichmann A. (2007) The Notch ligand Delta-like 4 negatively regulates endothelial tip cell formation and vessel branching. Proc Natl Acad Sci USA, 104:3225-3230

258. Lobov IB, Renard RA, Papadopoulos N, Gale NW, Thurston G, Yancopoulos GD, Wiegand SJ. (2007) Delta-like ligand 4 (Dll4) is induced by VEGF as a negative regulator of angiogenic sprouting. Proc Natl Acad Sci USA, 104:3219-3224

259. Williams CK, Li JL, Murga M, Harris AL, Tosato G. (2006) Up-regulation of the Notch ligand Delta-like 4 inhibits VEGF-induced endothelial cell function. Blood, 107:931-939

260. Harrington LS, Sainson RC, Williams CK, Taylor JM, Shi W, Li JL, Harris AL. (2008) Regulation of multiple angiogenic pathways by Dll4 and Notch in human umbilical vein endothelial cells. Microvasc Res, 75:144-154

261. Ausprunk DH, Folkman J. (1977) Migration and proliferation of endothelial cells in preformed and newly formed blood vessels during tumor angiogenesis. Microvasc Res, 14:53-65

262. Paku S, Paweletz N. (1991) First steps of tumor-related angiogenesis. Lab Invest, 65:334-346

263. Thompson WD, Shiach KJ, Fraser RA, McIntosh LC, Simpson JG. (1987) Tumours acquire their vasculature by vessel incorporation, not vessel ingrowth. J Pathol, 151:323-332

264. Holash J, Wiegand SJ, Yancopoulos GD. (1999) New model of tumor angiogenesis: dynamic balance between vessel regression and growth mediated by angiopoietins and VEGF. Oncogene, 18:5356-5362

265. Holash J, Maisonpierre PC, Compton D, Boland P, Alexander CR, Zagzag D, Yancopoulos GD, Wiegand SJ. (1999) Vessel cooption, regression, and growth in tumors mediated by angiopoietins and VEGF. Science, 284:1994-1998

266. Patan S, Munn LL, Jain RK. (1996) Intussusceptive microvascular growth in a human colon adenocarcinoma xenograft: a novel mechanism of tumor angiogenesis. Microvasc Res, 51:260-272

267. Paku S, Dezso K, Bugyik E, Tovari J, Timar J, Nagy P, Laszlo V, Klepetko W, Dome B. (2011) A new mechanism for pillar formation during tumor-induced intussusceptive angiogenesis: inverse sprouting. Am J Pathol, 179:1573-1585

268. Makanya AN, Stauffer D, Ribatti D, Burri PH, Djonov V. (2005) Microvascular growth, development, and remodeling in the embryonic avian kidney: the interplay between sprouting and intussusceptive angiogenic mechanisms. Microsc Res Tech, 66:275-288

269. Makanya AN, Hlushchuk R, Baum O, Velinov N, Ochs M, Djonov V. (2007) Microvascular endowment in the developing chicken embryo lung. Am J Physiol Lung Cell Mol Physiol, 292:L1136-1146

270. Patan S. (1998) TIE1 and TIE2 receptor tyrosine kinases inversely regulate embryonic angiogenesis by the mechanism of intussusceptive microvascular growth. Microvasc Res, 56:1-21

271. Wnuk M, Hlushchuk R, Janot M, Tuffin G, Martiny-Baron G, Holzer P, Imbach-Weese P, Djonov V, Huynh-Do U. (2012) Podocyte EphB4 signaling helps recovery from glomerular injury. Kidney Int, 81:1212-1225

272. Fujimoto A, Onodera H, Mori A, Isobe N, Yasuda S, Oe H, Yonenaga Y, Tachibana T, Imamura M. (2004) Vascular endothelial growth factor reduces mural cell coverage of endothelial cells and induces sprouting rather than luminal division in an HT1080 tumour angiogenesis model. Int J Exp Path, 85:355-364

273. Baum O, Suter F, Gerber B, Tschanz SA, Buergy R, Blank F, Hlushchuk R, Djonov V. (2010) VEGF-A promotes intussusceptive angiogenesis in the developing chicken chorioallantoic membrane. Microcirculation, 17:447-457

274. Semela D, Piguet AC, Kolev M, Schmitter K, Hlushchuk R, Djonov V, Stoupis C, Dufour JF. (2007) Vascular remodeling and antitumoral effects of mTOR inhibition in a rat model of hepatocellular carcinoma. J Hepatol, 46:840-848

275. Hlushchuk R, Riesterer O, Baum O, Wood J, Gruber G, Pruschy M, Djonov V. (2008) Tumor recovery by angiogenic switch from sprouting to intussusceptive angiogenesis after treatment with PTK787/ZK222584 or ionizing radiation. Am J Pathol, 173:1173-1185

276. Ohtani H. (1992) Glomeruloid structures as vascular reaction in human gastrointestinal carcinoma. Jpn J Cancer Res, 83:1334-1340

277. Sundberg C, Nagy JA, Brown LF, Feng D, Eckelhoefer IA, Manseau EJ, Dvorak AM, Dvorak HF. (2001) Glomeruloid microvascular proliferation follows adenoviral vascular permeability factor/vascular endothelial growth factor-164 gene delivery. Am J Pathol, 158:1145-1160

278. Dome B, Timar J, Paku S. (2003) A novel concept of glomeruloid body formation in experimental cerebral metastases. J Neuropathol Exp Neurol, 62:655-661

279. Straume O, Chappuis PO, Salvesen HB, Halvorsen OJ, Haukaas SA, Goffin JR, Begin LR, Foulkes WD, Akslen LA. (2002) Prognostic importance of glomeruloid microvascular proliferation indicates an aggressive angiogenic phenotype in human cancers. Cancer Res, 62:6808-6811

280. Asahara T, Takahashi T, Masuda H, Kalka C, Chen D, Iwaguro H, Inai Y, Silver M, Isner JM. (1999) VEGF contributes to postnatal neovascularization by mobilizing bone marrow-derived endothelial progenitor cells. EMBO J, 18:3964-3972

281. Asahara T, Masuda H, Takahashi T, Kalka C, Pastore C, Silver M, Kearne M, Magner M, Isner JM. (1999) Bone marrow origin of endothelial progenitor cells responsible for postnatal vasculogenesis in physiological and pathological neovascularization. Circ Res, 85:221-228

282. Kellner B. (1941) Die Fettmorphologie der Sarkome. Z Krebsforsch,240-246

283. Chang YS, di Tomaso E, McDonald DM, Jones R, Jain RK, Munn LL. (2000) Mosaic blood vessels in tumors: frequency of cancer cells in contact with flowing blood. Proc Natl Acad Sci USA, 97:14608-14613

284. Maniotis AJ, Folberg R, Hess A, Seftor EA, Gardner LM, Pe'er J, Trent JM, Meltzer PS, Hendrix MJ. (1999) Vascular channel formation by human melanoma cells in vivo and in vitro: vasculogenic mimicry. Am J Pathol, 155:739-752

285. Dome B, Hendrix MJ, Paku S, Tovari J, Timar J. (2007) Alternative vascularization mechanisms in cancer: Pathology and therapeutic implications. Am J Pathol, 170:1-15

286. Erben RG, Odorfer KI, Siebenhutter M, Weber K, Rohleder S. (2008) Histological assessment of cellular half-life in tissues in vivo. Histochem Cell Biol, 130:1041-1046

287. LeBleu VS, Macdonald B, Kalluri R. (2007) Structure and function of basement membranes. Exp Biol Med, 232:1121-1129

288.van Dijk CG, Nieuweboer FE, Pei JY, Xu YJ, Burgisser P, van Mulligen E, el Azzouzi H, Duncker DJ, Verhaar MC, Cheng C. (2015) The complex mural cell: pericyte function in health and disease. Int J Cardiol 190:75-89

289. Yasumoto K, Kowata Y, Yoshida A, Torii S, Sogawa K. (2009) Role of the intracellular localization of HIF-prolyl hydroxylases. Biochim Biophys Acta, 1793:792-797

290. Morikawa S, Baluk P, Kaidoh T, Haskell A, Jain RK, McDonald DM. (2002) Abnormalities in pericytes on blood vessels and endothelial sprouts in tumors. Am J Pathol, 160:985-1000

291. Ozawa MG, Yao VJ, Chanthery YH, Troncoso P, Uemura A, Varner AS, Kasman IM, Pasqualini R, Arap W, McDonald DM. (2005) Angiogenesis with pericyte abnormalities in a transgenic model of prostate carcinoma. Cancer, 104:2104-2115

292. Baluk P, Morikawa S, Haskell A, Mancuso M, McDonald DM. (2003) Abnormalities of basement membrane on blood vessels and endothelial sprouts in tumors. Am J Pathol, 163:1801-1815

293. Martin TA, Jiang WG. (2009) Loss of tight junction barrier function and its role in cancer metastasis. Biochim Biophys Acta, 1788:872-891

294. Padera TP, Stoll BR, Tooredman JB, Capen D, di Tomaso E, Jain RK. (2004) Pathology: cancer cells compress intratumour vessels. Nature, 427:695

295. Chaplin DJ, Olive PL, Durand RE. (1987) Intermittent blood flow in a murine tumor: radiobiological effects. Cancer Res, 47:597-601

296.di Tomaso E, Capen D, Haskell A, Hart J, Logie JJ, Jain RK, McDonald DM, Jones R, Munn LL. (2005) Mosaic tumor vessels: cellular basis and ultrastructure of focal regions lacking endothelial cell markers. Cancer Res, 65:5740-5749

297. Yonenaga Y, Mori A, Onodera H, Yasuda S, Oe H, Fujimoto A, Tachibana T, Imamura M. (2005) Absence of smooth muscle actin-positive pericyte coverage of tumor vessels correlates with hematogenous metastasis and prognosis of colorectal cancer patients. Oncology, 69:159-166

298. Hagendoorn J, Tong R, Fukumura D, Lin Q, Lobo J, Padera TP, Xu L, Kucherlapati R, Jain RK. (2006) Onset of abnormal blood and lymphatic vessel function and interstitial hypertension in early stages of carcinogenesis. Cancer Res, 66:3360-3364

299. Boucher Y, Jain RK. (1992) Microvascular pressure is the principal driving force for interstitial hypertension in solid tumors: implications for vascular collapse. Cancer Res, 52:5110-5114

300. Ganapathy-Kanniappan S, Geschwind JF. (2013) Tumor glycolysis as a target for cancer therapy: progress and prospects. Mol Cancer, 12:152

301. Sullivan R, Graham CH. (2007) Hypoxia-driven selection of the metastatic phenotype. Cancer metastasis Rev, 26:319-331

302. Hompland T, Ellingsen C, Ovrebo KM, Rofstad EK. (2012) Interstitial fluid pressure and associated lymph node metastasis revealed in tumors by dynamic contrast-enhanced MRI. Cancer Res, 72:4899-4908

303. Qian BZ, Pollard JW. (2010) Macrophage diversity enhances tumor progression and metastasis. Cell, 141:39-51

304. Carmeliet P, Jain RK. (2011) Principles and mechanisms of vessel normalization for cancer and other angiogenic diseases. Nat Rev Drug Discov, 10:417-427

305. Jain RK. (2005) Normalization of tumor vasculature: an emerging concept in antiangiogenic therapy. Science, 307:58-62

306. Pasquier E, Andre N, Braguer D. (2007) Targeting microtubules to inhibit angiogenesis and disrupt tumour vasculature: implications for cancer treatment. Curr Cancer Drug Targets, 7:566-581

307.D'Amato RJ, Loughnan MS, Flynn E, Folkman J. (1994) Thalidomide is an inhibitor of angiogenesis. Proc Natl Acad Sci USA, 91:4082-4085

308. Lu L, Payvandi F, Wu L, Zhang LH, Hariri RJ, Man HW, Chen RS, Muller GW, Hughes CC, Stirling DI, Schafer PH, Bartlett JB. (2009) The anti-cancer drug lenalidomide inhibits angiogenesis and metastasis via multiple inhibitory effects on endothelial cell function in normoxic and hypoxic conditions. Microvasc Res, 77:78-86

309. Ching LM, Cao Z, Kieda C, Zwain S, Jameson MB, Baguley BC. (2002) Induction of endothelial cell apoptosis by the antivascular agent 5,6-Dimethylxanthenone-4-acetic acid. Br J Cancer, 86:1937-1942

310. McGown AT, Fox BW. (1989) Structural and biochemical comparison of the anti-mitotic agents colchicine, combretastatin A4 and amphethinile. Anticancer Drug Des, 3:249-254

311. Philpott M, Baguley BC, Ching LM. (1995) Induction of tumour necrosis factor-alpha by single and repeated doses of the antitumour agent 5,6-dimethylxanthenone-4-acetic acid. Cancer Chemother and Pharmacol, 36:143-148

312. Smith GP, Calveley SB, Smith MJ, Baguley BC. (1987) Flavone acetic acid (NSC 347512) induces haemorrhagic necrosis of mouse colon 26 and 38 tumours. Eur J Cancer Clin Oncol, 23:1209-1211

313. Ching LM, Zwain S, Baguley BC. (2004) Relationship between tumour endothelial cell apoptosis and tumour blood flow shutdown following treatment with the antivascular agent DMXAA in mice. Br J Cancer, 90:906-910

314. Subbiah IM, Lenihan DJ, Tsimberidou AM. (2011) Cardiovascular toxicity profiles of vascular-disrupting agents. Oncologist, 16:1120-1130

315. Tozer GM, Kanthou C, Lewis G, Prise VE, Vojnovic B, Hill SA. (2008) Tumour vascular disrupting agents: combating treatment resistance. Br J Radiol, 81 Spec No 1:S12-20

316. Epstein AL, Mizokami MM, Li J, Hu P, Khawli LA. (2003) Identification of a protein fragment of interleukin 2 responsible for vasopermeability. J Natl Cancer Inst, 95:741-749

317. Watanabe N, Niitsu Y, Umeno H, Kuriyama H, Neda H, Yamauchi N, Maeda M, Urushizaki I. (1988) Toxic effect of tumor necrosis factor on tumor vasculature in mice. Cancer Res, 48:2179-2183

318. Ten Hagen TL, Van Der Veen AH, Nooijen PT, Van Tiel ST, Seynhaeve AL, Eggermont AM. (2000) Low-dose tumor necrosis factor-alpha augments antitumor activity of stealth liposomal doxorubicin (DOXIL) in soft tissue sarcoma-bearing rats. Int J Cancer, 87:829-837

319. Hayes AJ, Neuhaus SJ, Clark MA, Thomas JM. (2007) Isolated limb perfusion with melphalan and tumor necrosis factor alpha for advanced melanoma and soft-tissue sarcoma. Ann Surg Oncol, 14:230-238

320. Brunstein F, Hoving S, Seynhaeve AL, van Tiel ST, Guetens G, de Bruijn EA, Eggermont AM, ten Hagen TL. (2004) Synergistic antitumor activity of histamine plus melphalan in isolated limb perfusion: preclinical studies. J Natl Cancer Inst, 96:1603-1610

321. Xia Y, Choi HK, Lee K. (2012) Recent advances in hypoxia-inducible factor (HIF)-1 inhibitors. Eur J Med Chem, 49:24-40

322. Ranieri G, Patruno R, Ruggieri E, Montemurro S, Valerio P, Ribatti D. (2006) Vascular endothelial growth factor (VEGF) as a target of bevacizumab in cancer: from the biology to the clinic. Curr Med Chem, 13:1845-1857

323. Rahimi N, Dayanir V, Lashkari K. (2000) Receptor chimeras indicate that the vascular endothelial growth factor receptor-1 (VEGFR-1) modulates mitogenic activity of VEGFR-2 in endothelial cells. J Biol Chem, 275:16986-16992

324. Kendall RL, Rutledge RZ, Mao X, Tebben AJ, Hungate RW, Thomas KA. (1999) Vascular endothelial growth factor receptor KDR tyrosine kinase activity is increased by autophosphorylation of two activation loop tyrosine residues. J Biol Chem, 274:6453-6460

325. Gomez-Manzano C, Holash J, Fueyo J, Xu J, Conrad CA, Aldape KD, de Groot JF, Bekele BN, Yung WK. (2008) VEGF Trap induces antiglioma effect at different stages of disease. Neuro Oncol, 10:940-945

326. Witte L, Hicklin DJ, Zhu Z, Pytowski B, Kotanides H, Rockwell P, Bohlen P. (1998) Monoclonal antibodies targeting the VEGF receptor-2 (Flk1/KDR) as an anti-angiogenic therapeutic strategy. Cancer Metastasis Rev, 17:155-161

327. Gotink KJ, Verheul HM. (2010) Anti-angiogenic tyrosine kinase inhibitors: what is their mechanism of action? Angiogenesis, 13:1-14

328. Wan PT, Garnett MJ, Roe SM, Lee S, Niculescu-Duvaz D, Good VM, Jones CM, Marshall CJ, Springer CJ, Barford D, Marais R, Cancer Genome P. (2004) Mechanism of activation of the RAF-ERK signaling pathway by oncogenic mutations of B-RAF. Cell, 116:855-867

329. Wissner A, Fraser HL, Ingalls CL, Dushin RG, Floyd MB, Cheung K, Nittoli T, Ravi MR, Tan X, Loganzo F. (2007) Dual irreversible kinase inhibitors: quinazoline-based inhibitors incorporating two independent reactive centers with each targeting different cysteine residues in the kinase domains of EGFR and VEGFR-2. Bioorg Med Chem, 15:3635-3648

330. Kim BS, Goligorsky MS. (2003) Role of VEGF in kidney development, microvascular maintenance and pathophysiology of renal disease. Korean J Intern Med, 18:65-75

331. Gao Z, Sasaoka T, Fujimori T, Oya T, Ishii Y, Sabit H, Kawaguchi M, Kurotaki Y, Naito M, Wada T, Ishizawa S, Kobayashi M, Nabeshima Y, Sasahara M. (2005) Deletion of the PDGFR-beta gene affects key fibroblast functions important for wound healing. J Biol Chem, 280:9375-9389

332. Bhojani N, Jeldres C, Patard JJ, Perrotte P, Suardi N, Hutterer G, Patenaude F, Oudard S, Karakiewicz PI. (2008) Toxicities associated with the administration of sorafenib, sunitinib, and temsirolimus and their management in patients with metastatic renal cell carcinoma. Eur Urol, 53:917-930

333. Moreno Garcia V, Basu B, Molife LR, Kaye SB. (2012) Combining antiangiogenics to overcome resistance: rationale and clinical experience. Clin Cancer Res, 18:3750-3761

334. Lu C, Kamat AA, Lin YG, Merritt WM, Landen CN, Kim TJ, Spannuth W, Arumugam T, Han LY, Jennings NB, Logsdon C, Jaffe RB, Coleman RL, Sood AK. (2007) Dual targeting of endothelial cells and pericytes in antivascular therapy for ovarian carcinoma. Clin Cancer Res, 13:4209-4217

335. Xian X, Hakansson J, Stahlberg A, Lindblom P, Betsholtz C, Gerhardt H, Semb H. (2006) Pericytes limit tumor cell metastasis. J Clin Invest, 116:642-651

336. Hayman SR, Leung N, Grande JP, Garovic VD. (2012) VEGF inhibition, hypertension, and renal toxicity. Curr Oncol Rep, 14:285-294

337. Presta LG, Chen H, O'Connor SJ, Chisholm V, Meng YG, Krummen L, Winkler M, Ferrara N. (1997) Humanization of an anti-vascular endothelial growth factor monoclonal antibody for the therapy of solid tumors and other disorders. Cancer Res, 57:4593-4599

338. Krupitskaya Y, Wakelee HA. (2009) Ramucirumab, a fully human mAb to the transmembrane signaling tyrosine kinase VEGFR-2 for the potential treatment of cancer. Curr Opin Investig Drugs, 10:597-605

339. Hu-Lowe DD, Zou HY, Grazzini ML, Hallin ME, Wickman GR, Amundson K, Chen JH, Rewolinski DA, Yamazaki S, Wu EY, McTigue MA, Murray BW, Kania RS, O'Connor P, Shalinsky DR, Bender SL. (2008) Nonclinical antiangiogenesis and antitumor activities of axitinib (AG-013736), an oral, potent, and selective inhibitor of vascular endothelial growth factor receptor tyrosine kinases 1, 2, 3. Clin Cancer Res, 14:7272-7283

340. You WK, Sennino B, Williamson CW, Falcon B, Hashizume H, Yao LC, Aftab DT, McDonald DM. (2011) VEGF and c-Met blockade amplify angiogenesis inhibition in pancreatic islet cancer. Cancer Res, 71:4758-4768

341. Hilberg F, Roth GJ, Krssak M, Kautschitsch S, Sommergruber W, Tontsch-Grunt U, Garin-Chesa P, Bader G, Zoephel A, Quant J, Heckel A, Rettig WJ. (2008) BIBF 1120: triple angiokinase inhibitor with sustained receptor blockade and good antitumor efficacy. Cancer Res, 68:4774-4782

342. Kumar R, Knick VB, Rudolph SK, Johnson JH, Crosby RM, Crouthamel MC, Hopper TM, Miller CG, Harrington LE, Onori JA, Mullin RJ, Gilmer TM, Truesdale AT, Epperly AH, Boloor A, Stafford JA, Luttrell DK, Cheung M. (2007) Pharmacokinetic-pharmacodynamic correlation from mouse to human with pazopanib, a multikinase angiogenesis inhibitor with potent antitumor and antiangiogenic activity. Mol Cancer Ther, 6:2012-2021

343. Wilhelm SM, Dumas J, Adnane L, Lynch M, Carter CA, Schutz G, Thierauch KH, Zopf D. (2011) Regorafenib (BAY 73-4506): a new oral multikinase inhibitor of angiogenic, stromal and oncogenic receptor tyrosine kinases with potent preclinical antitumor activity. Int J Cancer, 129:245-255

344. Wilhelm SM, Carter C, Tang L, Wilkie D, McNabola A, Rong H, Chen C, Zhang X, Vincent P, McHugh M, Cao Y, Shujath J, Gawlak S, Eveleigh D, Rowley B, Liu

L, Adnane L, Lynch M, Auclair D, Taylor I, Gedrich R, Voznesensky A, Riedl B, Post LE, Bollag G, Trail PA. (2004) BAY 43-9006 exhibits broad spectrum oral antitumor activity and targets the RAF/MEK/ERK pathway and receptor tyrosine kinases involved in tumor progression and angiogenesis. Cancer Res, 64:7099-7109

345. Sun L, Liang C, Shirazian S, Zhou Y, Miller T, Cui J, Fukuda JY, Chu JY, Nematalla A, Wang X, Chen H, Sistla A, Luu TC, Tang F, Wei J, Tang C. (2003) Discovery of 5-[5-fluoro-2-oxo-1,2- dihydroindol-(3Z)-ylidenemethyl]-2,4-dimethyl-1H-pyrrole-3-carboxylic acid (2-diethylaminoethyl)amide, a novel tyrosine kinase inhibitor targeting vascular endothelial and platelet-derived growth factor receptor tyrosine kinase. J Med Chem, 46:1116-1119

346. Wedge SR, Ogilvie DJ, Dukes M, Kendrew J, Chester R, Jackson JA, Boffey SJ, Valentine PJ, Curwen JO, Musgrove HL, Graham GA, Hughes GD, Thomas AP, Stokes ES, Curry B, Richmond GH, Wadsworth PF, Bigley AL, Hennequin LF. (2002) ZD6474 inhibits vascular endothelial growth factor signaling, angiogenesis, and tumor growth following oral administration. Cancer Res, 62:4645-4655

347. Holash J, Davis S, Papadopoulos N, Croll SD, Ho L, Russell M, Boland P, Leidich R, Hylton D, Burova E, Ioffe E, Huang T, Radziejewski C, Bailey K, Fandl JP, Daly T, Wiegand SJ, Yancopoulos GD, Rudge JS. (2002) VEGF-Trap: a VEGF blocker with potent antitumor effects. Proc Natl Acad SciUSA, 99:11393-11398

348. Takahashi Y, Kitadai Y, Bucana CD, Cleary KR, Ellis LM. (1995) Expression of vascular endothelial growth factor and its receptor, KDR, correlates with vascularity, metastasis, and proliferation of human colon cancer. Cancer Res, 55:3964-3968

349. Speed B, Bu HZ, Pool WF, Peng GW, Wu EY, Patyna S, Bello C, Kang P. (2012) Pharmacokinetics, distribution, and metabolism of [14C]sunitinib in rats, monkeys, and humans. Drug Metab Dispos, 40:539-555

350. Starling N, Vazquez-Mazon F, Cunningham D, Chau I, Tabernero J, Ramos FJ, Iveson TJ, Saunders MP, Aranda E, Countouriotis AM, Ruiz-Garcia A, Wei G, Tursi JM, Guillen-Ponce C, Carrato A. (2012) A phase I study of sunitinib in combination with FOLFIRI in patients with untreated metastatic colorectal cancer. Ann Oncol 23:119-127

351. Strumberg D, Richly H, Hilger RA, Schleucher N, Korfee S, Tewes M, Faghih M, Brendel E, Voliotis D, Haase CG, Schwartz B, Awada A, Voigtmann R, Scheulen ME, Seeber S. (2005) Phase I clinical and pharmacokinetic study of the Novel Raf kinase and vascular endothelial growth factor receptor inhibitor BAY 43-9006 in patients with advanced refractory solid tumors. J Clin Oncol, 23:965-972

352. Tabernero J, Garcia-Carbonero R, Cassidy J, Sobrero A, Van Cutsem E, Kohne CH, Tejpar S, Gladkov O, Davidenko I, Salazar R, Vladimirova L, Cheporov S, Burdaeva O, Rivera F, Samuel L, Bulavina I, Potter V, Chang YL, Lokker NA, O'Dwyer PJ. (2013) Sorafenib in combination with oxaliplatin, leucovorin, and fluorouracil (modified FOLFOX6) as first-line treatment of metastatic colorectal cancer: the RESPECT trial. Clin Cancer Res, 19:2541-2550

353. Benedito R, Rocha SF, Woeste M, Zamykal M, Radtke F, Casanovas O, Duarte A, Pytowski B, Adams RH. (2012) Notch-dependent VEGFR3 upregulation allows angiogenesis without VEGF-VEGFR2 signalling. Nature, 484:110-114

354. Heinrich MC, Maki RG, Corless CL, Antonescu CR, Harlow A, Griffith D, Town A, McKinley A, Ou WB, Fletcher JA, Fletcher CD, Huang X, Cohen DP, Baum CM, Demetri GD. (2008) Primary and secondary kinase genotypes correlate with the biological and clinical activity of sunitinib in imatinib-resistant gastrointestinal stromal tumor. J Clin Oncol, 26:5352-5359

355. Gajiwala KS, Wu JC, Christensen J, Deshmukh GD, Diehl W, DiNitto JP, English JM, Greig MJ, He YA, Jacques SL, Lunney EA, McTigue M, Molina D, Quenzer T, Wells PA, Yu X, Zhang Y, Zou A, Emmett MR, Marshall AG, Zhang HM, Demetri GD. (2009) KIT kinase mutants show unique mechanisms of drug resistance to imatinib and sunitinib in gastrointestinal stromal tumor patients. Proc Natl Acad Sci USA, 106:1542-1547

356. Dai Y, Bae K, Siemann DW. (2011) Impact of hypoxia on the metastatic potential of human prostate cancer cells. Int J Radiat Oncol Biol Phys, 81:521-528

357. Elice F, Rodeghiero F, Falanga A, Rickles FR. (2009) Thrombosis associated with angiogenesis inhibitors. Best Pract Res Clin Haematol, 22:115-128

358. Cooke VG, LeBleu VS, Keskin D, Khan Z, O'Connell JT, Teng Y, Duncan MB, Xie L, Maeda G, Vong S, Sugimoto H, Rocha RM, Damascena A, Brentani RR, Kalluri R. (2012) Pericyte depletion results in hypoxia-associated epithelial-to-

mesenchymal transition and metastasis mediated by met signaling pathway. Cancer Cell, 21:66-81

359. Hu S, Chen Z, Franke R, Orwick S, Zhao M, Rudek MA, Sparreboom A, Baker SD. (2009) Interaction of the multikinase inhibitors sorafenib and sunitinib with solute carriers and ATP-binding cassette transporters. Clin Cancer Res, 15:6062-6069

360. Bruneel A, Labas V, Mailloux A, Sharma S, Vinh J, Vaubourdolle M, Baudin B. (2003) Proteomic study of human umbilical vein endothelial cells in culture. Proteomics, 3:714-723

361. Bruneel A, Labas V, Mailloux A, Sharma S, Royer N, Vinh J, Pernet P, Vaubourdolle M, Baudin B. (2005) Proteomics of human umbilical vein endothelial cells applied to etoposide-induced apoptosis. Proteomics, 5:3876-3884

362. Geiger T, Wisniewski JR, Cox J, Zanivan S, Kruger M, Ishihama Y, Mann M. (2011) Use of stable isotope labeling by amino acids in cell culture as a spike-in standard in quantitative proteomics. Nat Protoc, 6:147-157

363. Andersen JS, Mann M. (2006) Organellar proteomics: turning inventories into insights. EMBO Rep, 7:874-879

364. Burghoff S, Schrader J. (2011) Secretome of human endothelial cells under shear stress. J Proteome Res, 10:1160-1169

365. Nagel T, Meyer B. (2014) Simultaneous characterization of sequence polymorphisms, glycosylation and phosphorylation of fibrinogen in a direct analysis by LC-MS. Biochim Biophys Acta, 1844:2284-2289

366. Hoffmann BR, Wagner JR, Prisco AR, Janiak A, Greene AS. (2013) Vascular endothelial growth factor-A signaling in bone marrow-derived endothelial progenitor cells exposed to hypoxic stress. Physiol Genomics, 45:1021-1034

367. Gu H, Qiu W, Shi Y, Chen S, Yin J. (2014) Variant alleles of VEGF and risk of esophageal cancer and lymph node metastasis. Biomarkers, 19:252-258

368. Ai J, Tan Y, Ying W, Hong Y, Liu S, Wu M, Qian X, Wang H. (2006) Proteome analysis of hepatocellular carcinoma by laser capture microdissection. Proteomics, 6:538-546

369. Murphy RC, Hankin JA, Barkley RM. (2009) Imaging of lipid species by MALDI mass spectrometry. J Lipid Res, 50 Suppl:S317-322

370. Taban IM, Altelaar AF, van der Burgt YE, McDonnell LA, Heeren RM, Fuchser J, Baykut G. (2007) Imaging of peptides in the rat brain using MALDI-FTICR mass spectrometry. J Am Soc Mass Spectrom, 18:145-151

371. Seeley EH, Caprioli RM. (2008) Molecular imaging of proteins in tissues by mass spectrometry. Proc Natl Acad Sci USA, 105:18126-18131

372. Greer T, Sturm R, Li L. (2011) Mass spectrometry imaging for drugs and metabolites. J Proteomics, 74:2617-2631

373. Shariatgorji M, Nilsson A, Bonta M, Gan J, Marklund N, Clausen F, Kallback P, Loden H, Limbeck A, Andren PE. (2016) Direct imaging of elemental distributions in tissue sections by laser ablation mass spectrometry. Methods, 104:86-92

374. Solon EG. (2012) Use of radioactive compounds and autoradiography to determine drug tissue distribution. Chem Res Toxicol, 25:543-555

375. Solon EG, Schweitzer A, Stoeckli M, Prideaux B. (2010) Autoradiography, MALDI-MS, and SIMS-MS imaging in pharmaceutical discovery and development. AAPS J, 12:11-26

376. Kola I, Landis J. (2004) Can the pharmaceutical industry reduce attrition rates? Nat Rev Drug Discov, 3:711-715

377. Hillenkamp F, Karas M. (1990) Mass spectrometry of peptides and proteins by matrix-assisted ultraviolet laser desorption/ionization. Methods Enzymol, 193:280-295

378. Nordhoff E, Ingendoh A, Cramer R, Overberg A, Stahl B, Karas M, Hillenkamp F, Crain PF. (1992) Matrix-assisted laser desorption/ionization mass spectrometry of nucleic acids with wavelengths in the ultraviolet and infrared. Rapid Commun Mass Spectrom, 6:771-776

379. Schwartz SA, Reyzer ML, Caprioli RM. (2003) Direct tissue analysis using matrix-assisted laser desorption/ionization mass spectrometry: practical aspects of sample preparation. J Mass Spectrom, 38:699-708

380. Gusev AI, Muddiman DC, Proctor A, Sharkey AG, Hercules DM, Tata PN, Venkataramanan R. (1996) A quantitative study of in vitro hepatic metabolism of tacrolimus (FK506) using secondary ion and matrix-assisted laser desorption/ionization mass spectrometry. Rapid Commun Mass Spectrom, 10:1215-1218

381. Marko-Varga G, Vegvari A, Rezeli M, Prikk K, Ross P, Dahlback M, Edula G, Sepper R, Fehniger TE. (2012) Understanding drug uptake and binding within targeted disease micro-environments in patients: a new tool for translational medicine. Clin Transl Med, 1:8

382. Sharma K, Suresh PS, Mullangi R, Srinivas NR. (2015) Quantitation of VEGFR2 (vascular endothelial growth factor receptor) inhibitors--review of assay methodologies and perspectives. Biomed Chromatogr, 29:803-834

383. Ait-Belkacem R, Berenguer C, Villard C, Ouafik L, Figarella-Branger D, Beck A, Chinot O, Lafitte D. (2014) Monitoring therapeutic monoclonal antibodies in brain tumor. MAbs, 6:1385-1393

384. Kilkenny C, Browne W, Cuthill IC, Emerson M, Altman DG, Group NCRRGW. (2010) Animal research: reporting in vivo experiments: the ARRIVE guidelines. Br J Pharmacol, 160:1577-1579

385. Polverino A, Coxon A, Starnes C, Diaz Z, DeMelfi T, Wang L, Bready J, Estrada J, Cattley R, Kaufman S, Chen D, Gan Y, Kumar G, Meyer J, Neervannan S, Alva G, Talvenheimo J, Montestruque S, Tasker A, Patel V, Radinsky R, Kendall R. (2006) AMG 706, an oral, multikinase inhibitor that selectively targets vascular endothelial growth factor, platelet-derived growth factor, and kit receptors, potently inhibits angiogenesis and induces regression in tumor xenografts. Cancer Res, 66:8715-8721

386. Mendel DB, Laird AD, Xin X, Louie SG, Christensen JG, Li G, Schreck RE, Abrams TJ, Ngai TJ, Lee LB, Murray LJ, Carver J, Chan E, Moss KG, Haznedar JO, Sukbuntherng J, Blake RA, Sun L, Tang C, Miller T, Shirazian S, McMahon G, Cherrington JM. (2003) In vivo antitumor activity of SU11248, a novel tyrosine kinase inhibitor targeting vascular endothelial growth factor and platelet-derived growth factor receptors: determination of a pharmacokinetic/pharmacodynamic relationship. Clin Cancer Res, 9:327-337

387. Wood JM, Bold G, Buchdunger E, Cozens R, Ferrari S, Frei J, Hofmann F, Mestan J, Mett H, O'Reilly T, Persohn E, Rosel J, Schnell C, Stover D, Theuer A, Towbin H, Wenger F, Woods-Cook K, Menrad A, Siemeister G, Schirner M, Thierauch KH, Schneider MR, Drevs J, Martiny-Baron G, Totzke F. (2000) PTK787/ZK 222584, a novel and potent inhibitor of vascular endothelial growth factor receptor

tyrosine kinases, impairs vascular endothelial growth factor-induced responses and tumor growth after oral administration. Cancer Res, 60:2178-2189

388. Blanc J, Geney R, Menet C. (2013) Type II kinase inhibitors: an opportunity in cancer for rational design. Anticancer Agents Med Chem, 13:731-747

389. Jost LM, Gschwind HP, Jalava T, Wang Y, Guenther C, Souppart C, Rottmann A, Denner K, Waldmeier F, Gross G, Masson E, Laurent D. (2006) Metabolism and disposition of vatalanib (PTK787/ZK-222584) in cancer patients. Drug Metab Dispos, 34:1817-1828

390. Kane RC, Farrell AT, Saber H, Tang S, Williams G, Jee JM, Liang C, Booth B, Chidambaram N, Morse D, Sridhara R, Garvey P, Justice R, Pazdur R. (2006) Sorafenib for the treatment of advanced renal cell carcinoma. Clin Cancer Res, 12:7271-7278

391. Samalin E, Bouche O, Thezenas S, Francois E, Adenis A, Bennouna J, Taieb J, Desseigne F, Seitz JF, Conroy T, Galais MP, Assenat E, Crapez E, Poujol S, Bibeau F, Boissiere F, Laurent-Puig P, Ychou M, Mazard T. (2014) Sorafenib and irinotecan (NEXIRI) as second- or later-line treatment for patients with metastatic colorectal cancer and KRAS-mutated tumours: a multicentre Phase I/II trial. Br J Cancer, 110:1148-1154

392. Tsuji Y, Satoh T, Tsuji A, Muro K, Yoshida M, Nishina T, Nagase M, Komatsu Y, Kato T, Miyata Y, Mizutani N, Hashigaki S, Lechuga MJ, Denda T. (2012) First-line sunitinib plus FOLFIRI in Japanese patients with unresectable/metastatic colorectal cancer: a phase II study. Cancer Sci, 103:1502-1507

393. Yoshino T, Yamazaki K, Hamaguchi T, Shimada Y, Kato K, Yasui H, Boku N, Lechuga MJ, Hirohashi T, Shibata A, Hashigaki S, Li Y, Ohtsu A. (2012) Phase I study of sunitinib plus modified FOLFOX6 in Japanese patients with treatment-naive colorectal cancer. Anticancer Res, 32:973-979

394. Fu S, Hou MM, Naing A, Janku F, Hess K, Zinner R, Subbiah V, Hong D, Wheler J, Piha-Paul S, Tsimberidou A, Karp D, Araujo D, Kee B, Hwu P, Wolff R, Kurzrock R, Meric-Bernstam F. (2015) Phase I study of pazopanib and vorinostat: a therapeutic approach for inhibiting mutant p53-mediated angiogenesis and facilitating mutant p53 degradation. Ann Oncol, 26:1012-1018

395. Bennouna J, Deslandres M, Senellart H, de Labareyre C, Ruiz-Soto R, Wixon C, Botbyl J, Suttle AB, Delord JP. (2015) A phase I open-label study of the safety, tolerability, and pharmacokinetics of pazopanib in combination with irinotecan and cetuximab for relapsed or refractory metastatic colorectal cancer. Invest New Drugs, 33:138-147

396. Tebbutt N, Kotasek D, Burris HA, Schwartzberg LS, Hurwitz H, Stephenson J, Warner DJ, Chen L, Hsu CP, Goldstein D. (2015) Motesanib with or without panitumumab plus FOLFIRI or FOLFOX for the treatment of metastatic colorectal cancer. Cancer Chemother Pharmacol, 75:993-1004

397. Giatromanolaki A, Koukourakis MI, Sivridis E, Gatter KC, Trarbach T, Folprecht G, Shi MM, Lebwohl D, Jalava T, Laurent D, Meinhardt G, Harris AL, Tumour, Angiogenesis Research G. (2012) Vascular density analysis in colorectal cancer patients treated with vatalanib (PTK787/ZK222584) in the randomised CONFIRM trials. Br J Cancer, 107:1044-1050

398. Koukourakis MI, Giatromanolaki A, Sivridis E, Gatter KC, Trarbach T, Folprecht G, Shi MM, Lebwohl D, Jalava T, Laurent D, Meinhardt G, Harris AL. (2011) Prognostic and predictive role of lactate dehydrogenase 5 expression in colorectal cancer patients treated with PTK787/ZK 222584 (vatalanib) antiangiogenic therapy. Clin Cancer Res, 17:4892-4900

399. Banerjee S, A'Hern R, Detre S, Littlewood-Evans AJ, Evans DB, Dowsett M, Martin LA. (2010) Biological evidence for dual antiangiogenic-antiaromatase activity of the VEGFR inhibitor PTK787/ZK222584 in vivo. Clin Cancer Res, 16:4178-4187

400. Carlo-Stella C, Locatelli SL, Giacomini A, Cleris L, Saba E, Righi M, Guidetti A, Gianni AM. (2013) Sorafenib inhibits lymphoma xenografts by targeting MAPK/ERK and AKT pathways in tumor and vascular cells. PLoS One, 8:e61603

401.de Bouard S, Herlin P, Christensen JG, Lemoisson E, Gauduchon P, Raymond E, Guillamo JS. (2007) Antiangiogenic and anti-invasive effects of sunitinib on experimental human glioblastoma. Neuro Oncol, 9:412-423

402. Gril B, Palmieri D, Qian Y, Anwar T, Ileva L, Bernardo M, Choyke P, Liewehr DJ, Steinberg SM, Steeg PS. (2011) The B-Raf status of tumor cells may be a

significant determinant of both antitumor and anti-angiogenic effects of pazopanib in xenograft tumor models. PLoS One, 6:e25625

403. Schaiberger AM, Moss JA. (2008) Optimized sample preparation for MALDI mass spectrometry analysis of protected synthetic peptides. J Am Soc Mass Spectrom, 19:614-619

404. Smirnov IP, Zhu X, Taylor T, Huang Y, Ross P, Papayanopoulos IA, Martin SA, Pappin DJ. (2004) Suppression of alpha-cyano-4-hydroxycinnamic acid matrix clusters and reduction of chemical noise in MALDI-TOF mass spectrometry. Anal Chem, 76:2958-2965

405. MALDI ionization. https://nationalmaglab.org/user-facilities/icr/techniques/maldi.

406. Strupat K, Kovtoun V, Bui H, Viner R, Stafford G, S. H. (2009) MALDI Produced Ions Inspected with a Linear Ion Trap-Orbitrap Hybrid Mass Analyzer. J Am Soc Mass Spectrom, 20:1451-1463

407. Schneider BB, Lock C, Covey TR. (2005) AP and vacuum MALDI on a QqLIT instrument. J Am Soc Mass Spectrom, 16:176-182

408. Structure of quadrupole. . http://www.chemicool.com/definition/quadrupole_mass_spectrometry.html.

409. LTQ XL Hardware Manual.

410. Makarov A. (2000) Electrostatic axially harmonic orbital trapping: a high-performance technique of mass analysis. Anal Chem, 72:1156-1162

411. Structure of the orbitrap. https://www.thermofisher.com/hu/en/home/industrial/mass-spectrometry/liquid-chromatography-mass-spectrometry-lc-ms/lc-ms-systems/orbitrap-lc-ms.html.

412. Olsen JV, Macek B, Lange O, Makarov A, Horning S, Mann M. (2007) Higher-energy C-trap dissociation for peptide modification analysis. Nat Methods, 4:709-712

413. Folkman J. (1990) What is the evidence that tumors are angiogenesis dependent? J Nat Cancer Inst, 82:4-6

414. Li C, Kuchimanchi M, Hickman D, Poppe L, Hayashi M, Zhou Y, Subramanian R, Kumar G, Surapaneni S. (2009) In vitro metabolism of the novel, highly selective oral angiogenesis inhibitor motesanib diphosphate in preclinical species and in humans. Drug Metab Dispos, 37:1378-1394

415. Deng Y, Sychterz C, Suttle AB, Dar MM, Bershas D, Negash K, Qian Y, Chen EP, Gorycki PD, Ho MY. (2013) Bioavailability, metabolism and disposition of oral pazopanib in patients with advanced cancer. Xenobiotica, 43:443-453

416. Rais R, Zhao M, He P, Xu L, Deeken JF, Rudek MA. (2012) Quantitation of unbound sunitinib and its metabolite N-desethyl sunitinib (SU12662) in human plasma by equilibrium dialysis and liquid chromatography-tandem mass spectrometry: application to a pharmacokinetic study. Biomed Chromatogr, 26:1315-1324

417. Laschke MW, Elitzsch A, Vollmar B, Vajkoczy P, Menger MD. (2006) Combined inhibition of vascular endothelial growth factor (VEGF), fibroblast growth factor and platelet-derived growth factor, but not inhibition of VEGF alone, effectively suppresses angiogenesis and vessel maturation in endometriotic lesions. Hum Reprod, 21:262-268

418. Lankheet NA, Blank CU, Mallo H, Adriaansz S, Rosing H, Schellens JH, Huitema AD, Beijnen JH. (2011) Determination of sunitinib and its active metabolite N-desethylsunitinib in sweat of a patient. J Anal Toxicol, 35:558-565

419. Rodriguez J, Castaneda G, Munoz L, Villa JC. (2015) Quantitation of sunitinib, an oral multitarget tyrosine kinase inhibitor, and its metabolite in urine samples by nonaqueous capillary electrophoresis time of flight mass spectrometry. Electrophoresis, 36:1580-1587

420. Zhou Q, Gallo JM. (2010) Quantification of sunitinib in mouse plasma, brain tumor and normal brain using liquid chromatography-electrospray ionization-tandem mass spectrometry and pharmacokinetic application. J Pharm Biomed Anal, 51:958-964

421. Gotink KJ, Broxterman HJ, Labots M, de Haas RR, Dekker H, Honeywell RJ, Rudek MA, Beerepoot LV, Musters RJ, Jansen G, Griffioen AW, Assaraf YG, Pili R, Peters GJ, Verheul HM. (2011) Lysosomal sequestration of sunitinib: a novel mechanism of drug resistance. Clin Cancer Res; 17:7337-7346

422. Gottesman MM, Pastan IH. (2015) The Role of Multidrug Resistance Efflux Pumps in Cancer: Revisiting a JNCI Publication Exploring Expression of the MDR1 (P-glycoprotein) Gene. J Nat Cancer Inst, 107

423. Huang L, Perrault C, Coelho-Martins J, Hu C, Dulong C, Varna M, Liu J, Jin J, Soria C, Cazin L, Janin A, Li H, Varin R, Lu H. (2013) Induction of acquired drug

resistance in endothelial cells and its involvement in anticancer therapy. J Hematol Oncol, 6:49

424. Domingues I, Rino J, Demmers JA, de Lanerolle P, Santos SC. (2005) VEGFR2 translocates to the nucleus to regulate its own transcription. PLoS One 2011; 6:e25668

425. Bergers G, Song S. The role of pericytes in blood-vessel formation and maintenance. Neuro Oncol, 7:452-464

426. Van der Veldt AA, Lubberink M, Bahce I, Walraven M, de Boer MP, Greuter HN, Hendrikse NH, Eriksson J, Windhorst AD, Postmus PE, Verheul HM, Serne EH, Lammertsma AA, Smit EF. (2012) Rapid decrease in delivery of chemotherapy to tumors after anti-VEGF therapy: implications for scheduling of anti-angiogenic drugs. Cancer Cell, 21:82-91

427. Goel S, Wong AH, Jain RK. (2012) Vascular normalization as a therapeutic strategy for malignant and nonmalignant disease. Cold Spring Harb Perspect Med, 2:a006486

428. Wehland M, Bauer J, Magnusson NE, Infanger M, Grimm D. (2013) Biomarkers for anti-angiogenic therapy in cancer. Int J Mol Sci, 14:9338-9364

12. PUBLICATIONS

Connected to the thesis:

- Connell JJ, Sugihara Y, Torok S, Dome B, Tovari J, Fehniger TE, Marko-Varga G, Vegvari A. Localization of sunitinib in in vivo animal and in vitro experimental models by MALDI mass spectrometry imaging. *ANALYTICAL AND BIOANALYTICAL CHEMISTRY* 407:(8) pp. 2245-2253. (2015)
- Kwon HJ, Kim Y, Sugihara Y, Baldetorp B, Welinder C, Watanabe K, Nishimura T, Malm J, Torok S, Dome B, Vegvari A, Gustavsson L, Fehniger TE, Marko-Varga G. Drug compound characterization by mass spectrometry imaging in cancer tissue. *ARCHIVES OF PHARMACAL RESEARCH* 38:(9) pp. 1718-1727. (2015)
- Torok S, Vegvari A, Rezeli M, Fehniger TE, Tovari J, Paku S, Laszlo V, Hegedus B, Rozsas A, Dome B, Marko-Varga G. Localization of sunitinib, its metabolites and its target receptors in tumour bearing mice: a MALDI mass spectrometry imaging study. *BRITISH JOURNAL OF PHARMACOLOGY* 172:(4) pp. 1148-1163. (2015)
- Torok S, Dome B. A tumor-indukált angiogenezis gátlásának lehetőségei: eredmények multi-target tirozin kináz gátlókkal. *MAGYAR ONKOLÓGIA* 56: pp. 3-15. (2012)
- Torok S, Cserepes T M, Renyi-Vamos F, Dome B. Nintedanib (BIBF 1120) a szolid daganatok kezelésében: biológia és klinikai tapasztalatok áttekintése. *MAGYAR ONKOLÓGIA* 56:(3) pp. 199-208. (2012)

Not connected to the thesis:

- Hoda MA, Rozsas A, Lang E, Klikovits T, Lohinai Z, Torok S, Berta J, Bendek M, Berger W, Hegedus B, Klepetko W, Renyi-Vamos F, Grusch M, Dome B, Laszlo V. High circulating activin A level is associated with tumor progression and predicts poor prognosis in lung adenocarcinoma. *ONCOTARGET* 7:(12) pp. 13388-13399. (2016)
- Berta J, Hoda MA, Laszlo V, Rozsas A, Garay T, Torok S, Grusch M, Berger W, Paku S, Renyi-Vamos F, Masri B, Tovari J, Groger M, Klepetko W, Hegedus B, Dome B. Apelin promotes lymphangiogenesis and lymph node metastasis. *ONCOTARGET* 5:(12) pp. :4426-:4437. (2014)

- Sarosi V, Losonczy G, Francovszky E, Tolnay E, Torok S, Galffy G, Hegedus B, Dome B, Ostoros G. Effectiveness of erlotinib treatment in advanced KRAS mutation-negative lung adenocarcinoma patients: Results of a multicenter observational cohort study (MOTIVATE). *LUNG CANCER* 86:(1) pp. 54-58. (2014)
- Schelch K, Hoda MA, Klikovits T, Munzker J, Ghanim B, Wagner C, Garay T, Laszlo V, Setinek U, Dome B, Filipits M, Pirker C, Heffeter P, Selzer E, Tovari J, Torok S, Kenessey I, Holzmann K, Grasl-Kraupp B, Marian B, Klepetko W, Berger W, Hegedus B, Grusch M. Fibroblast growth factor receptor inhibition is active against mesothelioma and synergizes with radio- and chemotherapy. *AMERICAN JOURNAL OF RESPIRATORY AND CRITICAL CARE MEDICINE* 190:(7) pp. 763-772. (2014)
- Rozsas A, Berta J, Rojko L, Horvath LZ, Keszthelyi M, Kenessey I, Laszlo V, Berger W, Grusch M, Hoda MA, Torok S, Klepetko W, Renyi-Vamos F, Hegedus B, Dome B, Tovari J. Erythropoietin receptor expression is a potential prognostic factor in human lung adenocarcinoma. *PLOS ONE* 8:(10) p. e77459. (2013)
- Török Sz, Hegedűs B, Döme B, Ostoros Gy. Az epidermális növekedési faktor-receptor tirozinkináz-inhibitorok elleni rezisztencia okai és a potenciális terápiás lehetőségek. *MEDICINA THORACALIS* 66:(4) pp. 178-188. (2013)
- Hoda MA, Munzker J, Ghanim B, Schelch K, Klikovits T, Laszlo V, Sahin E, Bedeir A, Lackner A, Dome B, Setinek U, Filipits M, Eisenbauer M, Kenessey I, Torok S, Garay T, Hegedus B, Catania A, Taghavi S, Klepetko W, Berger W, Grusch M. Suppression of activin A signals inhibits growth of malignant pleural mesothelioma cells.. *BRITISH JOURNAL OF CANCER* 107:(12) pp. 1978-1986. (2012)
- Torok S, Hegedus B, Laszlo V, Hoda MA, Ghanim B, Berger W, Klepetko W, Dome B, Ostoros G. Lung cancer in never smokers. *FUTURE ONCOLOGY* 7:(10) pp. 1195-1211. (2011)

13. ACKNOWLEDGEMENT

Hereby I would like to thank everybody who helped me in my PhD work:

- my supervisors, Balázs Döme MD, PhD for employing me, finding me an interesting topic, bothering me to work hard, tolerating me in the bad times and sometimes also appreciating what I was doing; and György Marko-Varga for giving me the opportunity to get to know Sweden, Swedish culture, people and also mass spectrometry and MALDI imaging;
- Imre Barta PhD opponent for his useful remarks;
- the staff at the Department of Tumor Biology, National Korányi Institute of Pulmonology, especially Anita Horváth-Rózsás, Judit Berta PhD, Olga Kelemen PhD, Magdolna Keszthelyi, Krisztina Gönczi-Pető, Ildikó Koralovszkiné Kovács and Erzsébet Schlegl for their professional support and friendship
- József Tóvári PhD for all the mice he offered for my experiments and the staff in the Department of Experimental Pharmacology, National Institute of Oncology, for the professional care of the mice. Special thanks for Irén Bodrogi-Mayer and Anita Hidvégi for teaching me most things I know about animal experiments, and Mónika Kovaljovné Hegedűs for having a good word to me even in bad times;
- every employee of the Department of Tumor Progression, National Institute of Oncology for their help during my work there;
- the collegues at Lund University for accepting me, presenting real multi-cultural atmosphere and specially for Ákos Végvári PhD and Melinda Rezeli PhD for their Hungarian words and undiminished enthusiasm to ascertain how and why the MALDI instrument works or not;
- Balázs Hegedűs PhD and the members of the Division of Thoracic Surgery, Department of Surgery, Comprehensive Cancer Center, Medical University of Vienna, for supporting my life and experiments in Vienna;
- Sándor Paku DSc for his useful advices and directions during the personal consultations;
- Anna Tisza and Tímea Márton for working with me, for checking my knowledge from time to time and for accepting me as I am;

- and last, but not least I thank my husband, my family and all of my friends, for taking my side in the past few years. Special thanks to Dániel Török for checking my grammar every now and then, and Balázs Somogyi, Péter Martinek PhD and Csaba Mravik for asking or answering real scientific questions and solving real methodological problems. I really thank my daughter to let me write this dissertation in time.